



**Politecnico
di Torino**

Politecnico di Torino

Corso di Laurea Magistrale in
Ingegneria Energetica e Nucleare

**Exergetic potential of an organic
Rankine cycle coupled with a
concentrated solar power system**

Relatore

Ph.D. Davide Papurello

Candidata

Luisa Livia Pia Lambertino

A. A. 2020/2021

Contents

| | |
|--|----|
| Abstract | 3 |
| Part I – Exergy as a measure of energy quality | 4 |
| Energy, environment and sustainable development | 4 |
| Renewables to avoid resource degradation | 9 |
| Exergy aspects of CSP-driven ORCs: Literature review | 12 |
| Part II – Case study | 20 |
| Thermodynamic fundamentals | 20 |
| Exergy of a closed system | 23 |
| Exergy of a matter flow | 24 |
| Exergy of thermal energy | 24 |
| Exergy of work | 25 |
| Exergy of electricity | 26 |
| Exergy consumption | 26 |
| Exergy balance | 26 |
| Reference environment and general remarks | 27 |
| Efficiencies and other measures of merit | 29 |
| Base-case system | 31 |
| Working fluid | 34 |
| Expander | 36 |
| Condenser | 36 |
| Pump | 37 |
| Evaporator | 37 |
| Recuperator | 39 |
| System coupling | 40 |
| Design-point exergy performance | 42 |
| Revised system | 45 |
| Valves and tank | 45 |
| Thermal energy storage | 47 |
| Control strategy | 50 |
| Productivity | 57 |
| Exergy analysis | 62 |
| Sensitivity analysis | 68 |
| Part III – Final remarks | 73 |
| Bibliography | 75 |

Abstract

The relationship between sustainable development and the use of resources, particularly the energy ones, is currently of great significance. Attaining sustainable development requires also sustainable energy resources to be used, and it is more easily assisted if resources are exploited efficiently.

Exergy methods are important too since they are a useful tool for improving processes efficiency. Exergy analysis provides a true measure of how and how nearly actual performances approach the ideal ones and identifies, more clearly than energy analysis, causes and locations of thermodynamic losses.

The work carried out in this thesis shows the importance that exergy analysis assumes if applied when designing energy systems, especially having unconventional layouts.

After having illustrated the concept of exergy analysis, we move on to explore the scientific literature currently available that deals with non-conventional plants, especially the hybrid ones, powered by renewable sources.

Next, we focus on a system consisting of an organic Rankine cycle, powered by a concentrating solar thermal system, previously sized starting from the solar dish concentrator installed on the rooftop of Politecnico di Torino's Energy Center building. This system is analyzed from the exergetic point of view in its initial setting.

Then, some modifications are made: considering the organic Rankine cycle circuit, we focus on valves and on the condenser. After that, moving to the solar circuit, we install a thermocline-type thermal storage, carefully sized, which acts as a connection between the solar circuit and the power one, to improve the performance of the system by attenuating the typical intermittency of the solar resource.

The results obtained from the exergy analysis, expressed through specific indicators, are shown to emphasize the influence of the single element in the entire system, and are compared with the results reported in the literature. What is obtained is in line with what is reported in scientific papers.

The operating mode of such a system is then analyzed, deciding to give priority to electricity production, to make the most of the potential offered by a power cycle operating at low temperatures such as our organic Rankine one.

Finally, thanks to a sensitivity analysis, we focus on the influence that certain operating parameters - specifically the temperature and pressure at the inlet of the expander and the operating temperatures at the evaporator and condenser - have on exergetic performance, with particular attention given to the evaluation of unavoidable irreversibility and the consequent improvement potential of the entire system, in the wake of advanced exergy analysis.

In conclusion, the use of exergo-economic and exergo-environmental analyses is suggested as they are tools that can be used in any future research and development work, starting from the results obtained from the work carried out in this thesis.

Part I – Exergy as a measure of energy quality

Energy, environment and sustainable development

It is widely acknowledged that modern energy systems should embrace in their design the concerns of energy security, sustainability and affordability, as suggested by the United Nations Sustainable Development Goal 7, aiming at *ensuring access to affordable, reliable, sustainable, and modern energy for all*. The world is making progress towards Goal 7, with some encouraging signs that energy is becoming more sustainable and widely available: access to electricity in poorer countries has begun to accelerate, energy efficiency continues to improve, and renewable energy is making impressive gains in the electricity sector. Nevertheless, despite significant progress over the past decade, we are still falling short in providing affordable, reliable, sustainable and modern energy for all.

Clean and sustainable energy should be at the heart of the COVID-19 response and of efforts to combat climate change as, as we know, energy is the dominant contributor to climate change, accounting for around 60 per cent of total global greenhouse gas emissions (UN, 2021). Sustainable development requires a supply of energy resources that is available at reasonable cost and causes no or minimal negative societal impacts. Environmental concerns are also a major issue, as activities that degrade the environment cannot be considered sustainable. Clearly, limitations on sustainable development due to environmental emissions can be overcome in part through increased efficiency, as this usually leads to less environmental impact for the same services or products. There is a strong need to place efforts on meeting the environmental and energy efficiency requirements and drive for better sustainable development. This requires careful considerations of the energy crisis and environmental concerns by dwelling on potential solutions.

In this regard, the importance of renewable energy sources has been gradually increasing for cleaner applications. The share of renewable energy in total final energy consumption increased gradually from 16,4% in 2010 to 17,1% in 2018. However, the share of modern renewable sources in total final energy consumption rose by only 2,5% in a decade, remaining below 11% in 2018. The pandemic, also, is having a mixed impact on renewable energy development across end-use sectors: global electricity demand declined by 2% in 2020 compared to 2019, but the use of renewables for power generation increased by almost 7% year on year. International financial flows to developing countries in support of clean and renewable energy reached \$14 billion in 2018, 35% lower than in 2017 but 32% higher than in 2010. Hydropower projects received 27% of flows in 2018, while projects relating to solar received 26%, geothermal 8%, wind 5% and multiple or other renewable energies 34%.

The diversity of energy choices is but one reason why exergy plays a key role in the context of sustainable development. Ideally, a society seeking sustainable development utilizes only energy resources that cause no environmental impact. Such a condition can be attained or nearly attained by using energy resources in ways that cause little or no wastes to be emitted into the environment, and/or that produce only waste emissions that have no or minimal negative impact on the environment. This latter condition is usually met when relatively inert emissions that do not react in the environment are released, or when the waste emissions are

in or nearly in equilibrium (thermal, mechanical, and chemical) with the environment, that is, when the waste exergy emissions are minimal.

However, all resource use leads to some degree of environmental impact. A direct relation exists between exergy efficiency - and sometimes energy efficiency - and environmental impact, in that through increased efficiency, a fixed level of services can be satisfied with less energy resources and, in most instances, reduced levels of related waste emissions. Exergy is the quality of a flow of energy or matter that represents the useful part of the energy or matter, and it can be considered the confluence of energy, environment, and sustainable development.

Exergy methods can be used to improve sustainability. For example, in a study on thermodynamics and sustainable development (Cornelissen, 1997) it has been pointed out that one important element in obtaining sustainable development is the use of exergy analysis. By noting that energy can never be lost, as it is conserved according to the First Law of Thermodynamics, while exergy can be lost due to internal irreversibilities, that study suggests that exergy losses, particularly due to the use of non-renewable energy forms, should be minimized to obtain sustainable development. Further, the study shows that environmental effects associated with emissions and resource depletion can be expressed in terms of one exergy-based indicator, which is founded on physical principles.

Figure 1 illustratively presents the relation between exergy and sustainability and environmental impact. There, sustainability is seen to increase and environmental impact to decrease as the process exergy efficiency increases. The two limiting efficiency cases are significant. First, as exergy efficiency approaches 100%, environmental impact approaches zero, since exergy is only converted from one form to another without loss, either through internal consumptions or waste emissions. Also, sustainability approaches infinity because the process approaches reversibility. Second, as exergy efficiency approaches 0%, sustainability approaches zero because exergy-containing resources are used but nothing is accomplished. Also, environmental impact approaches infinity because, to provide a fixed service, an ever-increasing quantity of resources must be used and a correspondingly increasing number of exergy-containing wastes are emitted (Dincer & Rosen, 2013).

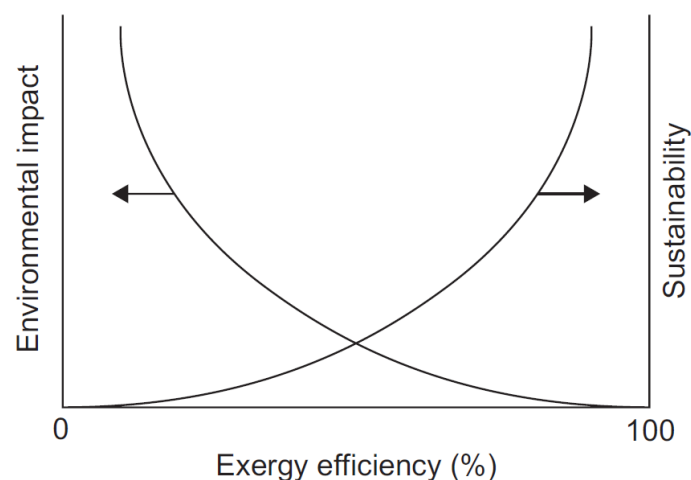


Figure 1 - Qualitative illustration of the relation between the environmental impact and sustainability of a process and its exergy efficiency (Dincer & Rosen, 2013)

Some important contributions that can be derived from exergy methods for increasing the sustainability of development, which is non-sustainable, are presented in Figure 2. Development typical of most modern processes, which are generally non-sustainable, is shown at the bottom of the figure. A future in which development is sustainable is shown at the top of the figure, while some key exergy-based contributions toward making development more sustainable are shown, and include increased exergy efficiency, reduction of exergy-based environmental degradation, and use of sustainable exergy resources.

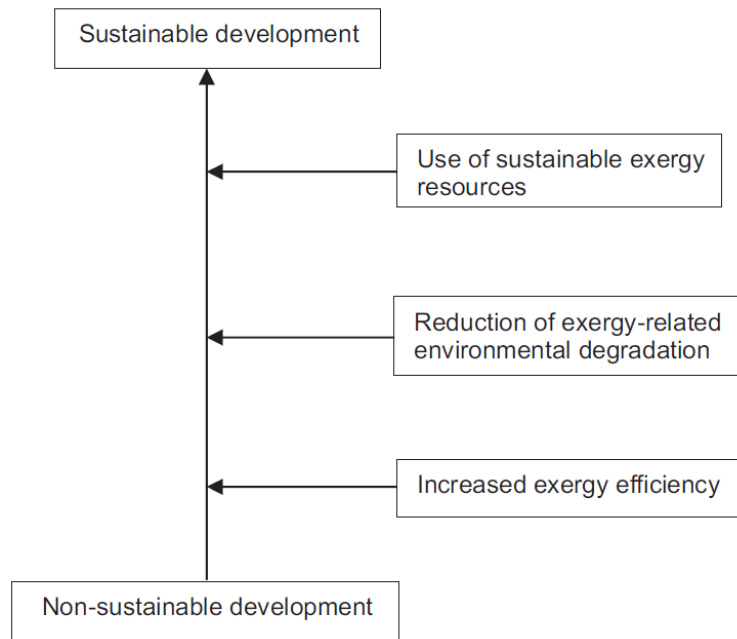


Figure 2 - Some key contributions of exergy methods to increase the sustainability of non-sustainable systems and processes (Dincer & Rosen, 2013)

An energy system is normally designed to work under various conditions to meet different expectations, not only regarding the technical load, but also the environment and, more generally, social expectations. Among the various environmental tools available to study an energy system, like the Life Cycle Assessment, the Environmental Impact Assessment or the Risk Assessment, there is the exergy analysis. It is, in fact, found that using the exergy concept to estimate the consumption of physical resources can improve the quality of the data necessary for LCA. The thermodynamic approach to LCA and design accounts for economic and ecological inputs and services and the impact of emissions.

The results of exergy analyses of processes and systems have direct implications on application decisions and on research and development directions. Further, exergy analyses provide more insights than energy analyses into the “best” directions for R&D effort. Here, best is loosely taken to mean “most promising for significant efficiency gains.” There are two main reasons for this statement:

Exergy losses represent true losses of the potential that exists to generate the desired product from the given driving input. This is not true in general for energy losses. Thus, if the objective is to increase efficiency, focusing on exergy losses permits R&D to focus on reducing losses that will affect the objective;

Exergy efficiencies always provide a measure of how nearly the operation of a system approaches the ideal, or theoretical upper limit. In general, this is not true for energy efficiencies. By focusing R&D effort on those plant sections or processes with the lowest exergy efficiencies, the effort is being directed to those areas that inherently have the largest margins for efficiency improvement. By focusing on energy efficiencies, on the other hand, one can expend R&D effort on topics for which little margins for improvement, even theoretically, exist.

Exergy analysis results typically suggest that R&D efforts should concentrate more on internal rather than external exergy losses, based on thermodynamic considerations, with a higher priority for the processes having larger exergy losses. Although this statement suggests focusing on those areas for which margins for improvement are greatest, it does not indicate that R&D should not be devoted to those processes having low exergy losses, as simple and cost-effective ways to increase efficiency by reducing small exergy losses should certainly be considered when identified. Of course, application and R&D allocation decisions should not be based exclusively on the results of energy and exergy analyses, even though these results provide useful information to assist in such decision making: other factors must be considered also, such as economics, safety, and social and political implications. Further, as energy policies increasingly play an important role in addressing sustainability issues and a broad range of local, regional, and global environmental concerns, policy makers also need to appreciate the exergy concept and its ties to these concerns (Dincer & Rosen, 2013).

Myron Tribus and Edward C. McIrvine (Tribus & McIrvine, 1971) already suggested that performing exergy – at the time named *Evans essergy* after Robert B. Evans, Ph.D. at the Georgia Institute of Technology devoted to the topic - analyses of the natural processes occurring on the Earth could form a foundation for ecologically sound planning, because it would indicate the disturbance caused by large-scale changes.

Rosen and Dincer (Rosen & Dincer, 1997) also noted that a relationship between exergy and environmental impact can be seen in resource degradation, as it is a form of environmental damage, basing their definition of resource on Kestin (Kestin, 1980) who defined a resource as a material, found in nature or created artificially, which is in a state of disequilibrium with the environment, and notes that resources have exergy because of this disequilibrium.

$$S_o = \frac{E + P_o V - \sum \mu_{io} N_i}{T_o}$$

$$I = \frac{E + P_o V - T_o S - \sum \mu_{io} N_i}{T_o}$$

$$T_o I = E + P_o V - T_o S - \sum \mu_{io} N_i$$

THREE EQUATIONS show the derivation of the concept of thermodynamic information. The top equation is based on classical thermodynamics: S_o is the uncertainty when energy (E), volume (V) and the number of moles of various chemical species (N_i) are unrecognizable because they are distributed in an environment at a temperature T_o , a pressure P_o and chemical potentials μ_{io} . The middle equation is derived from the top one on the basis of the relation $I = S_o - S$, where I is information and S is the uncertainty about the system formed with energy E , volume V and composition N_i , and the system is now discernible from the environment. These equations were derived by Robert B. Evans, now at the Georgia Institute of Technology, in 1969. He showed that a new quantity obtained by multiplying the middle equation by T_o is the most general measure of disequilibrium or "potential work." Evans has named this new quantity "essergy" (for the essential aspect of energy).

186

© 1971 SCIENTIFIC AMERICAN, INC

Thermodynamic information is defined as the difference between two entropies: $I = S_o - S$. S refers to the entropy of a system of given energy, volume and composition. S_o is the entropy of the same system of energy, volume and composition when it is diffused into (indistinguishable in) a referenced environment. It measures the loss of information in not being able to distinguish the system from its surroundings (as when an iceberg melts in the open sea).

The idea of using thermodynamic information as a generalized measure of the "availability" of energy was first put forward tentatively by Evans in 1965. (Although heat energy, mechanical energy and chemical energy can be converted into one another, they are not equally "available" to do work. What we call Carnot efficiency and Gibbs free energy were invented to deal with the availability of energy.) By 1969 Evans submitted his doctoral dissertation containing an entirely classical proof that a new quantity, obtained by multiplying his formula for thermodynamic information by an appropriate reference temperature, has most unusual properties. Evans has called this new function "essergy," for the essential aspect of energy [see illustration at left]. He has demonstrated that essergy is a unique measure of "potential work." Moreover, it incor-

Figure 3 - Frame taken from the article *Energy and Information*, published in 1971, dealing with the concept of "essergy" (Tribus & McIrvine, 1971)

According to the above-mentioned studies, some principal general approaches exist to reduce the environmental impact associated with resource degradation:

Increasing efficiency. Increased efficiency preserves exergy by reducing the exergy necessary for a process, therefore reducing environmental damage. Increased efficiency also usually reduces exergy emissions which also play a role in environmental damage;

Using external exergy resources like solar energy. The earth is an open system subject to a net influx of exergy from the sun. It is the exergy delivered with solar radiation that is valued; all the energy received from the sun is ultimately radiated out to the universe. Environmental damage can be reduced by taking advantage of the openness of the earth and utilizing solar radiation instead of degrading resources found in nature to supply exergy demands.

In view of this, a possible strategy to be implemented in policy making is to rely more and more on energy coming from the solar source.

Renewables to avoid resource degradation

As already stated, among renewable energy sources, solar energy has great potential to produce energy in a sustainable way. Environmental damage can be reduced by utilizing solar radiation, that means to lower exergy degradation. Among solar-based technologies, concentrated solar power has a great potential. CSP is a thermal technology that utilizes reflecting surfaces, such as mirrors, to concentrate solar radiation energy and transfer it to a heat transfer fluid, which further drives a thermodynamic engine, such as steam turbine or Stirling engine, coupled to a generator to produce electrical power. The concentrating systems can be line-focusing (parabolic trough and linear Fresnel) or point-focusing (solar tower and parabolic dish). This kind of superiority with respect to other RES technologies happens since CSP keeps a downstream conversion section almost close to the present conventional type, that of a common thermoelectric plant. Simply, conventional combustion is replaced by concentrated solar energy.

Furthermore, there is a growing number of research on the hybridization of renewable energy technologies with poly-generation systems, of which solar energy, biomass, and biofuels are the main sources. As a result, they are regarded as promising solutions, regardless of the lack of continuous energy production within 24 hours a day, which can be solved using several hybrid energetic sources. For example, combining geothermal and solar energy takes advantage of both technologies, because solar energy is inherently alternative, while geothermal energy can provide the baseload power.

Solar energy is a great option for hybridization due to its many advantages (IRENA, 2020):

it is a free and inexhaustible energy resource;

it contributes to the diversification of the energy supply;

it reduces non-renewable primary energy consumption;

it has very low or zero greenhouse gas emissions during the operation of the system;

it presents a growing economic viability and wide social acceptance.

There are several technology options within CSP whose selection is generally based on the power capacity and operating temperatures involved in a system. While conventional power blocks such as steam Rankine and air Brayton cycles are suited for large-scale CSP capacities – in the MW-scale - the solar organic Rankine cycle permits operation at lower temperatures and offers workable efficiencies even at decentralized capacity levels, ranging from a few kW up to a few MW. Also, low-grade thermal energy is attaining a renewed relevance: it is generally at disposal at temperatures up to 300 °C, readily available in thermal processes, combustion exhausts, cooling or condensing systems, as well as from equipment such as compressors. It also exists in nature, in geothermal form or as solar irradiation. There is a wide range of technologies and design options for the recovery of LGTE for power production and combined heat and power applications. Suitable thermodynamic cycles exactly include organic Rankine cycle. ORC power systems make use of an organic working fluid with high molar weight, flowing in a cycle whose peak temperatures range between 250-350 °C. These low operating temperatures make the

technology suitable for applications where use of water/steam as a working fluid becomes inefficient and uneconomical (Tchanche, Petrissans, & Papadakis, 2014).

When the temperature level of the heat sources has a low-to-medium value, an ORC is especially useful to produce mechanical work or electricity due to their potential to operate with a relatively high energy efficiency (Borunda, Jaramillo, Dorantes, & Reyes, 2016). Compared to steam at the same pressure levels, organic fluids are characterized by lower evaporation and condensation temperatures, which have substantial implications (Macchi & Astolfi, 2016). The heat supplied to the ORC in the evaporator can be produced externally, which favors the combination of different heat sources, such as solar field and biomass boiler (Bellos, Vellios, Theodosiou, & Tzivanidis, 2018) and solar field and geothermal well (Buonomano, Calise, Palombo, & Vicidomini, 2015).

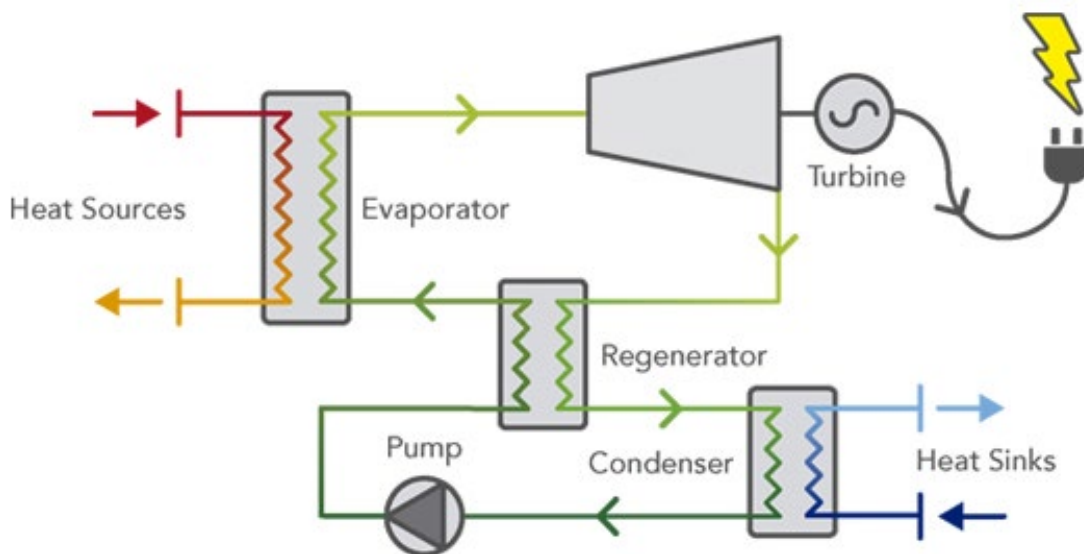


Figure 4 - Schematics of a regenerative organic Rankine cycle (Rank®, 2019)

Also, for the case of CSP, ORCs enable a substantial cost reduction in the solar field which is, by large, the dominant cost driver (Casati, Galli, & Colonna, Thermal energy storage for solar-powered organic Rankine cycles engines, 2013). This cost reduction comes from the lower temperature heat transfer fluid, as opposed to those employed in state-of-the-art steam turbine power plants, and from the possibility to use linear Fresnel collectors in lieu of the more expensive parabolic troughs or tower-heliostat technologies (Cocco & Serra, 2015); (Cau & Cocco, 2014). For the cited reasons, Organic Rankine Cycles are preferred to steam cycles in small scale solar thermal applications (Casati, Galli, & Colonna, Thermal energy storage for solar-powered organic Rankine cycles engines, 2013).

Over the years, ORC systems have gained a moderate level of maturity and reliability, allowing heat recovery from different sources. Although ORCs are characterized by rather low efficiencies, typically in the range of 8–12% (Schuster, Karellas, Kakaras, & Spliethoff, 2009), they are particularly viable for small-scale unsupervised power generation systems: ORC exhibits great flexibility, high safety, good reliability, and simplicity. Absence of fuel cost, improved reliability and low maintenance may also contribute to making ORCs commercially attractive (Nishith & Bandyopadhyay, 2009). Compared with the steam Rankine cycle, the ORC is scalable to smaller unit sizes and higher efficiencies during cooler ambient temperatures, immune from

freezing at cold winter nighttime temperatures, and adaptable for conducting semi-attended or unattended operations (Prabhu, 2006). In the case of a dry fluid, ORC can be employed at lower temperatures without requiring superheating. This results in a practical increase in efficiency over the use of the cycle with water as the working fluid (Andersen & T.J., 2005). Feasibility of the ORC technology is reinforced by high technological maturity of majority of its components, spurred by extensive use in refrigeration applications (Quoilin & Lemort, 2009).

Exergy aspects of CSP-driven ORCs: Literature review

A large number of researchers have worked on the above-mentioned issues, focusing on concentrating solar plants and organic Rankine cycle units. Although initially the greatest interest in this type of plant was mainly linked to the purpose of water desalination, in recent years distributed energy systems have drawn much attention due to their small-scale capacity, flexibility and high efficiency, and only in the last ten years a number of researchers have worked on improving the applications of organic Rankine cycles using renewable energy for electricity generation, from an exergy analysis point of view.

In most of the cases, however, such a type of system is considered as hybridized, that is to say that the solar energy system is assisted by another renewable energy system, which is able to ensure a continuous energy baseload, overcoming the intermittences of the solar source. Concentrated solar power is, indeed, found to be well suited to regions with good direct-solar irradiance conditions, but less so when diffuse irradiation accounts for a significant fraction of the total solar resource. Therefore, CSP is considered a good option for hybridization, as it has good summer performance but poor performance at low solar radiation levels, therefore offering promising options for integration during winter or during the night, and since geothermal and biomass are among the most dispatchable of all renewable energy resources, their suitability for hybridization with solar systems in ORC plants are widely studied.

Back in 2011, (Al-Sulaiman, Dincer, & Hamdullahpur, 2011) performed an exergy modeling of a novel trigeneration system using parabolic trough solar collectors and an organic Rankine cycle. The exergy efficiencies and exergy destruction rates were examined under the variation of the ORC evaporator pinch point temperature, ORC pump inlet temperature, and turbine inlet pressure. The study revealed that such a system had a higher exergy efficiency in comparison with the electrical and heating cogeneration as well as the cooling cogeneration. Moreover, this study showed that the main sources of exergy destruction rate were the solar collectors and ORC evaporators.

In 2014, in their *Off-design performance analysis of a solar-powered organic Rankine cycle* (Wang, Yan, Zhao, & Dai, 2014), the authors performed an off-design model of an organic Rankine cycle driven by solar energy with compound parabolic collector to collect the solar radiation and thermal storage unit to achieve the continuous operation of the overall system. The system off-design behavior was examined under the change in environment temperature, as well as thermal oil mass flow rates of vapor generator and CPC, over a whole day and in different months. The system obtained the maximum average exergy efficiency in December and the maximum net power output in June or in September, and both the net power output and the average exergy efficiency reached minimum values in August.

In the same year, (Al-Sulaiman, 2014) described a detailed exergy analysis of selected thermal power systems driven by parabolic trough solar collectors. Al-Sulaiman reported some exergetic parameters: exergetic efficiency, exergy destruction rate, fuel depletion ratio, irreversibility ratio, and improvement potential. He concluded that parabolic trough solar collectors were the main source of the exergy destruction in which more than 50% of the solar inlet exergy was destructed. This value accounted for around 70% of the total exergy destructed. The evaporator was another source of exergy destruction in which around 13% of the solar inlet exergy was

deconstructed. This value accounted for around 19% of the total exergy destructed in the system. The overall exergetic improvement potential of the systems was estimated to be around 75%.

Still in 2014, (Al-Ali & Dincer, 2014) examined the combination of solar parabolic trough collector and geothermal energy for electricity, cooling, space heating, hot water and industrial heat. A parametric study was conducted to investigate the effects of operating conditions and environment parameters on the system performance. The examined system included absorption chiller, ORCs and heat exchangers and it performed 78% energetically and 36,6% exergetically. The results showed that 75% of the exergy destruction on the system took place in the solar collectors.

In the same year (Suleman, Dincer, & Agelin-Chaab, 2014) examined a new integrated, solar and geothermal energy-based system for multigeneration applications, which comprises two ORCs for power generation, an absorption chiller cycle for cooling production and a drying system to dry wet products. In addition, some useful heat was recovered from the condensers of the ORC for heating applications. The overall energy and exergy efficiencies of the system were found to be 54,7% and 76,4%, respectively. Moreover, to analyze the system efficiently, parametric studies were also performed to observe the effects of different substantial parameters, namely inlet pressure and temperature of the ORC turbine, and reference environment temperature, in order to investigate the variations in the system performance in terms of the energy and exergy efficiencies.

In 2015, (Grosu, Marin, Dobrovicescu, & Queiros-Conde, 2015) used exergy analysis to evaluate the performance of a combined cycle: organic Rankine cycle and absorption cooling system using LiBr–H₂O, powered by a solar field with linear concentrators. Solar ACS was combined with the ORC system—its coefficient of performance was depending on the inlet temperature of the generator which was imposed by the outlet of the ORC. The ORC components, listed from the most to the least exergetic efficient were: pump, turbine, hot heat exchanger and condenser. Thus, a way to improve the performance of this system was to add a recovery heat exchanger at the inlet of the condenser, because of its high exergy dissipation.

Also in 2015, (Boyaghchi & Heidarnejad, 2015) proposed a novel micro solar Combined Cooling, Heating and Power (CCHP) cycle integrated with Organic Rankine Cycle (ORC) for summer and winter seasons. A thermal storage tank was installed to correct the mismatch between the supply of the solar energy and the demand of thermal source consumed by the CCHP subsystem, thus the desired system could continuously and stably operate. For summer mode, the thermal efficiency and exergy efficiency were found to be 23,66% and 9,51%, while for winter mode 48,45% and 13,76%. Five key parameters, namely turbine inlet temperature, turbine inlet pressure, turbine back pressure, evaporator temperature and heater outlet temperature were selected as the decision variables to examine the performance of the overall system.

Also in 2015, (Hassoun & Dincer, 2015) examined a solar driven, ORC-based multi-generation system for electricity, fresh-hot water, seasonal heating and cooling production with final exergetic efficiency close to 14%. This system was a complex system with ORC, absorption chiller, storage tanks and batteries. A comprehensive thermodynamic analysis through energy and exergy, and a parametric study to assess the sensitivity and improvements of the overall

system was conducted. Furthermore, exergo-economic analysis and a follow-up optimization study for optimizing the total system cost to the overall system efficiency were carried out.

In the same 2015 year, (F., Dincer, Rosen, & ., 2015) examined the use of a central solar receiver with ORCs, absorption chiller and gas turbine for producing power, cooling, hot water and heated air. Energy and exergy analyses were used to assess the performance of the cycle, and the effects of various system parameters on energy and exergy efficiencies of the overall system and its subsystems were examined. The overall energy and exergy efficiencies of the system were found to be 66,5% and 39,7% respectively. Furthermore, the effect was also investigated of reference-environment temperature on energy and exergy efficiencies for the system, when operated only on biomass and solar energy. This system was found to have 39.7% exergy efficiency and 66.5% energy efficiency.

At the same time, (Karellas & Braimakis, 2015) investigated a domestic trigeneration system capable of combined heat and power production and refrigeration, based on the joint operation of an Organic Rankine Cycle and a Vapor Compression Cycle. The ORC expander, VCC compressor and electricity generator were connected to the same shaft. The condensation of both cycles took place under a common pressure in a single condenser. A biomass boiler together with a module of Parabolic-Trough Collectors (PTC) provided heat to the ORC via two distinct intermediate pressurized water circuits. In trigeneration mode (summer operation), a portion of the power produced by the ORC expander was consumed by the VCC compressor, while any surplus power was converted to electricity. The heat generated in the condenser of the system was used to meet hot water demand. In cogeneration mode (winter operation) the VCC was disconnected, since no refrigeration was necessary. They found the system exergy efficiency to be 7%, the payback period to be close to 7 years and the IRR to be 12%.

In 2016, in (Borunda, Jaramillo, Dorantes, & Reyes, 2016) it was presented a study of a small CSP plant coupled to an ORC with a novel configuration since useful energy was directly used to feed the power block and to charge the thermal storage. The results showed that the system was a promising option for applications to medium temperature processes where electrical and heat generation was required. It was found that the energy and exergy efficiencies of the thermal storage systems decreased as the solar fraction increased. Likewise, the energy and exergy efficiencies of the solar- ORC power plant decreased as the incident solar radiation increased. On the other hand, the overall system efficiency was increased by using waste heat as a heat source. The energy recovery was close to 55% and the global efficiency enhanced.

In the same year (Javaherdeh, Amin Fard, & Zoghi, 2016) simulated the organic Rankine cycle (ORC) in order to generate electricity and hot water with the simultaneous stimulation of geothermal and solar energy, and evaluated from an energy, exergy and exergo-economic standpoint. In this configuration, 90 °C geothermal fluid was used for pre-heating and 150 °C solar fluid was used for super heating the organic fluid. The heat exchanger in the condenser was also used to produce hot water. The simulation results showed that at the base state, the efficiency of energy and exergy were 0,566 and 0,156, respectively. Solar collectors, evaporators and organic cycle condensers had the highest initial cost and exergy destruction from an exergo-economic perspective. The results of parametric analysis indicated that evaporator temperature had a positive effect on cycle performance and increased electrical efficiency and reduced

irreversibility, and increasing the pinch temperature has a negative effect on system performance.

Then, in 2016 solar, geothermal and wind energy are the renewable energy sources utilized by the system in (Khalid, Dincer, & Rosen, 2016). In this case, wind turbine gave electricity to a green building, while solar and geothermal energy fed a trigeneration system. In this system, solar energy feeds an ORC for electricity production and an absorption chiller for cooling production. The condenser of the ORC was cooperating with a geothermal field in a heat pump for heating production. The results proved 46,1% energetic efficiency and only 7,3% exergetic performance.

Finally, in 2016 the combination of a poly-generation system with geothermal and solar energy has been performed by (Calise, Dentice d'Accadia, Macaluso, Piacentino, & Vanoli, 2016). This system was designed for producing heating, cooling, electricity, and fresh water. The hybrid system was equipped with an Organic Rankine Cycle fueled by medium-enthalpy geothermal energy and by a Parabolic Trough Collector solar field. Geothermal brine was also used for space heating and cooling purposes. Finally, geothermal fluid supplied heat to a Multi-Effect Distillation unit, producing also desalinized water from seawater. The core of the examined system was an ORC which was fed by the heat sources. The authors of this work found the exergy efficiency to be up to 50% in the thermal recovery mode, up to 20% in the cooling mode and the simple payback period to be close to 5 years.

Next, in 2017, (Fontalvo, et al., 2017) combined thermodynamic optimization and economic analysis to assess the performance of single and dual pressure ORC operating with different organic fluids and targeting small-scale applications. The following conclusion was established: there were higher exergy destruction and lower exergy efficiency rates when net power was optimized as compared to the case in which thermal efficiency was optimized. The inclusion of the regenerative heat exchanger reduced the exergy destruction and increased the exergy efficiency, but dual pressure ORC was the configuration with the lowest exergy efficiency and the highest exergy destruction, especially at higher temperatures, where the working fluid was superheated.

Still in 2017, (Cocco, Petrollese, & Tola, 2017) investigated the use of concentrating solar technologies for supplying heat and power in industrial processes. The thermal energy produced by a solar field was stored in a TES system and subsequently used in a Heat and Power Generation (HPG) section. In particular, three different HPG configurations were analyzed. The electricity was generated in an Organic Rankine Cycle (ORC) unit while the heat was supplied by a heat generator placed in parallel or downstream of the ORC unit or by recovering the ORC waste heat. An exergy analysis was carried out and the plant exergy efficiency was chosen as marker to evaluate the best configuration. The use of the ORC waste heat was an interesting option for the hot water production, but it required the full use of available heat to avoid significant exergy degradations.

In the same 2017 year, a solar driven trigeneration system was investigated and optimized in energetic and exergetic terms (Bellos & Tzivanidis, 2017). Parabolic Trough collectors (PTC) were used for supplying the demanded heat input in the present configuration which included a storage tank, an Organic Rankine Cycle (ORC) module and an absorption heat pump operating

with the LiBr-H₂O working pair. The heat source from solar collectors drove the ORC which rejected heat to the generator of the absorption heat pump. This heat pump produced heating and cooling demand simultaneously, while electricity was produced from the ORC. The inlet temperature in the heat recovery system, the superheating, the maximum pressure in ORC, the heat rejection temperature of ORC, the evaporating temperature of the heat pump, as well as the solar beam irradiation were the examined parameters. According to the final results, toluene was the working fluid which leads to maximum exergetic output with n-octane and MDM to follow with 29,42%, 28,50% and 28,35% respectively.

Still in 2017, the ORC system driven by industrial low-temperature waste heat was analyzed and optimized by (Sun, Yue, & Wang, 2017). The impacts of the operational parameters, including evaporation temperature, condensation temperature, and degree of superheat, on the thermodynamic performances of ORC system were conducted, with R113 used as the working fluid. In addition, the ORC-based cycles, combined with the Absorption Refrigeration Cycle (ARC) and the Ejector Refrigeration Cycle (ERC), were investigated to recover waste heat from low temperature flue gas. The uncoupled ORC-ARC and ORC-ERC systems could generate both power and cooling for external uses. The exergy efficiency of both systems decreased with the increase of the evaporation temperature of the ORC. The net power output, the refrigerating capacity and the resultant exergy efficiency of the uncoupled ORC-ARC were all higher than those of the ORC-ERC for the evaporation temperature of the basic ORC >153 C, in the investigated application. Finally, suitable application conditions over other temperature ranges were also given.

Then in 2018 the objective of the work by (Bellos, Vellios, Theodosiou, & Tzivanidis, 2018) was the investigation of a poly-generation system which was driven by solar energy and a biomass boiler. Parabolic trough solar collectors coupled to a storage tank were used to produce useful heat at high-temperature levels (~350 °C). The system included an organic Rankine cycle and a vapor compression cycle for electricity and cooling to be produced respectively. Moreover, useful heat was produced at two temperatures levels (50 °C and 150 °C) and so there were totally four useful energy outputs. The system was optimized in steady-state conditions and then the most suitable design was investigated in dynamic conditions for all the year period. According to the results, the yearly energetic efficiency of the system was 51,26% while the yearly exergetic efficiency was 21,77%. Finally, the results of this work indicated that the suggested configuration could provide various useful outputs with high efficiency and the total investment was characterized as viable due to the suitable financial index values.

Still in 2018, within their two papers (Singh & Mishra, 2018); (Singh & Mishra, 2018) the researchers conducted their studies on combined S-CO₂ cycles and ORC-ORC cooperated as a low temperature cycle to recover waste heat from those cycles. In the first paper the authors carried out an energy and exergy analysis on the model of integrated solar PTSCs, combined with the simple recuperated S-CO₂ cycle and the ORC as a bottoming cycle. They concluded that the system's exergetic and energetic efficiency increased with solar irradiation. In the second work, indeed, they investigated the thermal performance of the solar operated combined recompression S-CO₂ and ORC as a bottoming cycle. They found that the combined system's thermal and energy efficiency increased with solar radiation and turbine inlet pressure. R123 and R290 showed the best and worst thermal performance of the system. In addition, they also

concluded that the solar collector was responsible for the maximum exergy destruction of the system.

In 2020, (Khan & Mishra, 2020) presented a thermodynamic analysis of the combined partial heating supercritical CO₂ (PSCO₂) cycle and ORC. The effects of the parabolic trough collectors (PTSCs) on the combined cycle performance were further examined. Without considering the performance of the PTSCs, the highest exergy and thermal efficiency of the combined cycle using R1233 was achieved by 83,26% and 48,61%, respectively at 950 W/m² of solar irradiation while considering the performance of PTSCs, the combined cycle achieved exergy efficiency by 42,31% because PTSCs alone accounted for 62,93% of the total exergy destruction. One of the other conclusions obtained from the results was that the highest solar incidence angle was responsible for poor system performance.

In the same year, (Alibaba, Pourdarbani, Khoshgoftar Manesh, Valencia Ochoa, & Duarte Forero, 2020) proposed the combined energy-exergy-economic-environmental analysis as the optimization method. First, optimal design of thermodynamic, exergo economic and exergo environmental was developed; the geothermal power plant was used as a complement to concentrated solar power (CSP) and then combined energy-exergy-economic-environmental analysis was conducted. A standalone geothermal cycle (first mode), as well as hybrid Geothermal-Solar cycle (second mode) were investigated to generate the heating/cooling power of the building. The close similarity of the results of the exergy and emergo-economic analysis was very interesting. For standalone geothermal cycle, both exergo and emergo-economic analysis implied that highest value (6.02E-04 \$/s and 3.1915Eþ09 sej/s) was related to turbine due to the heat generated by the impact of the blade, and the lowest value was related to ORC condenser. The exergo and emergo-economic analysis for geothermal-solar hybrid cycle, due to the increase in refrigerant pressure drop inside the coil, the evaporator (4.50E-03 \$/s and 4.4699Eþ09 sej/s) and turbine (2.40E-03 \$/s and 2.1920Eþ09 sej/s) had the highest amount. Also, for standalone cycle, exergo and emergo-environmental implied that ORC turbine had the highest value of 1.26E-06 pts/s and 9.7201Eþ09sej/s. For hybrid geothermal-solar cycle, the evaporator (3.77E-06 pts/s and 6.1814Eþ08sej/s) and turbine (3.27E-06 pts/s and 6.37Eþ08 sej/s) had the highest amount of exergo and emergo-environmental.

In 2021, (Sinac & Jianu, 2021) analyzed a power generation system involving a solar-powered organic Rankine cycle (ORC) with an intermediate thermal energy storage (TES) and complete flashing cycle (CFC). The system had better dispatchability over conventional power production methods as well as a simplified overall plant layout. The focus of this paper was to complete an energy and exergy analysis of each component of the system to identify locations of irreversibilities or losses and quantify them. Multiple parametric studies and performance improvements were also completed whereby optimal operating temperatures were chosen, to maximize the system's performance. Assumptions necessary for the analyses were stated and justified with a presentation of the findings. A discussion of the parametric studies and system alterations proposed potential improvements on the system regarding reduced exergy destruction and improved overall energy and exergy efficiencies.

Finally, (Zarei, Akhavan, Babaie Rabiee, & Elahi, 2021) proposed a novel poly-generation system powered by two solar sources. Photovoltaic thermal and parabolic trough collectors were used in a series configuration with water as working fluid for this purpose. The proposed system was

equipped with an ejector - compression refrigeration cycle (VCRC) with two different temperature levels (above zero and sub-zero) and an organic Rankine cycle (ORC) to provide cooling, heating, and power. The water out coming from the photovoltaic thermal (PVT) unit was used to cool the VCRC condenser, and hence it was preheated before entering the parabolic trough collector (PTC) resulting in reduced sizing and the cost of the PTC unit. In this study, the impact of parameters such as water flow rate in PVT-PTC circuit, the effect of working fluid in the ORC cycle, and solar irradiation were investigated using the first and second laws of thermodynamic and economic analysis. The results showed that in the same conditions, R123, R600, R245fa, R600a refrigerants have higher energy efficiency, respectively, so that the highest energy efficiency of 70,78% and exergy efficiency of 10,70% were calculated for R123 refrigerant. Furthermore, it was shown that the highest energy and exergy efficiency cannot be achieved together.

As it can be seen from the literature review, many configurations for highly efficient energy systems exist by combining different energetic devices. In the last ten years a lot of research has been focused on coupling different power systems. The basic idea was based on utilizing the rejected heat of the power cycles to feed another power unit. Moreover, other useful outputs as industrial heat, dried products and hydrogen can be produced in multigeneration systems.

Also, despite the numerous research papers published only in the past decade, most of the work was restricted to the theory, mainly focusing on mathematical modeling and feasibility study. The ongoing focus on the theory with little advances on the practical side leaves doubts about engineering and practical limitations of these concepts, meaning there was a lack of a suitable cost-effective technology ready for mass production. In that sense, it was more and more important to look at these technical solutions through the lens of an exergy analysis.

In the light of what has just been observed, the work of this thesis places itself in this empty space dedicated to the study of a real, existing system. As already stated, exergy analysis is a valuable tool especially for technicians involved in the research and development area: the results of exergy analyses have direct implications on application decisions and on research and development (R&D) directions. Further, exergy analyses provide more insights than energy analyses into the “best” directions for R&D effort. Here, it is now proposed to use this tool on existing elements, to understand the potential of the system. Rather than designing new and complex energy system *ex novo*, we choose to start from a small concentrating solar system, the core of which is represented by the solar dish concentrator installed on the rooftop of the Politecnico di Torino Energy Center building.

The solar concentrator in question has already been the subject of several master's degree theses, in particular of (Guerriero, 2021), where a small Organic Rankine Cycle was modeled to exploit the energy deriving from the parabolic dish concentrator itself. The cycle has been sized with the Aspen Plus software to produce both electrical and thermal energy in order the expander to generate about 10 kW of electric power, while the thermal power disposed of by the condenser allows to heat a water flow of up to about 80 °C. The cycle has been studied and modeled with 3 different working fluids: two silicone and a commercial fluid. The final configuration of the system provides a pump, an evaporator, an expander, a condenser, and a recuperator to allow preheating the liquid leaving the condenser by recovering part of the sensible heat possessed by the fluid at the outlet from the turbine.

In the next section of this thesis, the thermodynamic theory on which the exergetic analysis is based is illustrated. Then we proceed to conduct the exergetic analysis of the system object of (Guerrero, 2021) already designed and optimized from an energetic point of view in each of its components. Once the results of the exergetic analysis have been obtained, they are discussed and changes are made to the system topology, to make it more realistic. The assumptions made at the basis of the first and second law analysis of thermodynamics are also commented, so as to show the effect of the hypotheses made on the results of the analysis in question. Finally, through an appropriate sensitivity analysis, the exergetic performance of the system is studied as the operating conditions vary.

Part II – Case study

Thermodynamic fundamentals

This chapter aims at providing a theoretical background for understanding exergy concepts. The first and second laws of thermodynamics are described, as the first law places all forms of energy on the same level while the second law establishes a constraint on thermodynamic processes, from which it results that not all energy conversion processes are achievable: exergy combines the first and the second law together, in this way assigning a weighting factor to the various forms of energy, according to their ability to make certain thermodynamic processes feasible. The following discussion is taken from (Dincer & Rosen, 2013).

The First Law of Thermodynamics is the law of the conservation of energy, which states that, although energy can change form, it can be neither created nor destroyed. The FLT defines internal energy as a state function and provides a formal statement of the conservation of energy. However, it provides no information about the direction in which processes can spontaneously occur, that is, the reversibility aspects of thermodynamic processes. For a control mass, the energy interactions for a system may be divided into two parts: dQ , the amount of heat, and dW , the amount of work. Unlike the total internal energy dE , the quantities dQ and dW are not independent of the manner of transformation, so we cannot specify dQ and dW simply by knowing the initial and final states. Hence, it is not possible to define a function Q , which depends on the initial and final states, that is, heat is not a state function. The FLT for a control mass can be written as follows:

$$dQ = dE + dW \quad [1]$$

When Equation 1.1 is integrated from an initial state 1 to a final state 2, it results in the following:

$$Q_{1-2} = E_2 - E_1 + W_{1-2} \quad [2]$$

where E_1 and E_2 denote the initial and final values of the energy E of the control mass, Q_{1-2} is the heat transferred to the control mass during the process from state 1 to state 2, and W_{1-2} is the work done by the control volume during the process from state 1 to state 2. The energy E may include internal energy U , kinetic energy KE , and potential energy PE terms as follows:

$$E = U + KE + PE \quad [3]$$

For a change of state from state 1 to state 2 with a constant gravitational acceleration g , Equation 1.3 becomes the following:

$$E_2 - E_1 = U_2 - U_1 + \frac{m(v_2^2 - v_1^2)}{2} + mg(Z_2 - Z_1) \quad [4]$$

where m denotes the fixed amount of mass contained in the system, V the velocity, and Z the elevation. The quantities dQ and dW can be specified in terms of the rate laws for heat transfer and work. For a control volume, an additional term appears from the fluid flowing across the

control surface (entering at state i and exiting at state e). The FLT for a control volume can be written as the following:

$$\dot{Q}_{cv} = \dot{E}_{cv} + \dot{W}_{cv} + \sum \dot{m}_e \hat{h}_e - \sum \dot{m}_i \hat{h}_i \quad [5]$$

Where \dot{m} is mass flow rate per unit time, \hat{h} is total specific energy equal to the sum of specific enthalpy, kinetic energy, and potential energy, that is $\hat{h} = h + \frac{v^2}{2} + gz$.

The FLT provides no information about the inability of any thermodynamic process to convert heat fully into mechanical work, or any insight into why mixtures cannot spontaneously separate or unmix themselves. A principle to explain these phenomena and to characterize the availability of energy is required to do this. That principle is embodied in the Second Law of Thermodynamics (SLT). The SLT establishes the difference in the quality of different forms of energy and explains why some processes can spontaneously occur while others cannot. It is usually expressed as an inequality, stating that the total entropy after a process is equal to or greater than that before. The equality only holds for ideal or reversible processes. The SLT defines the fundamental quantity entropy as a randomized energy state unavailable for direct conversion to work. It also states that all spontaneous processes, both physical and chemical, proceed to maximize entropy; that is, to become more randomized and to convert energy to a less available form.

A direct consequence of fundamental importance is the implication that at thermodynamic equilibrium, the entropy of a system is at a relative maximum; that is, no further increase in disorder is possible without changing the thermodynamic state of the system by some external means (such as adding heat). A corollary of the SLT is the statement that the sum of the entropy changes of a system and that of its surroundings must always be positive. In other words, the universe (the sum of all systems and surroundings) is constrained to become forever more disordered and to proceed toward thermodynamic equilibrium with some absolute maximum value of entropy.

Although there are various formulations of the SLT, two are particularly well known as follows:

Clausius statement. It is impossible for heat to move by itself from a lower temperature reservoir to a higher temperature reservoir. That is, heat transfer can only occur spontaneously in the direction of temperature decrease. For example, we cannot construct a refrigerator that operates without any work input.

Kelvin-Planck statement. It is impossible for a system to receive a given amount of heat from a high-temperature reservoir and to provide an equal amount of work output. While a system converting work to an equivalent energy transfer as heat is possible, a device converting heat to an equivalent energy transfer as work is impossible. Alternatively, a heat engine cannot have a thermal efficiency of 100%.

The Clausius inequality provides a mathematical statement of the SLT, which is a precursor to SLT statements involving entropy. German physicist R.J.E. Clausius, one of the founders of thermodynamics, stated the following:

$$\oint (\delta Q/T) \leq 0 \quad [6]$$

where the integral symbol \oint shows the integration should be done for the entire system. The cyclic integral of $(\delta Q/T)$ is always less than or equal to zero. The system undergoes only reversible processes (or cycles) if the cyclic integral equals zero, and irreversible processes (or cycles) if it is less than zero.

The previous equation can be expressed without the inequality as the following:

$$S_{gen} = -\oint (\delta Q/T) \quad [7]$$

Where $S_{gen} = \Delta S_{total} = \Delta S_{sys} + \Delta S_{surr}$.

The quantity S_{gen} is the entropy generation associated with a process or cycle, due to irreversibilities. The following are cases for values of S_{gen} :

$S_{gen} = 0$ for a reversible process;

$S_{gen} > 0$ for an irreversible process;

$S_{gen} < 0$ for no process (i.e., negative values for S_{gen} are not possible).

Consequently, one can write for a reversible process as follows:

$$\Delta S_{sys} = (Q/T)_{rev} \quad [8]$$

$$\Delta S_{surr} = - (Q/T)_{rev} \quad [9]$$

For an irreversible process:

$$\Delta S_{sys} > (Q/T)_{surr} \quad [10]$$

Due to entropy generation within the system because of internal irreversibilities. Hence, although the change in entropy of the system and its surroundings may individually increase, decrease, or remain constant, the total entropy change, or the total entropy generation cannot be less than zero for any process.

It is helpful to list some common relations for a process involving a pure substance and assuming the absence of electricity, magnetism, solid distortion effects, and surface tension, as it happens throughout this thesis. The following four equations apply, subject to the noted restrictions:

$\delta q = du + \delta w$ (a FLT statement applicable to any simple compressible closed system);

$\delta q = du + pdv$ (a FLT statement restricted to reversible processes for a closed system);

$Tds = du + \delta w$ (a combined statement of the FLT and SLT, with $Tds = \delta q$);

$Tds = du + pdv$ (a combined statement of the FLT and SLT valid for all processes between equilibrium state).

With the SLT, the maximum work that can be produced can be determined. Exergy is a useful quantity that stems from the SLT and helps in analyzing energy and other systems and processes. The exergy of a system is defined as the maximum shaft work that can be done by the composite of the system and a specified reference environment. The reference environment is assumed to be infinite, in equilibrium, and to enclose all other systems. Typically, the environment is specified by stating its temperature, pressure, and chemical composition. Exergy is not simply a thermodynamic property; it is a property of both a system and the reference environment. The term exergy comes from the Greek words *ex* and *ergon*, meaning from and work. The exergy of a system can be increased if exergy is input (e.g., work is done on it).

Exergy has the characteristic that it is conserved only when all processes occurring in a system and the environment are reversible, while it is destroyed whenever an irreversible process occurs. When an exergy analysis is performed on a plant such as a power station, a chemical processing plant, or a refrigeration facility, the thermodynamic imperfections can be quantified as exergy destructions, which represent losses in energy quality or usefulness (e.g., wasted shaft work or wasted potential for the production of shaft work). Like energy, exergy can be transferred or transported across the boundary of a system. For each type of energy transfer or transport there is a corresponding exergy transfer or transport. Exergy analysis takes into account the different thermodynamic values of different energy forms and quantities, for example, work and heat. The exergy transfer associated with shaft work is equal to the shaft work. The exergy transfer associated with heat transfer, however, depends on the temperature at which it occurs in relation to the temperature of the environment.

Several quantities related to the conceptual exergy of systems and flows are described here.

Exergy of a closed system

The exergy $Ex_{nonflow}$ of a closed system of mass m , or the nonflow exergy, can be expressed as follows:

$$Ex_{nonflow} = Ex_{ph} + Ex_0 + Ex_{kin} + Ex_{pot} \quad [11]$$

$$Ex_{pot} = PE \quad [12]$$

$$Ex_{kin} = KE \quad [13]$$

$$Ex_0 = \sum_i (\mu_{i0} - \mu_{i00}) N_i \quad [14]$$

$$Ex_{nonflow} = (U - U_0) + P_0(V - V_0) - T_0(S - S_0) \quad [15]$$

where the system has a temperature T , pressure P , chemical potential μ_i for species i , entropy S , energy E , volume V , and number of moles N_i of species i . The system is within a conceptual environment in an equilibrium state with intensive properties T_0 , P_0 , and μ_{i00} . The quantity μ_{i0} denotes the value of μ_i at the environmental state (i.e., at T_0 and P_0). The terms on the right side of [11] represent, respectively, physical, chemical, kinetic, and potential components of the

nonflow exergy of the system. The exergy Ex is a property of the system and conceptual environment, combining the extensive properties of the system with the intensive properties of the environment. Physical nonflow exergy is the maximum work obtainable from a system as it is brought to the environmental state (i.e., to thermal and mechanical equilibrium with the environment), and chemical nonflow exergy is the maximum work obtainable from a system as it is brought from the environmental state to the dead state (i.e., to complete equilibrium with the environment).

Exergy of a matter flow

The exergy of a flowing stream of matter Ex_{flow} is the sum of nonflow exergy and the exergy associated with the flow work of the stream (with reference to P_0), i.e.:

$$Ex_{flow} = Ex_{nonflow} + (P - P_0)V \quad [16]$$

Alternatively, Ex_{flow} can be expressed following Equation [11] in terms of physical, chemical, kinetic, and potential components as follows:

$$Ex_{flow} = Ex_{ph} + Ex_0 + Ex_{kin} + Ex_{pot} \quad [17]$$

$$Ex_{pot} = PE \quad [18]$$

$$Ex_{kin} = KE \quad [19]$$

$$Ex_0 = \sum_i (\mu_{i0} - \mu_{i00})N_i \quad [20]$$

$$Ex_{flow,ph} = (H - H_0) - T_0(S - S_0) \quad [21]$$

Exergy of thermal energy

Consider a control mass, initially at the dead state, being heated or cooled at constant volume in an interaction with some other system. The heat transfer experienced by the control mass is Q . The flow of exergy associated with the heat transfer Q is denoted by Ex_Q , and can be expressed as follows:

$$Ex_Q = \int_i^f \left(1 - \frac{T_0}{T}\right) \delta Q \quad [22]$$

Where δQ is an incremental heat transfer, and the integral is from the initial state (i) to the final state (f). This “thermal” exergy is the minimum work required by the combined system of the control mass and the environment in bringing the control mass to the final state from the dead state. Often the dimensionless quantity in parentheses in this expression is called the exergetic temperature factor and denoted τ :

$$\tau = 1 - \frac{T_0}{T} \quad [23]$$

The relation between τ and the temperature ratio $\frac{T}{T_0}$ is illustrated in figure 3.

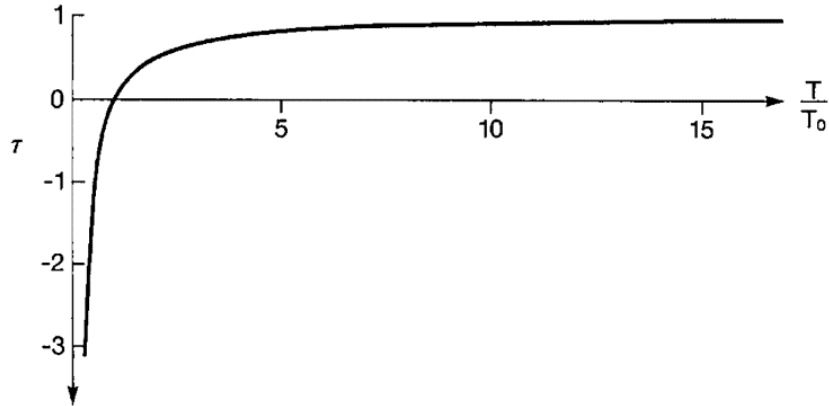


Figure 5 - The relation between the exergetic temperature factor τ and the absolute temperature ratio T/T_0 . The factor τ is equal to zero when $T = T_0$. For heat transfer at above-environment temperatures (i.e., $T > T_0$), $0 < \tau < 1$. For heat transfer at sub-environment temperatures (i.e., $T < T_0$), $\tau < 0$, implying that exergy and energy flow in opposite directions in such cases. Also, the magnitude of exergy flow exceeds that of the energy flow when $\tau < -1$, which corresponds to $T < T_0/2$

If the temperature T of the control mass is constant, the thermal exergy transfer associated with a heat transfer is the following:

$$Ex_Q = \left(1 - \frac{T_0}{T}\right) Q = \tau Q \quad [24]$$

For heat transfer across a region r on a control surface for which the temperature may vary:

$$Ex_Q = \int_r \left[q \left(1 - \frac{T_0}{T}\right) dA \right] r \quad [25]$$

Where q_r is the heat flow per unit area at a region on the control surface at which the temperature is T_r .

Exergy of work

The exergy transfer associated with work done by a system due to volume change is the net usable work due to the volume change and is denoted by W_{NET} . Thus, for a process in time interval t_1 to t_2 :

$$(W_{NET})_{1,2} = W_{1,2} - P_0(V_2 - V_1) \quad [26]$$

Where $W_{1,2}$ is the work done by the system due to volume change ($V_2 - V_1$). The term $P_0(V_2 - V_1)$ is the displacement work necessary to change the volume against the constant pressure P_0 exerted by the environment.

Exergy of electricity

As for shaft work, the exergy associated with electricity is equal to the energy.

Exergy consumption

For a process occurring in a system, the difference between the total exergy flows into and out of the system, less the exergy accumulation in the system, is the exergy consumption I , expressible as follows:

$$I = T_0 S_{gen} \quad [27]$$

Which points out that exergy consumption is proportional to entropy creation, as is known as the Gouy-Stodola relation.

Exergy balance

By combining the conservation law for energy and non-conservation law for entropy, the exergy balance can be obtained as follows:

$$\text{Exergy input} - \text{Exergy output} - \text{Exergy consumption} = \text{Exergy accumulation} \quad [28]$$

Following the physical interpretation of [28], for a non-steady flow process during time interval t_1 to t_2 :

$$\sum_i ex_i m_i - \sum_e ex_e m_e + \sum_r (Ex_{Q_r})_{1,2} - (Ex_W)_{1,2} - (W_{NET})_{1,2} - I_{1,2} = Ex_2 - Ex_1 \quad [29]$$

$$(W_{NET})_{1,2} = W_{1,2} - P_0(V_2 - V_1) \quad [30]$$

$$(Ex_{Q_r})_{1,2} = \int_{t_1}^{t_2} \left[\int_r \left(1 - \frac{T_0}{T_r}\right) q_r dA_r \right] dt \quad [31]$$

$$I_{1,2} = T_0 S_{gen,1,2} \quad [32]$$

$$Ex = \int \rho \xi dV \quad [33]$$

Here, I and S_{gen} , respectively, denote exergy consumption and entropy creation, Ex denotes exergy, and the integral for Ex is performed over the control volume. The first two terms on the left side of [29] represent the net input of exergy associated with matter, the third term represents the net input of exergy associated with heat, the fourth and fifth terms represent the net input of exergy associated with work, and the sixth term represents the exergy consumption. The right side of [29] represents the accumulation of exergy.

For a closed system, [29] simplifies to the following:

$$\sum_r (Ex_{Q_r})_{1,2} - (Ex_W)_{1,2} - (W_{NET})_{1,2} - I_{1,2} = Ex_2 - Ex_1 \quad [34]$$

When volume is fixed, $(W_{NET})_{1,2} = 0$ in Equations [29] and [34]. Also, when the initial and final states are identical, as in a complete cycle, the right sides of [29] and [34] are zero.

Reference environment and general remarks

Some important characteristics of exergy are described as follows:

A system in complete equilibrium with its environment does not have any exergy. No difference appears in temperature, pressure, concentration, and so forth, so there is no driving force for any process;

The exergy of a system increases the more it deviates from the environment. For instance, a specified quantity of hot water has a higher exergy content during winter than on a hot summer day. A block of ice carries little exergy in winter while it can have significant exergy in summer;

When energy loses its quality, exergy is destroyed. Exergy is the part of energy that is useful, therefore, it has economic value and is worth managing carefully;

Exergy by definition depends not just on the state of a system or flow, but also on the state of the environment;

Exergy efficiencies are a measure of approach to ideality (or reversibility). This is not necessarily true for energy efficiencies, which are often misleading.

Exergy can generally be considered a valuable resource. There are both energy or nonenergy resources and exergy is observed to be a measure of value for both:

Energy forms with high exergy contents are typically more valued and useful than energy forms with low exergy. Fossil fuels, for instance, have high energy and exergy contents. Waste heat at a near environmental condition, on the other hand, has little exergy, even though it may contain much energy, thus, it is of limited value. Solar energy, which is thermal radiation emitted at the temperature of the sun (approximately 5800 K), contains much energy and exergy;

A concentrated mineral deposit “contrasts” with the environment and thus has exergy. This contrast and exergy increase with the concentration of the mineral. When the mineral is mined the exergy content of the mineral is retained, and if it is enriched or purified, the exergy content increases. A poor-quality mineral deposit contains less exergy and can accordingly be utilized only through a larger input of external exergy. Today, this substitution of exergy often comes from exergy forms such as coal and oil. When a concentrated mineral is dispersed the exergy content is decreased.

Since the value of the exergy of a system or flow depends on the state of both the system or flow and a reference environment, a reference environment must be specified prior to the performance of an exergy analysis. The environment is often modeled as a reference environment similar to the actual environment in which a system or flow exists. This ability to tailor the reference environment to match the actual local environment is often an advantage of exergy analysis. Some, however, consider the need to select a reference environment a difficulty of exergy analysis. To circumvent this perceived difficulty, some suggest that a “standard environment” be defined with a specified chemical composition, temperature, and pressure. A possible chemical standard environment for global use could, for instance, be based

on a standard atmosphere, a standard sea, and a layer of the earth's crust. In accounting for local conditions, a reference environment can vary spatially and temporally. The need to account for spatial dependence is clear if one considers an air conditioning and heating system operating in the different climates across the earth. The importance of accounting for temporal dependence is highlighted by considering a technology like a seasonal thermal energy storage unit in which heating or cooling capacity can be stored from one season where it is available in the environment to another season when it is unavailable but in demand.

The reference environment is in stable equilibrium, with all parts at rest relative to one another. No chemical reactions can occur between the environmental components. The reference environment acts as an infinite system and is a sink and source for heat and materials. It experiences only internally reversible processes in which its intensive state remains unaltered (i.e., its temperature T_o , pressure P_o , and the chemical potentials μ_{i00} or each of the i components present remain constant). The exergy of the reference environment is zero. The exergy of a stream or system is zero when it is in equilibrium with the reference environment.

Consequently, models for the reference environment are used that try to achieve a compromise between the theoretical requirements of the reference environment and the actual behavior of the natural environment. The reference-environment model that is going to be used throughout this thesis is adapted from (Gaggioli & Petit, 1977) and is showed in the following figure:

Temperature: $T_o = 298.15 \text{ K}$
 Pressure: $P_o = 1 \text{ atm}$
 Composition: Atmospheric air saturated with H_2O at T_o and P_o , having the following composition:

| Air constituents | Mole fraction |
|----------------------|---------------|
| N_2 | 0.7567 |
| O_2 | 0.2035 |
| H_2O | 0.0303 |
| Ar | 0.0091 |
| CO_2 | 0.0003 |
| H_2 | 0.0001 |

The following condensed phases at T_o and P_o :

Water (H_2O)
 Limestone (CaCO_3)
 Gypsum ($\text{CaSO}_4 \cdot 2\text{H}_2\text{O}$)

Figure 6 - Reference-environment model

This choice is also consistent with the standard settings of Aspen Plus software, which is the main software used in the modeling and simulation phase of the energy system object of this thesis. All the simulations dealing with the case study of this work are based on the Peng-Robinson (PENG-ROB) property method and the standard state used by the Aspen Physical Property System, for any constituent element, which is at 298,15 K and 101325 Pa.

| | | |
|--|--------|-------|
| Exergy reference environment temperature | 298,15 | K |
| Exergy reference environment pressure | 101325 | N/sqm |

Figure 7 - Screenshot taken from the Aspen Plus Setup-Calculation Options window. The values shown are the reference ones.

Efficiencies and other measures of merit

In this section, the use of exergy efficiencies in assessing the utilization efficiency of energy and other resources is described.

First, the exergy efficiency is an efficiency based on the SLT. To illustrate the idea of a performance parameter based on the SLT and to contrast it with an analogous energy-based efficiency, consider a control volume at steady state for which energy and exergy balances can be written, respectively, as follows:

$$(Energy\ in) = (Energy\ output\ in\ product) + (Energy\ emitted\ with\ waste) \quad [35]$$

$$(Exergy\ in) = (Exergy\ output\ in\ product) + (Exergy\ emitted\ with\ waste) + (Exergy\ destruction) \quad [36]$$

In these equations, the term product might refer to shaft work, electricity, a certain heat transfer, one or more particular exit streams, or some combination of these. The latter two terms in the exergy balance (Eq. 1.11) combine to constitute the exergy losses. Losses include such emissions to the surroundings as waste heat and stack gases. The exergy destruction term in the exergy balance is caused by internal irreversibilities.

From energy or exergy viewpoints, a gauge of how effectively the input is converted to the product is the ratio of product to input. That is, the energy efficiency η can be written as follows:

$$Energy\ efficiency\ \eta = \frac{Energy\ output\ in\ product}{Energy\ input} = 1 - \left(\frac{Energy\ loss}{Energy\ input} \right) \quad [37]$$

And the exergy efficiency Ψ is:

$$Exergy\ efficiency\ \Psi = \frac{Exergy\ output\ in\ product}{Exergy\ input} = 1 - \left(\frac{Exergy\ loss}{Exergy\ input} \right) = 1 - \left[Exergy\ waste\ emission + \left(\frac{Exergy\ destruction}{Exergy\ input} \right) \right] \quad [38]$$

The exergy efficiency Ψ frequently gives a finer understanding of performance than the energy efficiency η . In evaluating η , the same weight is assigned to energy whether it is shaft work or a stream of low-temperature fluid. Also, the energy efficiency centers attention on reducing energy emissions to improve efficiency. The parameter Ψ weights energy flows by accounting for each in terms of exergy. It stresses that both waste emissions (or external irreversibilities) and internal irreversibilities need to be dealt with to improve performance. In many cases it is the irreversibilities that are more significant and more difficult to address. Efficiency expressions each define a class of efficiencies because judgment has to be made about what the product is,

what is counted as a loss, and what the input is. Different decisions about these lead to different efficiency expressions within the class.

Other SLT-based efficiency expressions also appear in the literature as follows, for steady-state devices:

$$\text{Rational efficiency} = \left(\frac{\text{Total exergy output}}{\text{Total exergy input}} \right) = 1 - \left(\frac{\text{Exergy consumption}}{\text{Total exergy input}} \right) \quad [39]$$

$$\text{Task efficiency} = \frac{\text{Theoretical minimum exergy input required}}{\text{Actual exergy input}} \quad [40]$$

(Van Gool, 1997) noted that the maximum improvement in the exergy efficiency for a process or system is achieved when the exergy destruction rate ($\dot{E}x_{in} - \dot{E}x_{out}$) is minimized. He suggested an exergetic improvement potential (IP) be used when analyzing processes. This improvement potential on a rate basis is given by (Hammond & Stapleton, 2001):

$$\text{Improvement potential IP} = \left(1 - \frac{\text{Net electrical exergy efficiency}}{100} \right) \text{Exergy destruction rate} \quad [41]$$

$$\text{Net electrical exergy efficiency} = \frac{W_{NET}}{\text{Total exergy input}} \quad [42]$$

In general, exergy efficiencies provide a measure of potential for improvement of the whole energy system. On the other hand, it can be interesting to evaluate the performance of an individual component considering interactions among components too. For this purpose, some other thermodynamic performance measures used for energy systems follow, as defined in (Xiang, Cali, & Santarelli, 2004):

$$\text{Relative irreversibility } \chi_i = \frac{\dot{E}x_i}{\dot{E}x_{tot}} \quad [43]$$

$$\text{Productivity lack } \xi_i = \frac{\dot{E}x_i}{\dot{P}_{tot}} \quad [44]$$

$$\text{Exergetic factor } f_i = \frac{\dot{F}_i}{\dot{F}_{tot}} \quad [45]$$

Base-case system

The energy system subject of this thesis consists of an organic Rankine cycle unit coupled with a concentrated solar power system. The plant as a whole does not currently exist, except for the solar concentrator, which is located on the rooftop of Politecnico di Torino's Energy Center building. It is precisely starting from the solar concentrator that the rest of the system is, then, modeled.

The solar concentrator installed at Energy Center belongs to the solar dish family. In general, parabolic dishes are commonly made up of different subsystems:

The dish, a paraboloidal shaped concentrator, aimed at focusing the solar flux on a little area, namely the focus of the parabola. The reflecting surface is made with metallized glass, plastic film, or anodized aluminum. The dish can have different set-ups, it can be constituted by a single piece, or by several units (as it more often happens for larger systems), in form of petals, squares or circles;

A receiver, the solar heat exchanger, located in the region where the sunlight is concentrated. It can have many different layouts, depending on the function of the CSP system and must be able to sustain very high temperatures;

A receiver support, a sustaining structure that keeps in place the solar heat exchanger. Again, there are different strategies for the same purpose, whether it being a mechanical arm starting from the center of the dish and holding it, or being suspended by a semicircular support;

A tracking system, able to always direct the solar dish towards the sun, so that the solar radiation will be approximately parallel to the parabola axis. The well-functioning of this system is extremely important, as the dish can concentrate the solar power on the geometric focus, only if the solar rays are as perpendicular as possible to the concentrator aperture. The tracking system is equipped with two motors, one for controlling the tilt, i.d. the zenith, and the other for controlling the azimuth, to always keep the dish in the right position;

A support structure that holds the dish at a certain height from the ground and allows its rotation around the two axes for tracking the Sun;

Foundations that anchor the support structure to the ground and hold it still;

A control unit that enables the user to control and move the paraboloid. It must be equipped with an anemometer, so that the tracking can be stopped in case of extreme wind speed and the dish is brought back to a safe position. The connection with a thermocouple - to be placed in the receiver - allows the control unit to slightly un-focus the system when the temperature exceeds a threshold.

In the examined case, the concentrator is designed by the Italian company El.Ma. s.r.l. on behalf of Politecnico di Torino, to carry out laboratory experiments for research purposes and for temporary use. Considering a design point value of Direct Normal Irradiance of $800 \frac{W}{m^2}$ and a capturing surface of $4,5 m^2$, and the optical efficiency equal to 80%, the rated power of the collector is:

$$\dot{Q}_{solar\ dish} = DNI \cdot S \cdot \eta_{optical} = 800 \frac{W}{m^2} \cdot 4,5 m^2 \cdot 0,8 = 2880 W \quad [46]$$

Also, the maximum temperature that the solar dish can withstand is 1800 °C (Borghero, 2021); (Guerriero, 2021).



Figure 8 - The solar dish concentrator by El.Ma., installed on the Energy Center rooftop (Borghero, 2021)

The reflecting surface of the solar dish is constituted by the conjunction of 6 petals covered by a plastic reflecting film which is pasted on them. The units are fixed together along their long side and to the structure in the center. In this point, there is no reflecting surface, as that is where the mechanic arm holding the receiver support is mounted. The arm consists of a large and short U-shaped iron arm that sustains the receiver support.

On the horizontal part opposite to the solar dish, two aluminum joints can swipec and move the receiver closer or further from the vertex of the paraboloid. Moreover, the support can also be raised or lowered thanks to two vertical aluminum joints, as it can be noticed from the figure.



Figure 9 - The support structure of the collector, at the end of the mechanical arm (Borghero, 2021).

The two vertical joints are kept at a stable distance of 20 cm by a horizontal aluminum joint of the same type on the bottom. They hold two iron U-shaped supports, where the receiver is placed. The initial receiver consists of a pipe made of alumina, Al_2O_3 , connected to two thinner tubes at the edges. The pipe is 22 cm long, so that part of it goes inside the supports at the tips. It has an external diameter of around 18 mm, an internal diameter of around 14 mm and is around 2 mm thick. The dimensions can slightly vary from one piece to another one, and sometimes even along the same piece. On one side, the pipe holder is equipped with a Q-type thermocouple of 10 cm length and 6 mm diameter, so that, if mounted correctly, reaches the middle of the pipe without impeding gas flow. The electric connection of the thermocouple is protected by a plastic sleeve and a metallic plate. The small tubes connected to the edges and the cable run inside the mechanical arm, the supporting pillar and reach the control cabinet by passing inside a duct installed on the floor.

The reflecting surface has a diameter of 2370 mm, and the depth of the dish has been measured to be 370 mm. The focal distance is 958 mm measured starting from the plate where the support is connected. The focus lies on the central axis of the parabola. With this information, it is possible to calculate the rim angle, which is found to be of $61,89^\circ$ (Borghero, 2021). It must be noted that the rim angle is higher than 45° , a value which is regarded as the one outputting the best performance (Hafez, Soliman, El-Metwally, & Ismail, 2017). Also, the theoretical concentration ratio is ≈ 8013 and the diameter of the focal point is 6.41 mm (Borghero, 2021).

The machine is also equipped with a control unit through which it is possible to modify the settings and orient with the desired coordination. The collector can work in two modes:

Automatic, when it automatically tracks the sun basing the time set;

Manual, if the user wants to decide the coordinates for the orientation. In this mode, it is possible to edit the parameters that regulate the solar tracking. It is possible to insert offsets for the azimuth and elevation tracking, choose the night position and the kind of tracking, whether the system should update its position on a temporal or angular basis.

The presence of the control unit is of fundamental importance because it allows to modulate the operating mode of the entire solar circuit. This feature takes on even greater importance when the solar system is connected to a thermal energy storage.

The aim of the first part of this thesis is to model an ORC unit, of moderate size, to be coupled to the solar system based on the above-described solar collector. Since a nominal size – in the sense of power output - must be set, the proposed model is a hybrid between a simulation model and a sizing model: on one hand, the design, the size and the parameters of the collector are set according to the collector technology; on the other hand, the size of the ORC cycle and of its components is recalculated by the model to obtain a good match between collector power and ORC engine power. To do so, the next steps are the discussion on the working fluid and on the various components of the power unit, the identification of the design conditions, the process simulation on Aspen Plus.

Working fluid

As previously mentioned, the organic Rankine cycle unit is modeled starting from the solar concentrator, the main element of the solar concentrating system that powers the ORC unit. The components of the organic Rankine cycle are sized following a sensitivity analysis aimed at establishing which, among three organic fluids compatible with this type of plant, allows the best exploitation of the solar resource.

Nowadays, it is important to use working fluids with low environmental impact and low risk. In this regard, about organic fluids, two indices can be used to make the best choice:

GWP, Global Warming Potential: the GWP of a chemical compound expresses the heat absorbed by any greenhouse gas in the atmosphere, as a multiple of the heat that would be absorbed by the same mass of carbon dioxide (CO₂), being fixed at 1,0 the GWP for CO₂. Each GWP value is calculated for a specific time frame, typically 20, 100 or 500 years;

ODP, Ozone Depletion Potential: the ODP of a chemical compound is the relative amount of degradation to the ozone layer it can cause, with trichlorofluoromethane (R-11 or CFC-11) being fixed at an ODP of 1,0. Specifically, the value of the ozone depletion potential associated with a substance is defined as the ratio of the loss of ozone for the substance under consideration and the loss of ozone produced by one equal mass of trichlorofluoromethane.

Also, the critical point of the working fluid should be similar to the target temperature range (100–200 °C). The working fluid should be a well-known fluid in both state-of-the-art ORC applications and in the scientific literature: in this way several conditions such as the toxicity, the cost or the flammability are easily known. Finally, the working fluid should have a null ODP in order to avoid the phasing-out of the Montreal Protocol (Quoilin, Orosz, Hemond, & Lemort, 2011).

The choice, faced in a previous thesis work, falls on the octa-methyl-tri-siloxane fluid $C_8H_{24}O_2Si_3$ (MDM), belonging to the siloxane family. Siloxanes are silicone chemical compounds, often used as working fluids in organic Rankine cycles at high temperature: they are neither toxic nor corrosive, they have a good thermal stability, they are not very flammable. As regards the environmental aspects, also, silicone fluids are characterized by a null Ozone Depletion Potential value and a very low Global Warming Potential. The critical temperature of MDM is equal to $290,98\text{ }^\circ\text{C}$ (Sebelev, Saychenko, Zabelin, & Smirnov, 2016) and the critical pressure is $14,15\text{ bar}$ (Lai, Wendland, & Fischer, 2011). These values are confirmed by the results obtained from Aspen Plus, which are critical temperature equal to $291\text{ }^\circ\text{C}$ and critical pressure to $14,55\text{ bar}$.

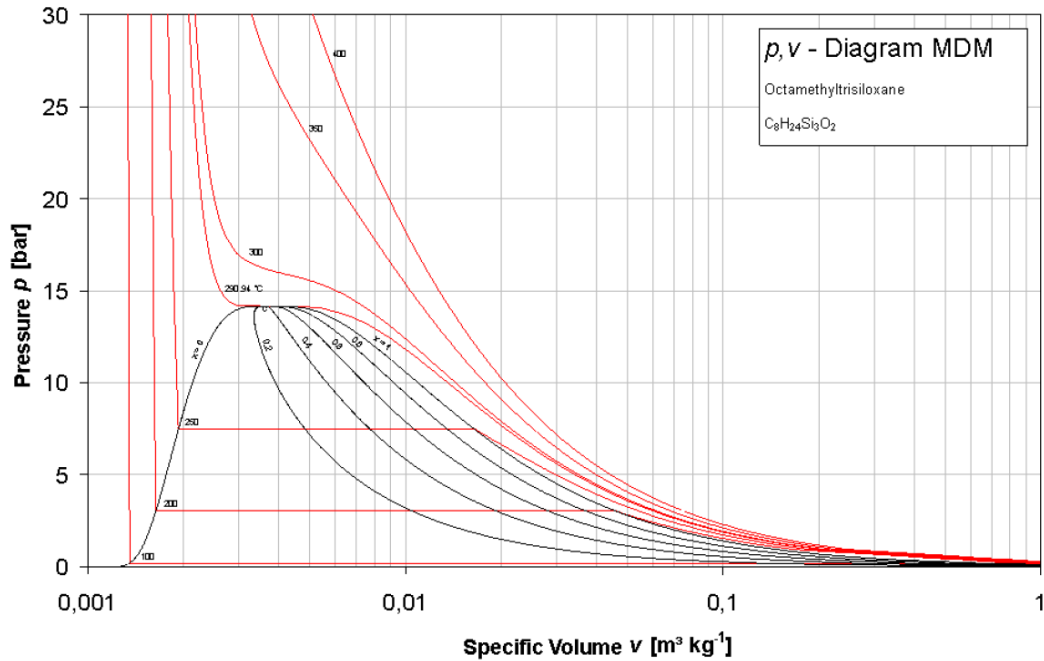


Figure 10 - MDM saturation curve on the P,v diagram (Kretzschmar, 2019)

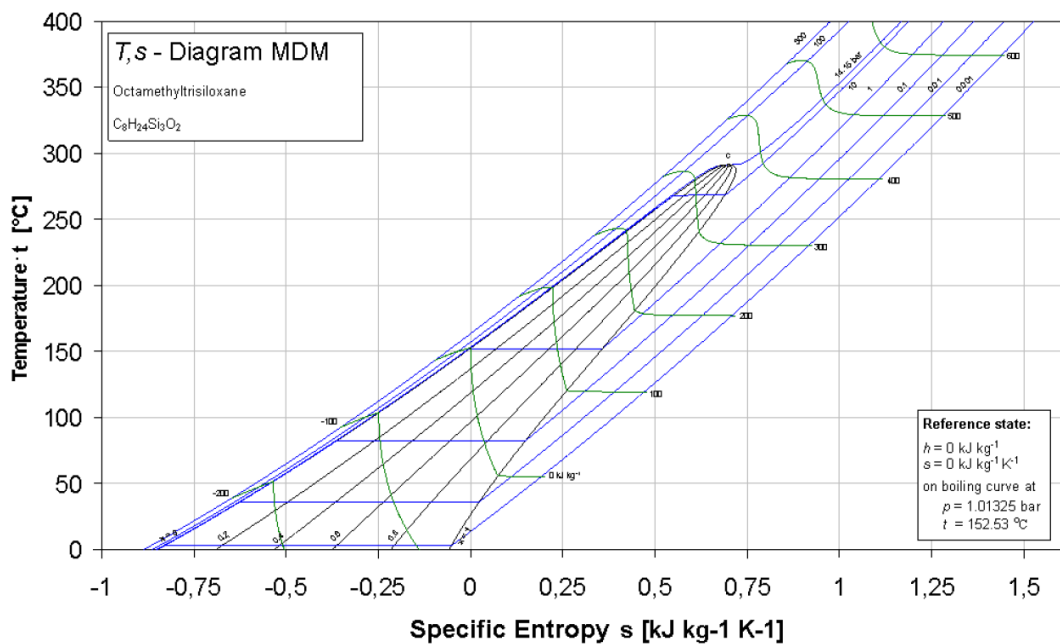


Figure 11 - MDM saturation curve on the T,s diagram (Kretzschmar, 2019)

The slope of the saturation limit curve is negative therefore the fluid is of the dry type; it is then suitable to be used as a working fluid in an ORC since in the case of a dry fluid, as already stated, the cycle can be employed at lower temperatures without requiring superheating: this results in a practical increase in efficiency over the use of the same Rankine cycle with water as working fluid (Andersen & T.J., 2005). Although the use of a dry fluid is convenient in most cases for ORCs, it is necessary pay attention not to excessively raise the evaporation pressure, since it could happen that in the expansion phase the fluid itself falls within the saturation curve, in the two-phase zone (Maccioni).

Expander

With respect to the cycle modeling, the main assumption is that the electrical power coming out of the expander is equal to 10 kW. It is imposed to set the turbine inlet temperature - which is equivalent to the steam generator outlet temperature - at 250 °C. The choice of limiting this temperature to 250 °C lies in avoiding any safety issue: the critical point of MDM is 291 °C and it is important that the fluid never reaches that temperature, to avoid instability phenomena. Furthermore, at a temperature of 250 °C a pressure of 7,72 bar corresponds on the saturation curve and, by further increasing the temperature, the pressure would also rise, causing an increase in the work done by the pump and a greater thickness of the pipes. Then, it is stated to let the fluid enter the turbine at a temperature of 250 °C and a pressure of 7,72 bar. The isentropic and mechanical efficiencies are set at 0,90 and 0,98 respectively. It is important to state that the constant isentropic efficiency is an important limitation of this thesis. However, the selected value of 90% is a reasonable value which gives acceptable results according to previous works (Bellos, Vellios, Theodosiou, & Tzivanidis, 2018). The efficiency of the alternator is also assumed to be 0,98. Electric power produced by the cycle is therefore 9,8 kW_{el}. The component used on Aspen Plus for modeling is a compressor from the Pressure Changers library, which is specified to work as a turbine. Finally, it has to be noted that because not many thermal power blocks are currently manufactured in the kilowatt range, a small-scale expander is based on modified commercially available components such as HVAC scroll expanders: the main challenge for ORC development is, up to now, the high cost of specially designed expander-generator equipment (Quoilin, 2011).

To choose the optimal fluid flow rate, focus must be made on the pressure at the turbine outlet. A lower flow rate of fluid would certainly bring benefits to the entire system because it would reduce the costs of the fluid and the work of the pump, however low flow rates correspond to low pressure values at the turbine outlet, even lower than atmospheric pressure. As a matter of safety, it is important that there is always a slight overpressure in the circuit with respect to the surrounding environment to avoid air infiltration inside the system. By setting the turbine outlet pressure at 1,15 bar, the flow rate corresponding to the chosen pressure is $0,39 \frac{kg}{s}$. Aspen Plus provides the temperature values that occur at the turbine outlet under the design conditions described above. The fluid leaving the turbine, as can be seen from the vapor fraction value, is still in the vapor phase therefore there are no issues with the formation of liquid particles in the turbine. The output temperature is equal to 225,32 °C.

Condenser

Since the ORC to be modeled is designed for production of both electrical and thermal energy, the condensation heat that is released by the hot fluid in the condenser must heat a cold fluid

that is used in applications where thermal power is required, such as in an industrial process or for space heating. The cooling fluid that is decided to be used is water, the most versatile fluid in engineering. A water temperature entering the condenser of 60 °C is assumed: this value is consistent with the temperature of the return loop of a district heating network.

On Aspen Plus the condenser is modeled using the HeatX component of the Exchangers library. The input values are the ones obtained as output of the expander, while the output values are calculated directly by the software. It is assumed that the pressure of the hot fluid does not undergo any variation during condensation. In the case of water, on the other hand, an inlet temperature of 60 °C and a pressure of 1 bar are assumed. It is taken a flowrate value such that the outlet water temperature is about 85 °C. Results are: 85,18 °C as water temperature leaving the condenser and $0,92 \frac{kg}{s}$ as water flowrate crossing the condenser. The thermal power exchanged in the condenser is equal to 105,42 kW_{th}.

In the following, the temperature profile of MDM, the hot fluid, and of water, the cold fluid, is showed.

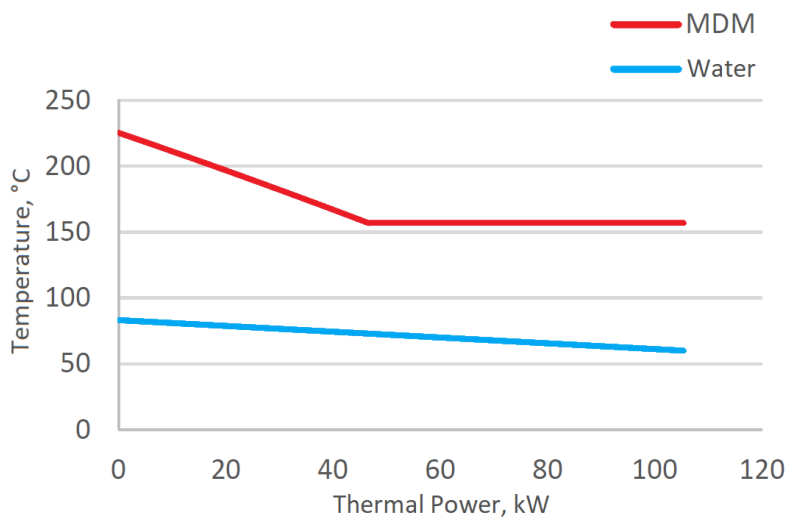


Figure 12 - Graphical representation of the heat exchange on the Temperature - Exchanged heat diagram

Pump

The pump allows to raise the pressure of the fluid after leaving the condenser. For the pump model, the Pump component present in the Aspen Plus Pressure Changers library is used. The inlet conditions are the same as those at the condenser outlet. The efficiency of the component is assumed to be 0,90. The pump outlet pressure is set equal to the turbine inlet pressure. Due to the irreversibility generation within the pump, the outgoing fluid has a slightly higher temperature than at the inlet. The values obtained and the electrical power absorbed by the pump – which is much lower than the electrical power obtained by the turbine – are respectively 157,43 °C and 0,42 kW_{el}.

Evaporator

The evaporator is the key component of the system: it allows the ORC to exploit the heat deriving from the solar concentrator. The evaporator is a heat exchanger that is by a hot and a cold flow: the hot fluid transfers heat to the cold one, which evaporates. The hot fluid comes from the

solar field, while the cold one is the working fluid used in the ORC. The quantity of heat exchanged between the two fluids must be enough to allow the phase change of the working fluid. The hot fluid that is chosen is a commercial, synthetic organic oil that is often used in solar fields: Therminol® VP-1. This thermal fluid is able to operate up to 400 °C with safety (Eastman, s.d.) and it is a usual choice for these applications (Bellos & Tzivanidis, 2017). Therminol® VP-1 is a promising option since it is able to stay in liquid state under ambient temperatures; however, due to high vapor pressures the usage of such an oil is restricted to temperatures below 400 °C, truncating the performance of the power plant (Reddy, Jawahar, Sivakumar, & Mallick, 2017).

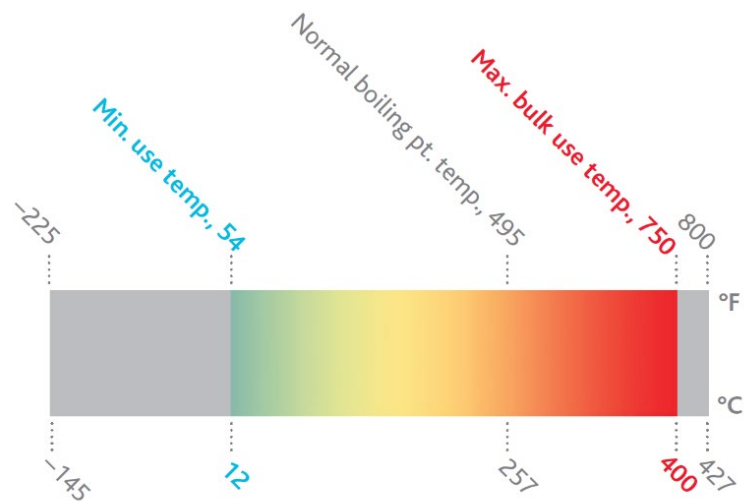


Figure 13 – Therminol® VP-1 optimum temperature use range (Eastman, s.d.)

On Aspen Plus the evaporator is modeled using the HeatX component of the Exchangers library. The values of the inlet flow correspond to the values obtained at the output of the pump model. It is assumed that the pressure remains constant during evaporation, so it is fixed at 1 bar. The outlet temperature of the evaporated fluid is the same as the one chosen for the fluid entering the expander: 350 °C. In this way, the outlet temperature of the Therminol® VP-1 flow is equal to 293,95 °C, being the flowrate equal to $0,45 \frac{kg}{s}$. The minimum temperature difference that occurs inside an exchanger is called the pinch point temperature. As this difference decreases, the temperature profiles of the two fluids get closer, and the efficiency of the heat exchanger increases because irreversibility decreases, but the exchange areas necessary to achieve it increases. The pinch point temperature difference is about 74 °C. The thermal power exchanged at the evaporator is equal to 115,19 kW_{th}.

In the following, the temperature profile of the thermal oil, the hot fluid, and of MDM, the cold fluid, is showed.

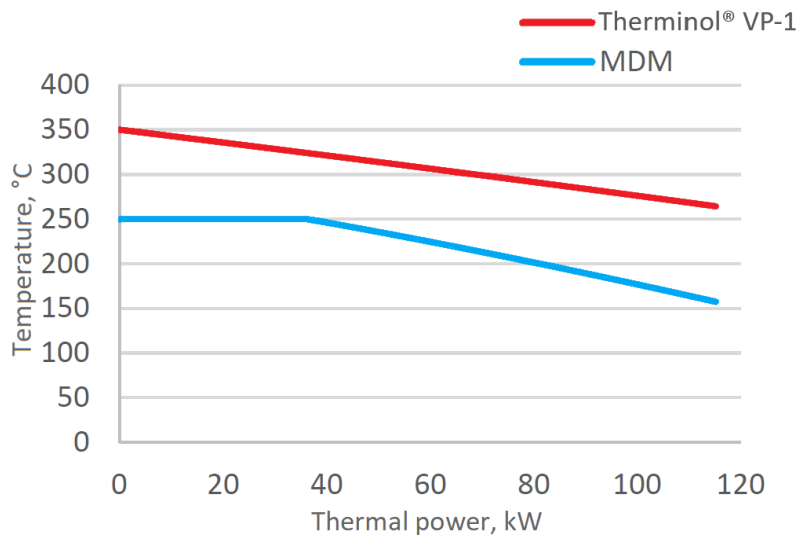


Figure 14 - Graphical representation of the heat exchange on the Temperature - Exchanged heat diagram

Recuperator

Owing to the molecular complexity of the organic fluid, a small enthalpy drop occurs in the expansion phase, resulting in a large thermal power availability at the turbine discharge (Petrollese, Cau, & Cocco, 2020). To increase the cycle efficiency, a heat recovery unit between the turbine and the condenser is introduced for a regenerative pre-heating. The recuperator is a counter-current heat exchanger that allows to preheat the liquid leaving the condenser by recovering part of the sensible heat possessed by the fluid that comes out of the expander. Thanks to this internal recovery, the thermal power to be supplied as input to the evaporator diminishes, allowing to decrease the area of the solar field necessary for the operation of the cycle. On the Aspen Plus software, the recovery unit is modeled using a HeatX from the Heat Exchangers library and setting a difference of 20 °C between the temperature of the hot fluid at the inlet and the temperature of the cold fluid at the outlet. This is the only assumption made since the remaining parameters of the flows are determined by the software when the simulation is launched. The results obtained from this analysis are the following: the water flowrate crossing the condenser is equal to $0,59 \frac{kg}{s}$, the water temperature at the outlet of the condenser is 85 °C, the thermal power recovered is 38,33 kW_{th}. A hypothetical T-Q diagram of the recuperator shows the trend of temperatures inside the counter-current exchanger: the hot fluid and the cold fluid have an almost parallel trend. This is because the heat exchange takes place between the same fluid therefore the specific heat is very similar, only temperature changes; in this case, irreversibility is minimized.

The next image shows the temperature profile of the organic fluid as it flows into the recuperator.

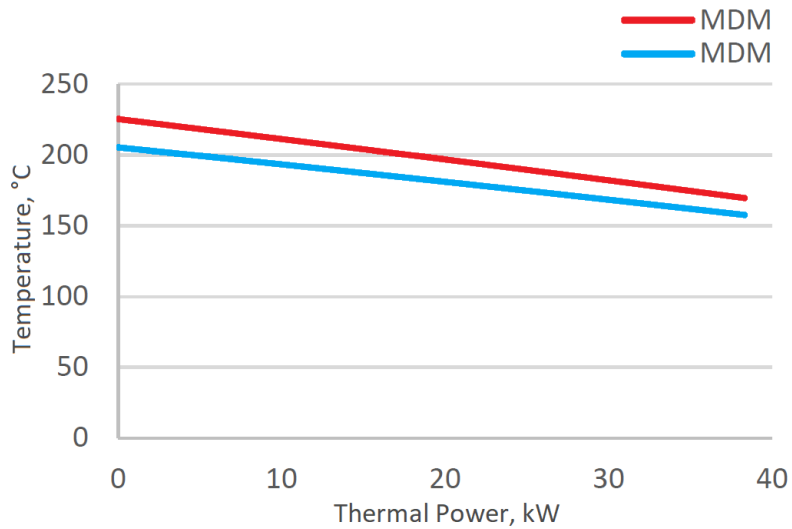


Figure 15 - Graphical representation of the heat exchange on the Temperature - Exchanged heat diagram

System coupling

In the following, an overview of the plant layout is presented.

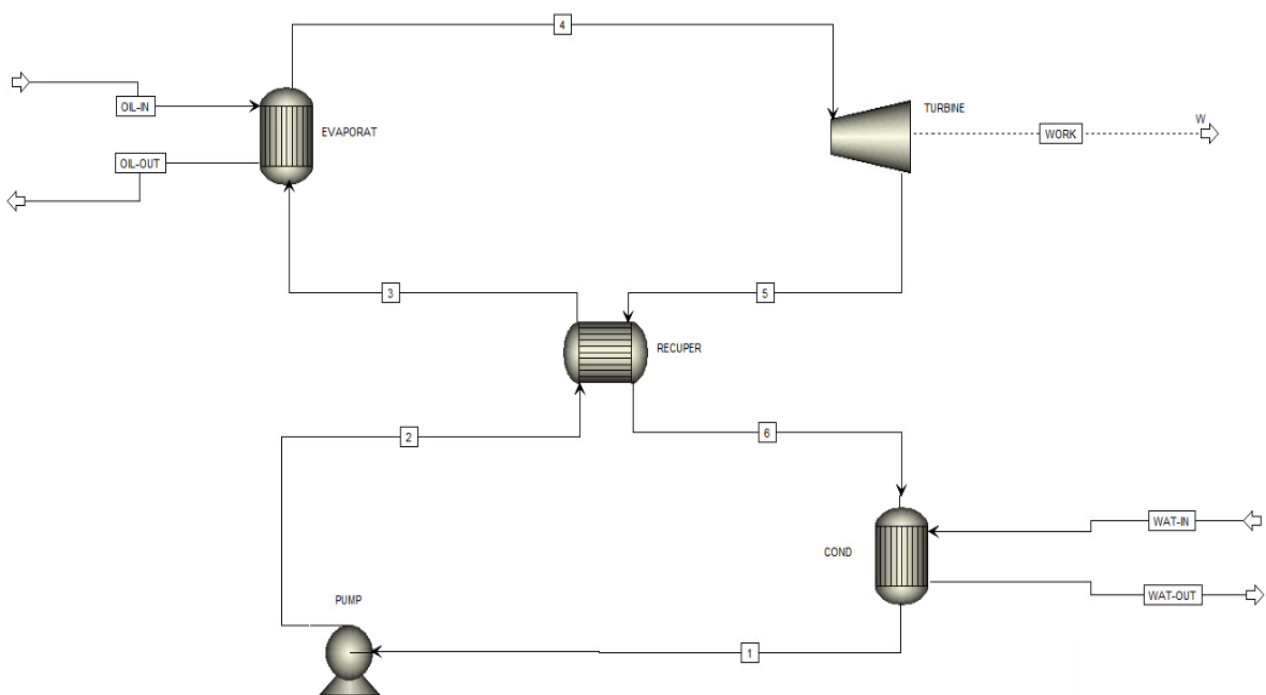


Figure 16 - ORC layout as displayed on the Aspen Plus workspace

In the graphical representation on the Gibbs chart, the organic Rankine cycle is drawn in red, while the heat recovery performed by the recuperator is outlined by the blue dashed line. On the top of the state diagram of the organic fluid, an orange line stands for the temperature profile of the thermal oil employed in the solar circuit that supplies thermal power to the ORC, while on the bottom the grey line represents the temperature profile of the water stream flowing in the condenser which acts as the second thermostat of the Rankine cycle.

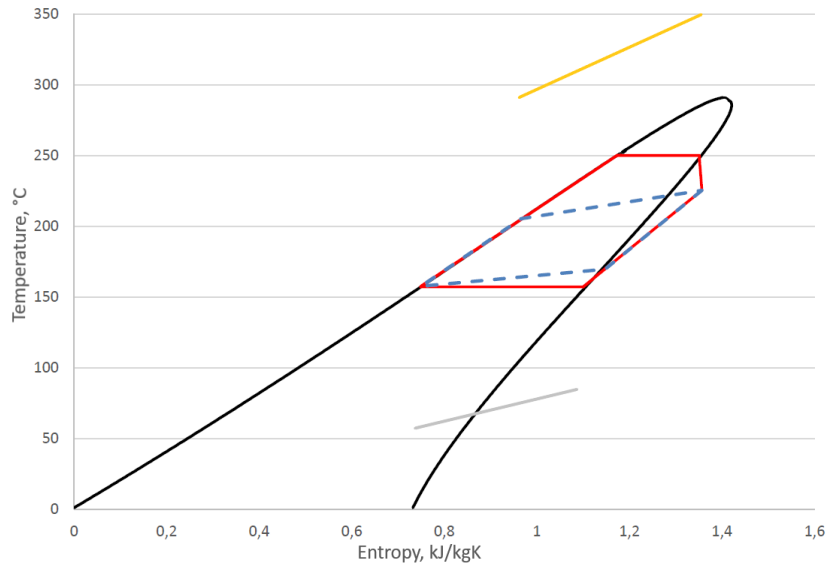


Figure 17 - Graphical representation of the thermodynamic cycle on the T-s plane

The organic Rankine cycle unit is modeled using Aspen Plus software. At this stage of the work, we focus on the ORC and the solar field is not taken into account in details: its contribution to the system is considered to lie between the input and the output state of the diathermic oil flowing in the evaporator.

The analysis is done considering steady-state operating conditions, since the system operates for long periods of time. The components are all considered perfectly insulated so that no heat losses occur. Also, the pressure drops in the evaporator and in the condenser are neglected. The dead state temperature and pressure, as previously stated, are assumed to be 25 °C and 1 bar, that are typical environment conditions. The output of the simulation is presented.

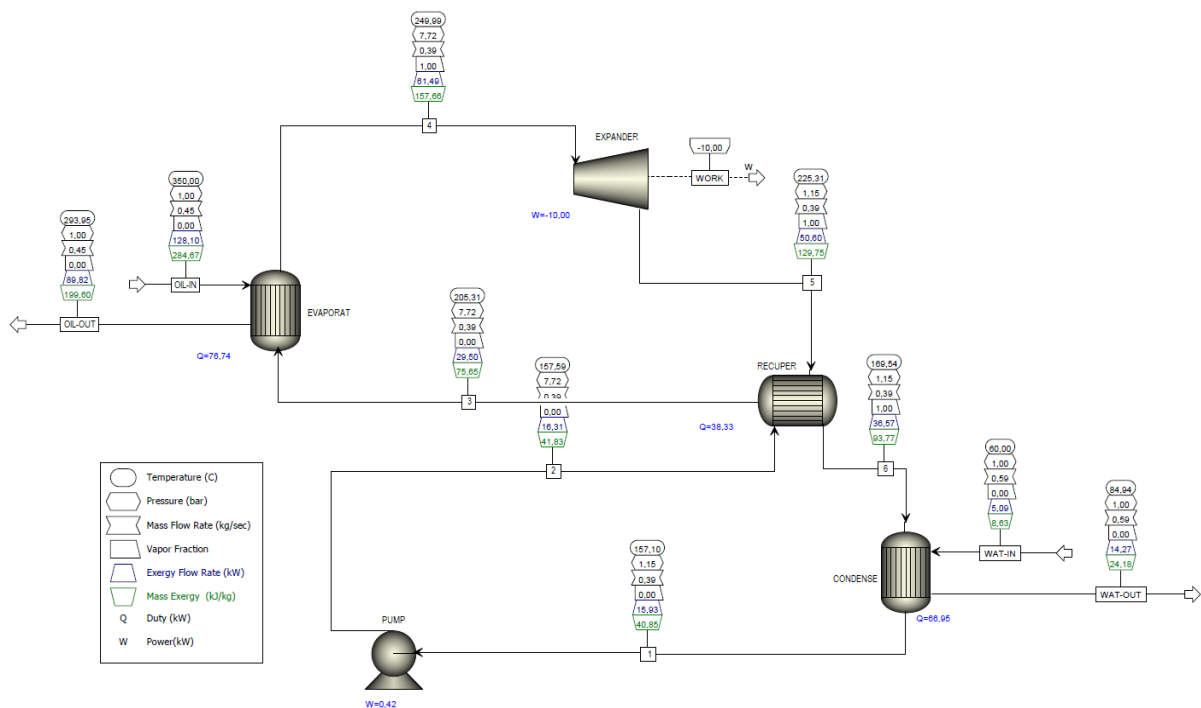


Figure 18 - Aspen Plus simulation output

As found in the analysis just carried out, the thermal power required by the cold fluid to the evaporator is equal to 115,07 kW. This power is partly supplied by the recuperator component, inside which the cold fluid, at the pump outlet, is pre-heated by the hot fluid leaving the turbine. The thermal power exchanged in the recuperator is 38,33 kW. The remaining thermal power required for the phase change of the fluid to occur in the evaporator, must be supplied by the solar fluid and is equal to the difference between the two:

$$115,07 \text{ kW}_{th} - 38,33 \text{ kW}_{th} = 76,86 \text{ kW}_{th} \quad [47]$$

The energy efficiency of the system, as defined by [37], results to be the following, according to what is considered to be the useful output of the plant:

| | Power generation | Combined heat and power generation |
|-----------------------------|-------------------------|---|
| Energy efficiency, % | 12,5% | 99,7% |

Table 1 - Obtained energy efficiency of the system

Design-point exergy performance

By applying FLT and SLT together, it is possible to write the exergy balance of each single component and then of the entire system. The application of [29] allows us to obtain the irreversibility generated in each single component, expressed in the following table:

| Component | Irreversibility, kW |
|------------------|----------------------------|
| Pump | 0,0378 |
| Recuperator | 0,8424 |
| Evaporator | 6,2976 |
| Turbine | 0,8849 |
| Condenser | 11,4643 |

Table 2 - Exergy consumption for each component

By applying, instead, [29] to the entire organic Rankine cycle, we obtain the following result.

| | Irreversibility, kW |
|---------------|----------------------------|
| System | 19,527 |

Table 3 - Exergy consumption of the ORC

While the exergy efficiency of the system, as defined in [38], results to be the following:

| | Power generation | Combined heat and power generation |
|-----------------------------|-------------------------|---|
| Exergy efficiency, % | 25,0% | 49,0% |

Table 4 - Obtained exergy efficiency of the system

This result practically means that the system can exploit only a quarter of its potential exergy. It is interesting to visualize these results by means of a pie chart showing the percentage weight of each component in exergy consumption:

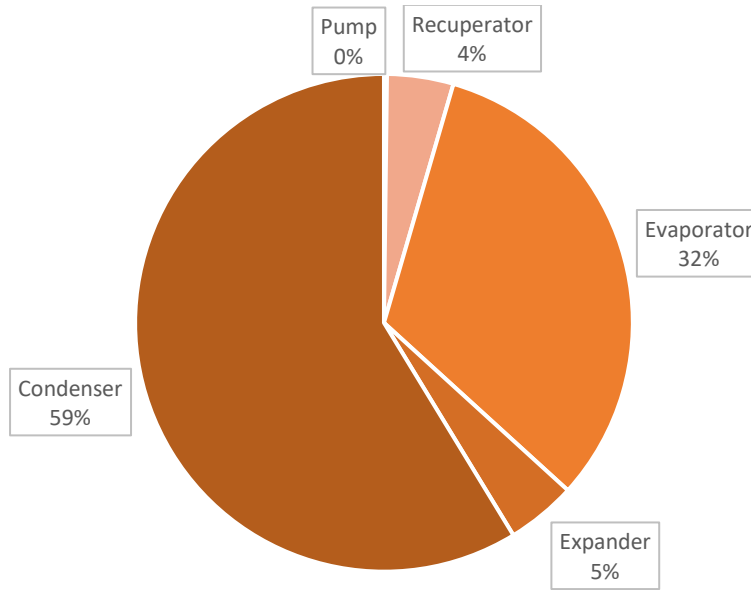


Figure 19 - Pie chart representing irreversibility generation

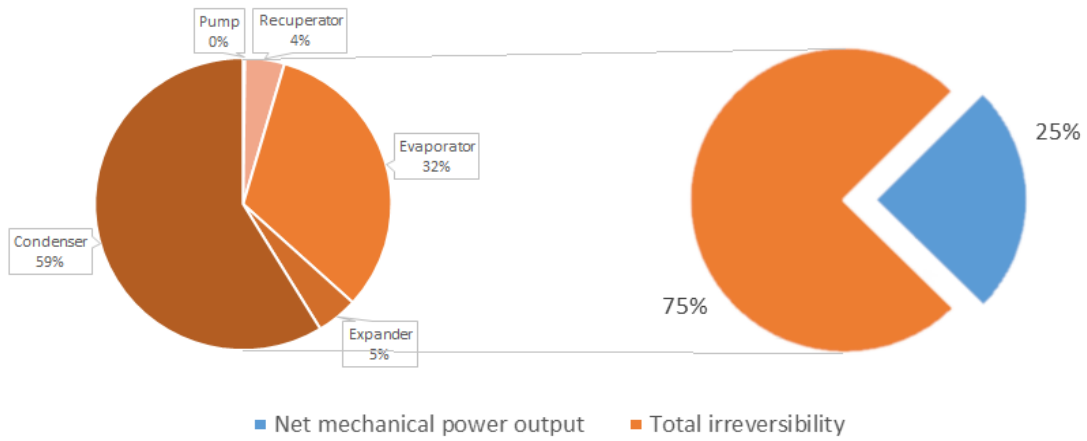


Figure 20 - Exergy output and destruction in the case of sole power generation

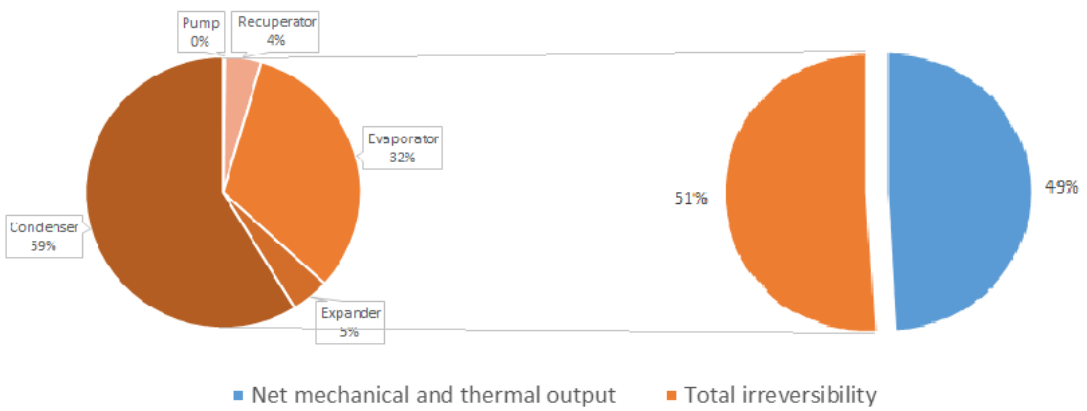


Figure 21 - Exergy output and destruction in the case of combined heat and power generation

First, the contribution of the pump in the consumption of exergy is negligible. After that, the least exergy-consuming component turns out to be the recuperator, followed by the turbine. Both components have a limited exergetic consumption. The components within which the greatest generation of entropy and, consequently, irreversibility occurs are the condenser and the evaporator. The condenser, alone, accounts for about 60% of total exergy consumption. Usually, the highest exergy loss occurs in heat exchangers due to the temperature difference between the hot and the cold fluids. A further indication of the not so satisfactory performance of the heat exchangers is given by the heat exchange efficiency:

$$\varepsilon_{evaporator} = \frac{T_{hot,in} - T_{hot,out}}{T_{hot,in} - T_{cold,in}} = \frac{350,00 - 293,95}{350,00 - 205,31} = 0,387 \quad [48]$$

$$\varepsilon_{condenser} = \frac{T_{hot,in} - T_{hot,out}}{T_{hot,in} - T_{cold,in}} = \frac{169,54 - 157,10}{169,54 - 60,00} = 0,114 \quad [49]$$

Nonetheless, despite the high efficiency of the regenerator, evaluated as:

$$\varepsilon_{recuperator} = \frac{T_{hot,in} - T_{hot,out}}{T_{hot,in} - T_{cold,in}} = \frac{225,31 - 169,54}{225,31 - 157,59} = 0,823 \quad [50]$$

An exergy loss is also present in this component due to the temperature difference between the exhaust vapor from the turbine and the liquid fluid from the pump. Other remarkable exergy losses occur in the expander, mainly due to frictions (Cocco, Petrollese, & Tola, 2017).

It is obvious that the condenser is the most critical component, so a focus on it is needed. The proposed strategy to improve its performance is to use water as condensation fluid, but at different temperatures. The exhaust working fluid is then sent to a water-cooled condenser where it returns to saturated liquid conditions. The water from the condenser is cooled in turn and, in case, used for other applications.

At this point, in a comparison between energetic and exergetic performance, what happens in the condenser if the temperature difference increases have to be addressed in the following sensitivity analysis.

We know that in heat exchangers, from an economic point of view, the optimal temperature difference is reduced the more the exchange temperatures are reduced, and we also know that the uses of heat and cold have a greater value the more the exchange temperature it differs from that of the environment. The following parameter named F can be, then, investigated and the goal is to find the optimum temperature difference value which leads to the maximum value of this parameter. This parameter is practically the geometrical dimensionless distance between the examined point and the ideal point, in a two-dimensional depiction of energy-exergy efficiency. This optimization strategy is usual and it can be found also in (Bellos, Tzivanidis, & Tsimpoukis, 2017):

$$F = \sqrt{\left(\frac{\eta_{ex} - \eta_{ex,max}}{\eta_{ex,max} - \eta_{ex,min}}\right)^2 + \left(\frac{\eta_{en} - \eta_{en,max}}{\eta_{en,max} - \eta_{en,min}}\right)^2} \quad [51]$$

Revised system

Up to now, energy and exergy balances of the organic Rankine cycle, at design conditions, are reported. Before going on with the calculation of the energy yield of the plant and, later, with the sensitivity analysis, it is proper to investigate the energy system as a whole.

The energy system includes three main sections: the Solar Field, where the solar energy is concentrated to heat up the HTF, a single-tank Thermal Energy Storage section, where the HTF is stored, and a Power Block, where the collected thermal energy is converted into electricity.

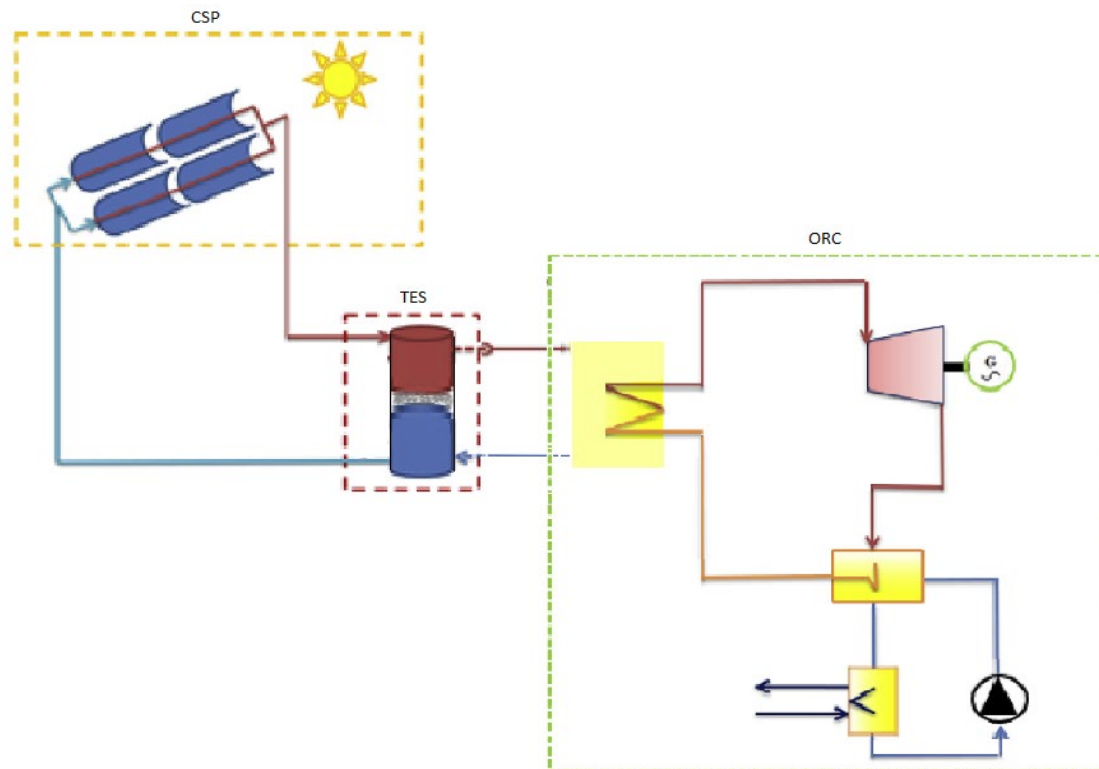


Figure 22 - Layout of the system blocks – Adapted from (Pantaleo, et al., 2020)

Valves and tank

The analysis starts with the power block. With respect to the previously analysed ORC system, the first modification stands into the introduction of valves. As pointed out in (Li, Hung, Feng, Xi, & Wang), the contribution of ducts and valves in exergy analyses is often – mistakenly – neglected, when in reality these components also have a certain effect on the energetic and exergetic performance of the entire system. The effect of valves, in particular, is greater than the one of pipelines, so in this thesis the pressure loss of pipes is attributed to the one of valves. To analyse a system having a fairly realistic behaviour, three valves are introduced. The two VALVE-TU and VALVE-CO valves are positioned in such a way as to allow the adjustment of the parameters subjected to the regulation of the system - VALVE-TU at the turbine inlet and VALVE-CO at the condenser inlet on the circuit cold fluid. The VALVE-TA valve is installed at the outlet of the newly introduced tank.

A tank, indeed, is another novelty of the layout, and it is modelled as a liquid separator with zero outlet-vapor flow rate to ensure that only liquid is present at the pump suction, to give to the plant a certain likelihood to represent a real system. The insertion of a tank downstream of the

condenser is commonly done, in fact, to guarantee a certain inertia of the system in the case of malfunctions, as well as to provide an appropriate flow rate at the pump inlet in the case of sudden shortages, avoiding failures (Maccioni). Due to the effect of the gravity, there is a pressure drop at the tank, because of the relatively higher density of the fluid. The pressure rise is expressed as:

$$\Delta P = \rho g z \quad [52]$$

Where z represents the relative elevation difference between the level of pump to the level of the liquid. In this way, the pressure rise due to the tank is equal to 0,053 bar. According to the result of experiments conducted on a similar system, z is consistent and can be assumed as 0,8 m (Li, Hung, Feng, Xi, & Wang). Regarding the modelling of valves, instead, the simulation software allows you to model such a component in three ways: by defining the pressure drop, the downstream pressure or the opening of the valve, in the latter case you also set the type of valve - ball, globe or butterfly. In this work, the pressure drop that the working fluid undergoes through the valve is estimated through the portion of dynamic pressure, and expressed, according to (Rampello, 2018) as:

$$\Delta P = \frac{\dot{V}}{0,5 \cdot C_v} \quad [53]$$

Where ΔP is expressed in psi, \dot{V} is the volumetric flowrate in gallon per minute, C_v is the flux coefficient and it can be evaluated as:

$$K_v = 0,865 \cdot C_v \quad [54]$$

K_v is the valve coefficient, and its values are set at 11,6 in the case of the two valves positioned along the liquid side of the pipelines, and at 89,0 in the case of the valve at the turbine inlet, due to relatively lower density and higher velocity of the fluid. These values are obtained from a regression analysis done on experimental data regarding a similar ORC unit (Li, Hung, Feng, Xi, & Wang). From the application of [50], a pressure drop of 0,004 bar is applied in the case of VALVE-TU, while it is equal to 0,0005 bar in the case of VALVE-TA and to 0,0008 bar in the case of VALVE-CO.

The power block is now represented as in the following figure, taken from the simulation software:

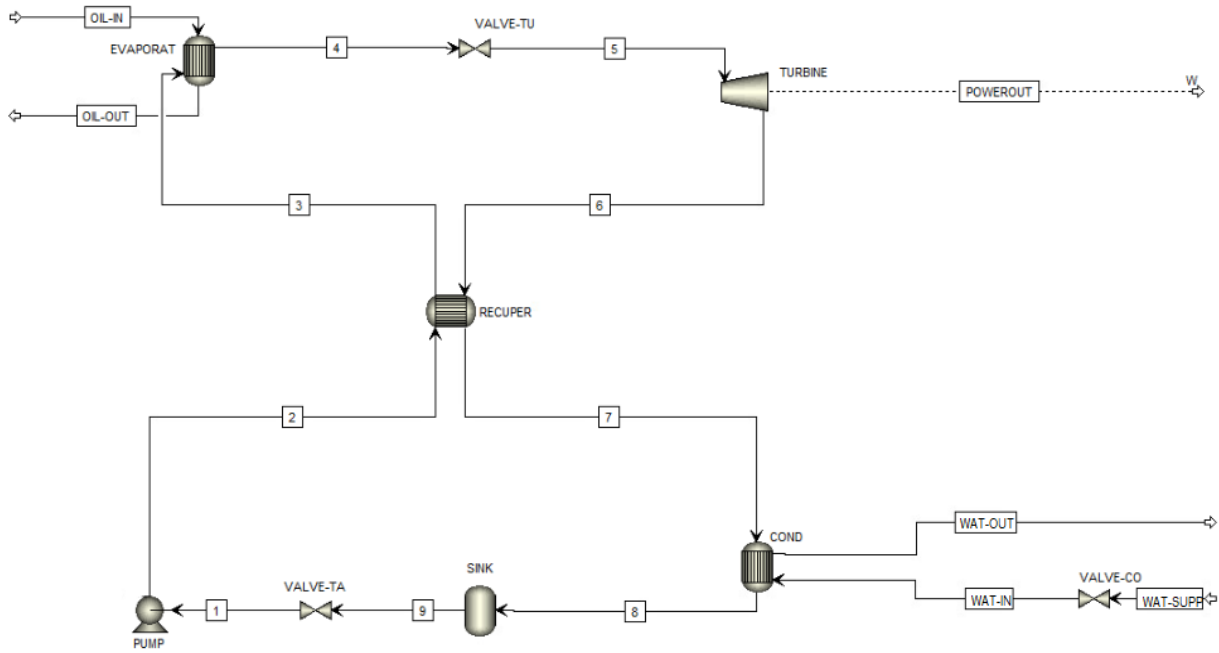


Figure 23 - Renewed ORC unit layout, as showed on the Aspen Plus software interface

Thermal energy storage

The second novelty is the introduction of a Thermal Energy Storage. Unlike conventional power generation systems, energy generation from a solar energy system does not always match energy demands when considering time and rate of use. In this case, a TES is required to meet energy needs. Several TES typologies can be used to recover heat from relatively high temperature: a critical review of technologies and materials is proposed in (Zhang, Baeyens, Cáceres, Degrève, & Lv, 2016). In this work, the single-tank thermocline technology is selected. This technology, referred as sensible heat storage with direct heating, has the advantage of a relatively low-cost medium for storage and fluid vector. In this way, the TES supplies heat for extended duration, multiplying the operational capacity of the power plant and, at the same time, increasing the ability of power dispatch.

A thermocline tank uses a single tank to store thermal energy, relying on the thermocline effect to reduce exergy losses due to mixing of the cold and the hot fluid (Casati, Desideri, Casella, & Colonna, 2012). Physical separation of the hot and cold region is maintained via buoyancy force, since cold oil is denser than hot oil, which induces stratification leading to two isothermal regions along the vertical direction. A narrow layer of substantial temperature gradient grows at the interface between the hot and cold region known as the thermocline or heat transfer region. The resultant temperature profile is a sigmoid-shaped curve which systematically travels up and down the height of the tank as the storage is charged and discharged; such a curve is showed by using the normalized temperature Θ , defined as:

$$\theta = \frac{T - T_c}{T_h - T_c}$$

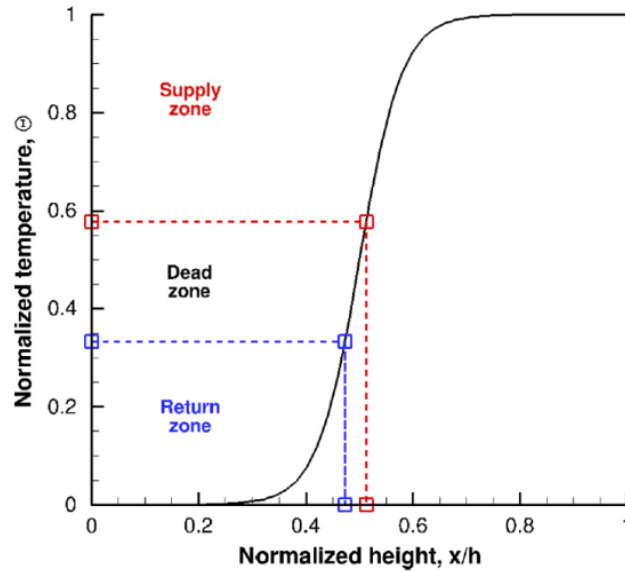


Figure 24 - Thermocline sigmoid-shaped curve (Ferruzza, 2015)

In addition to the HTF, thermocline tank is also filled with an inexpensive filler material that diminishes the volume of expensive HTF required for storage and enhances the fluid mixing that is crucial for thermal stratification.

About the working fluid, we know from the literature that, in case of CSP-ORC plants, the heat output to the power block is limited to the selection of the HTF materials like synthetic oils and molten salts, that remains in liquid state at very high temperatures. In particular, synthetic oils such as Eastman Therminol[®] and Dow Dowtherm[™] are a promising option as they remain in liquid state under ambient temperatures. On the other hand, due to high vapor pressures, the usage of such oils is restricted to temperatures below 400 °C (Bellos & Tzivanidis, 2017), and from the literature it is known that it may be difficult to use Therminol[®] VP-1 as a thermal storage media because its vapor pressure is too high (>1 MPa at 400 °C) to practically store in any significant quantity at its upper temperature: multiple thick-walled pressure-vessels would have to be used to store the hot oil, which would be too costly to be practical (Pacheco, J.E., Showalter, & Kolb, 2001). Despite that, this fluid has recently been studied as heat storage medium and, in particular, by studying its charging and discharging characteristics, Therminol[®] is found to be suitable for single-tank thermocline storage system (Reddy, Jawahar, Sivakumar, & Mallick, 2017). For this reason, Therminol[®] VP-1 is chosen as the storage medium, being it also the fluid flowing in the solar field. For sake of safety, the temperature at the inlet of the TES, on the solar system side, is fixed at 350 °C. The low-cost filler material – typically a mixture of quartzite and silica sand (Pacheco, J.E., Showalter, & Kolb, 2001) - is used, then, to displace the higher-cost liquid. The filler material as well as buoyant forces help to maintain the thermal gradient.

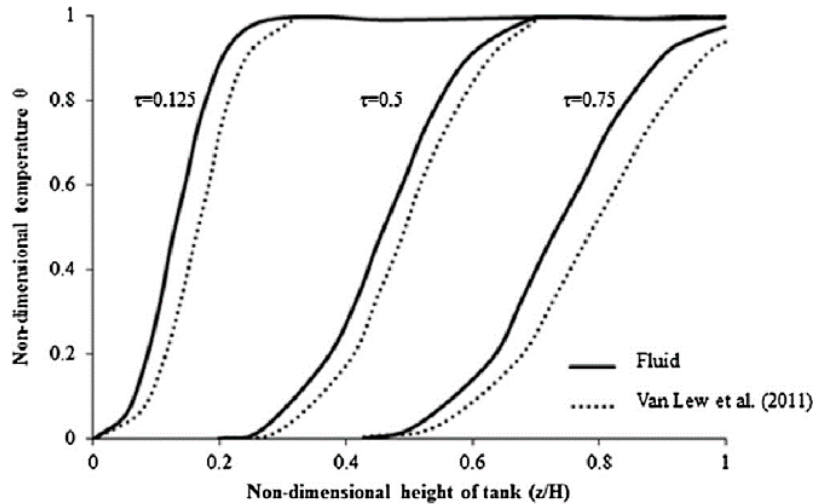


Figure 25 - Validation of the temperature profiles for Therminol® with results of (Van Lew, Li, Chan, Karaki, & Stephens, 2011). The temperature distribution for the selected fluid and quartzite rock is studied and plotted, and the results obtained are validated with (Van Lew, Li, Chan, Karaki, & Stephens, 2011). It is seen that the results are in good agreement (Reddy, Jawahar, Sivakumar, & Mallick, 2017).

When the system is charged, cold fluid is drawn from the bottom, heated with the receiver heat transfer fluid, and then it returns to the top of the tank. When the tank is discharged, hot fluid is drawn from the top, cooled as it passes through a heat exchanger – the ORC evaporator - to transfer heat for MDM phase change, and then it returns to the bottom of the tank. It is chosen to study a thermocline system not only because it has the potential to reduce the cost of the thermal storage system, but also because it can dispatch thermal energy at nearly a constant temperature over most of its discharge cycle (Pacheco, J.E., Showalter, & Kolb, 2001).

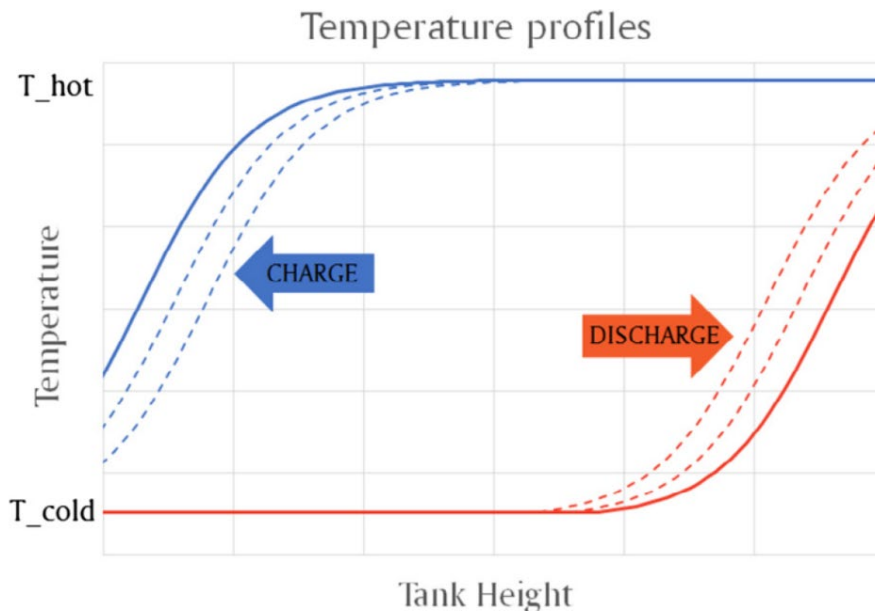


Figure 26 - Temperature distribution in a thermocline tank during charge and discharge. When the thermocline zone reaches the bottom part of the tank at the end of the charging process, the temperature of this lower section of the tank starts to increase. Conversely, the outlet temperature from the tank decreases if the thermocline region reaches the upper part of the tank during discharge (Rodríguez, Sánchez, Martínez, Bennouna, & Ikken, 2016)

Also, it is essentially to state that the temperature in the inlet of the collector field is assumed to be equal to the temperature inside the lowest zone of the tank and the temperature to the evaporator inlet is assumed to be equal to the temperature level in the highest zone of the storage tank: this is of fundamental importance for coupling the storage tank with the other devices of the plant.

About the geometry of the thermocline tank, although for sake of simplicity the diameter of the tank can be selected to be equal to its height, as seldom seen on the literature (Pavlovic, et al., 2017), because of height required for the thermal gradient, taller tanks with smaller diameters are favoured over shorter tanks with larger diameters. Also, as the device stores energy only by sensible heat in one tank, high volume is required; therefore, as the height of the tank is fixed to an upper limit due to the bearing capacity of the underlying soil, the diameter must increase (Ferruzza, 2015). The tallest tanks that can practically be fabricated for such a purpose have a bed height of 16 m (Pacheco, J.E., Showalter, & Kolb, 2001). Moreover, it is important to stress that the assumptions done for the storage tank shape and volume have a low impact on the results because the present study is done in steady-state conditions (Bellos & Tzivanidis, 2017). Constant pressure is prescribed in the tank, thus considering an ideal pressurization system. The adopted hypotheses account for changes in the volume of fluid, as a consequence of thermal expansion and mass balance.

In this analysis thermal losses are, again, neglected except for the thermocline tank: all components are thermally insulated to the environment except for it; the thermal losses of the component account for 2% of its nominal thermal power. This assumption is quite realistic and is commonly adopted in literature; also, when imperfect insulation of the TES tank is considered, heat losses to the environment are estimated to be less than 2% of the thermal power actually supplied by thermocline (Oyekale, Heberle, Petrollese, Brüggemann, & Cau, 2019); (Petrollese, Cau, & Cocco, 2020); (Rodríguez, Sánchez, Martínez, Bennouna, & Ikken, 2016); (Pina, Lozano, Serra, Hernandez, & Lazaro, 2021); (Sun, Yue, & Wang, 2017); (Borunda, Jaramillo, Dorantes, & Reyes, 2016). For what concerns exergy losses due to deterioration of the stratification, they are neglected: such simplification is typically justified for daily charge-discharge cycles, that means relatively short standstill times (Haller, et al., 2010).

Control strategy

The operating strategy of the overall CSP-TES-ORC power system greatly influences the reliability and profitability of the plant. In general, in case of small-to-medium scale solar ORC systems, the ORC power generation is completely devoted to cover the corresponding load demand, and the TES system, if present, is used to face some perturbations such as a cloud passing or a low temperature of the HTF loop. The main objective is related to the maximization of the energy production; sometimes the HTF is even directly sent to the power block, which often operates in off-design conditions, and only the energy surplus is diverted toward the storage system (Rodríguez, Sánchez, Martínez, Bennouna, & Ikken, 2016).

In this case, the hot heat transfer fluid delivered by the solar field is sent to the evaporator of the power block in order to maximise the production of electricity. Only when rated conditions are achieved - that is 100% output at generator terminals for the given ambient conditions - the surplus thermal power is diverted towards the storage system. This strategy is currently the standard practise in most CSP facilities worldwide because of its simplicity and because it

maximises the annual yield (Rodríguez, Sánchez, Martínez, Bennouna, & Ikken, 2016). At the same time though, the main disadvantage is the instability that comes about if there is a sudden, drastic reduction of incoming solar energy. As illustrated in figure, this would increase the number of start-up and shutdown events in the power block.

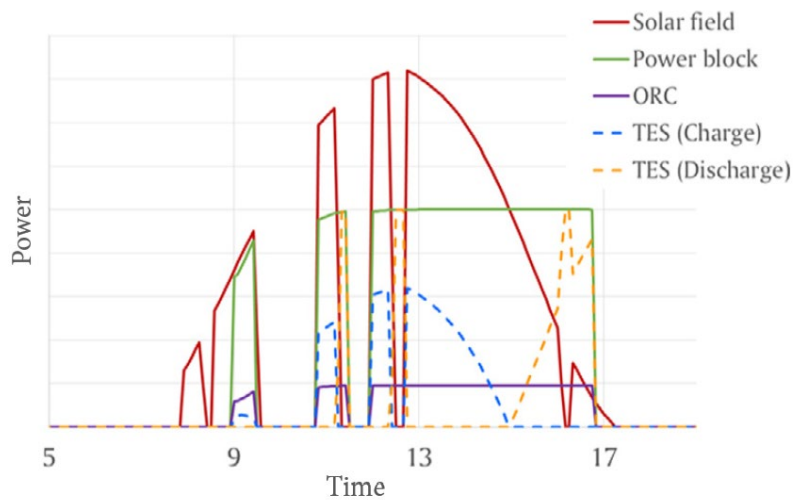


Figure 27 - General plant operation during a cloudy day with priority to power block strategy. Adapted from (Rodríguez, Sánchez, Martínez, Bennouna, & Ikken, 2016)

In alternative, as proposed in (Patil, et al., 2017), the thermal storage can be privileged and the power block operation is postponed when the TES is completely charged. Thermal storage utilisation is more intense with this second strategy, with higher values of total energy charged and discharged, that is nonetheless to be expected since this strategy is set to fully charge the storage system every day. Actually, the main advantage of the second strategy does not come from the energy balance but from an operational standpoint: the reduction of start/stops and the generation of power at constant output have several benefits for the plant: lower operation and maintenance costs, energy dispatchability regardless of the available solar resource, steady operation of the turbine at rated conditions, which means maximum efficiency, for longer periods.

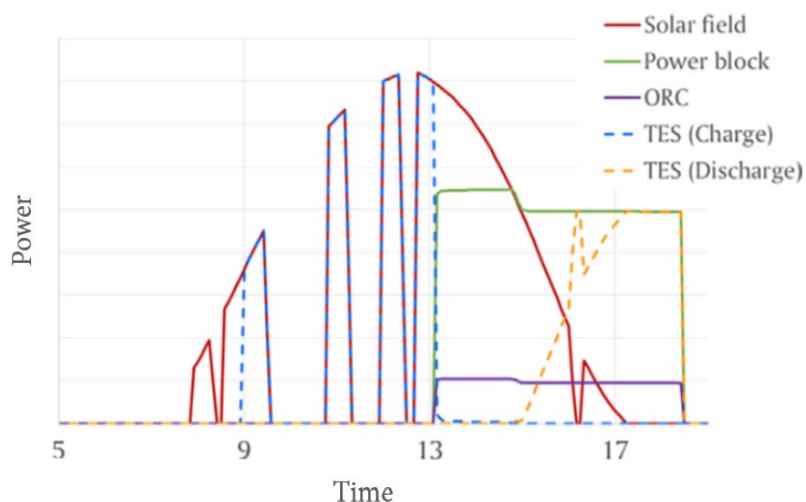


Figure 28 - General plant operation during a cloudy day with priority to TES strategy. Adapted from (Rodríguez, Sánchez, Martínez, Bennouna, & Ikken, 2016)

The first strategy systematically generates more energy than the alternative one. This surplus electricity production, averaging 11% (Rodríguez, Sánchez, Martínez, Bennouna, & Ikken, 2016), is to be expected though from the fact that electricity generation is prioritised with respect to energy storage. The first strategy also shows a better use of the solar resource throughout the year, with lower values of energy dumped out of the system. With the second strategy, the total amount of energy that cannot be exploited is higher. The increased production of electricity and the lower values of dumped energy yield higher efficiency when the first strategy is employed.

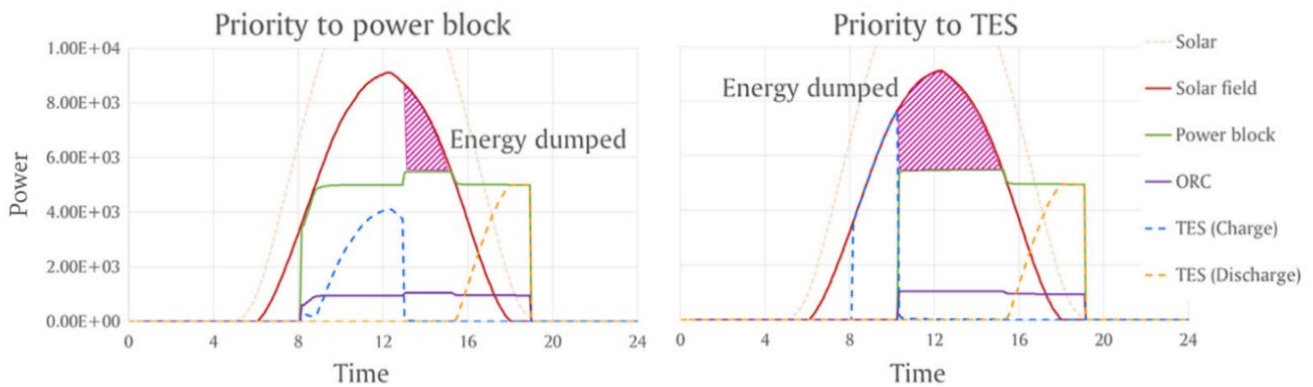


Figure 29 - Comparison of dumped energy for both operating strategies. Adapted from (Rodríguez, Sánchez, Martínez, Bennouna, & Ikken, 2016)

This suggests that prioritising power production is the most suitable scheme to operate the ORC power plant. To sum up, the control strategy provides that:

The system starts up only after a certain threshold of thermal energy available to the evaporator is surpassed by the solar fluid energy, in this way bypassing the TES;

When the energy supplied by the solar circuit is able to satisfy the evaporator request, the excess thermal energy goes to charge the TES;

In the afternoon, once there is no longer enough energy from the solar circuit, the TES supplies the necessary heat to the evaporator for a number of hours equal to its capacity, assumed to be equal to 4 hours;

Once the TES is discharged, the system no longer produces electricity.

About regulation, the solar loop is managed by a feedback controller operating on a variable speed pump. Such controller receives temperature readings measured at the bottom of the tank, that is the solar collector inlet temperature, and at the outlet of the solar collector loop, and it returns a control signal used to vary the pump mass flow rate, in order to achieve the desired outlet set point temperature equal to 350 °C. Notice that during the charging cycle, the temperature of the cold oil entering the heat exchanger is constant until the gradient reaches the bottom of the tank. At that point the temperature coming out of the bottom of the tank starts to rise. Similarly, during a discharge cycle, the hot oil coming off the top of the tank is nearly constant until the gradient enters the top. Then the hot salt temperature starts to decay. This ensures that the storage tank is always loaded from the top with fluid at the design temperature, thus avoiding as much as possible mixing phenomena that could reduce the efficiency of the downstream ORC system (Casati, Desideri, Casella, & Colonna, 2012). In

addition, the controller also stops the pump when the solar collector outlet temperature is lower than the tank bottom temperature, since in such case the solar field would dissipate heat. Such controller also receives the measured value of the incident solar radiation, stopping the pump when the irradiance falls below a certain value, thus preventing heat dissipation. Thus, the hot solar oil supplies the heat side of the thermocline.

On the load side of the thermocline tank, the fluid is pumped by a second pump to the ORC. The ORC is designed in order to operate at fixed flow rate, therefore the pump is a fixed speed pump (Calise, Dentice d'Accadia, Macaluso, Piacentino, & Vanoli, 2016). In fact, with decreasing mass flow rate of the heat source, the mass flow rate of ORC working fluid flowing through the turbine is decreased to, and this leads to a reduction in enthalpy difference: the overall consequence of this reduction stands in a lower turbine isentropic efficiency. Similarly, deviation of mass flow rate of heat source from design value would have considerable effect on the volume flow of organic fluid through the pump. Moreover, according to one of the main players in ORC power units manufacturing that is Turboden (Turboden, s.d.), generally the minimum thermal power that would keep the plant running is equivalent to 40-to-50% of its nominal value, below which an ORC unit of power rating comparable to the one of this thesis would not work in an efficient way.

It is, then, assumed that the plant is in operation only when there is enough solar resource available to drive the ORC, that is, when the solar thermal production is higher than 76,86 kW_t. The ORC is assumed to operate only at full load, thereby requiring a constant heat supply, which is made possible by the solar system sort-of-hybridization with the thermal energy storage. In this way, a feasible and more reliable operation, as well as a more secure energy supply, is achieved. By doing so, the operating hours of the solar system vary significantly throughout the year according to the solar resource availability. Such a variation in the solar resource would entail the implementation of large TES system in fixed approach, a situation that is unfavorable to its economic performance: in fact, despite the integration of TES systems in modern designs, most CSP-ORC plants are usually shut down for several hours within the year. This is usually due to insufficient TES capacity, as economic implications of implementing large TES systems and solar fields are often not favorable. Concentrating solar systems require high values of DNI to be cost-effective, resulting in a performance drop at high latitudes. Therefore, the exploitation of solar energy through concentrating solar technologies can be considered a valid and 100% renewable option for supplying heat and power when located in middle and low latitudes (Cocco, Petrollese, & Tola, 2017).

In this thesis, weather data for Torino are used for simulating the system performance for all year period. Torino is located in the North-West of Italy, having latitude of 45°04' N and longitude of 7°42' E (Google, s.d.). Weather data about the solar irradiation and the ambient temperature are obtained from the weather station of Politecnico di Torino. The available data have been recorded throughout the year 2020, with 15-minute intervals. The methodology used in this study has been to consider a monthly average, calculated starting from the measurement recorded at the specific time and repeated for all days of the month, and to make it the reference of the whole month. The graphs representing the daily air temperature and the direct normal irradiation trends are shown; since the DNI trend is much more scattered than the temperature one because of its implicit intermittence, due to the simple passage of clouds, the chart relative

to the temperature is more compact while the chart relative to the solar irradiation is split into four seasonal sub-charts.

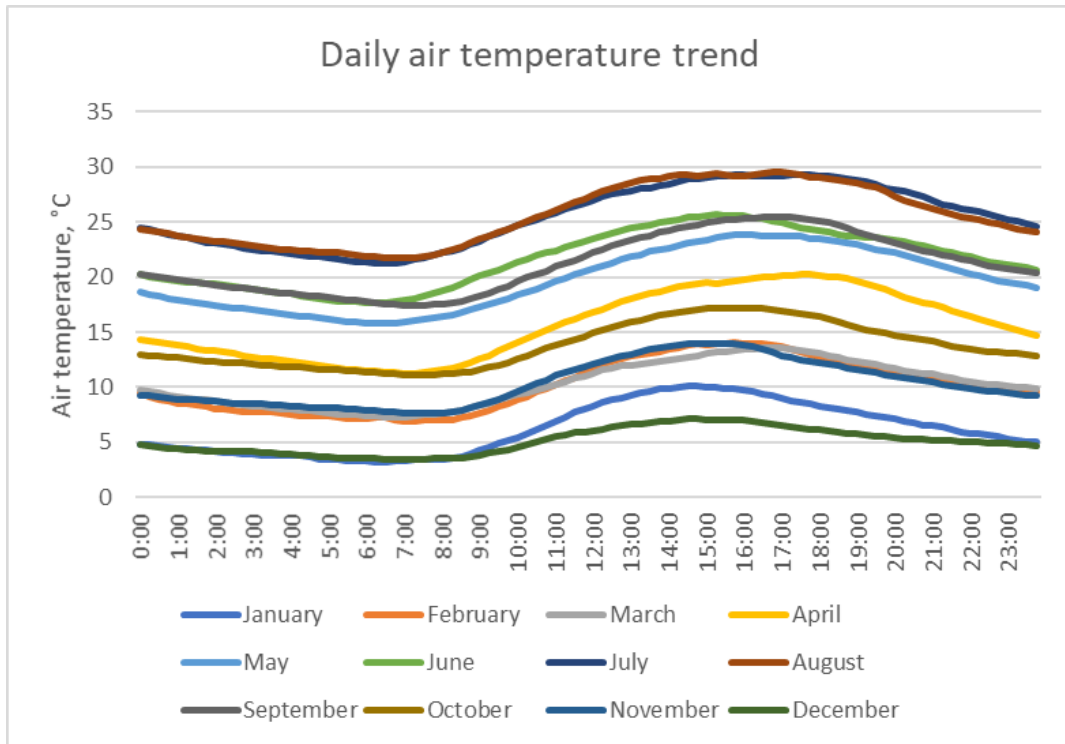


Figure 30 – Daily air temperature trend recorded in Torino during 2020. Each month's curve stands for its most significant-day's curve

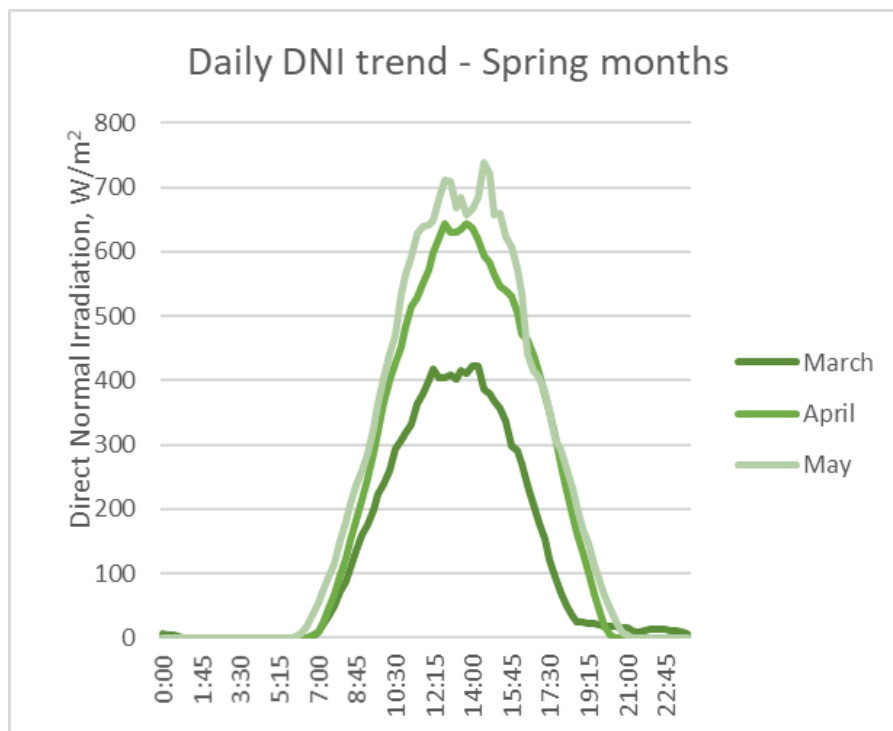


Figure 31 - Daily DNI trend recorded in Torino during Spring 2020. Each month's curve stands for its significant-day's curve

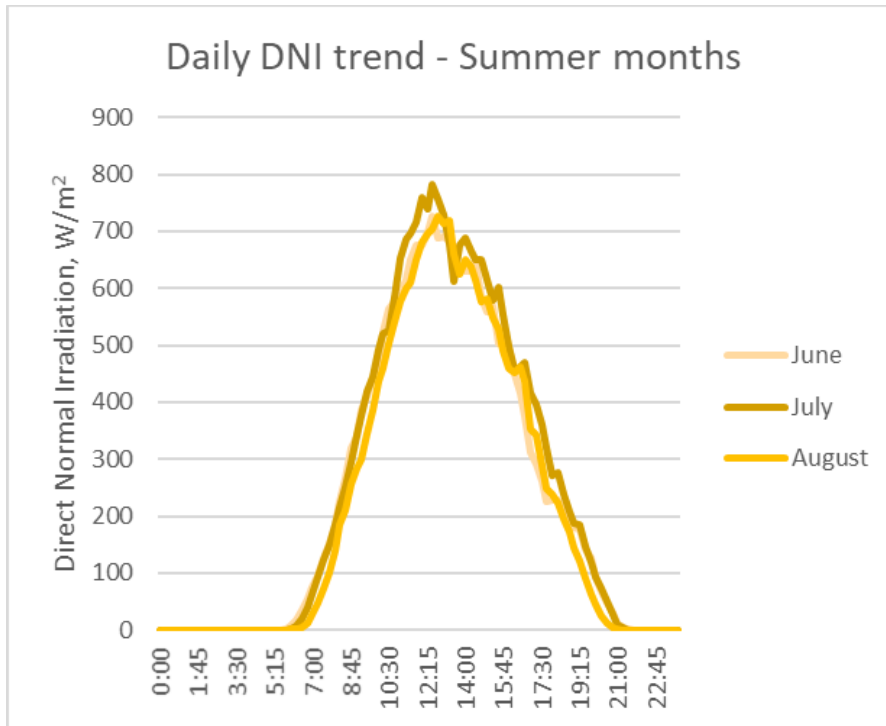


Figure 32 - Daily DNI trend recorded in Torino during Summer 2020. Each month's curve stands for its significant-day's curve

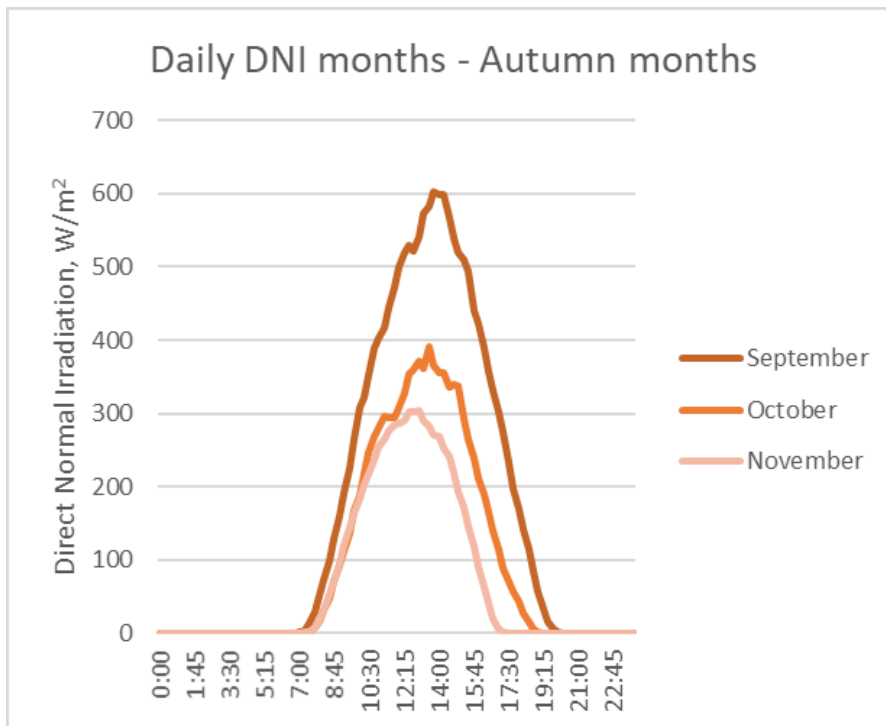


Figure 33 - Daily DNI trend recorded in Torino during Autumn 2020. Each month's curve stands for its significant-day's curve

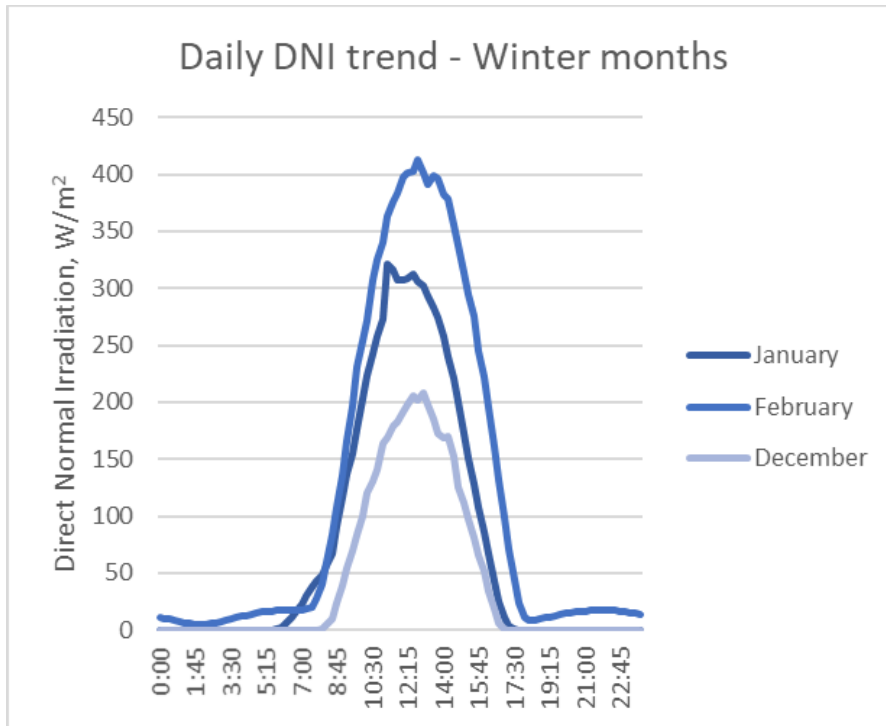


Figure 34 - Daily DNI trend recorded in Torino during Winter 2020. Each month's curve stands for its significant-day's curve

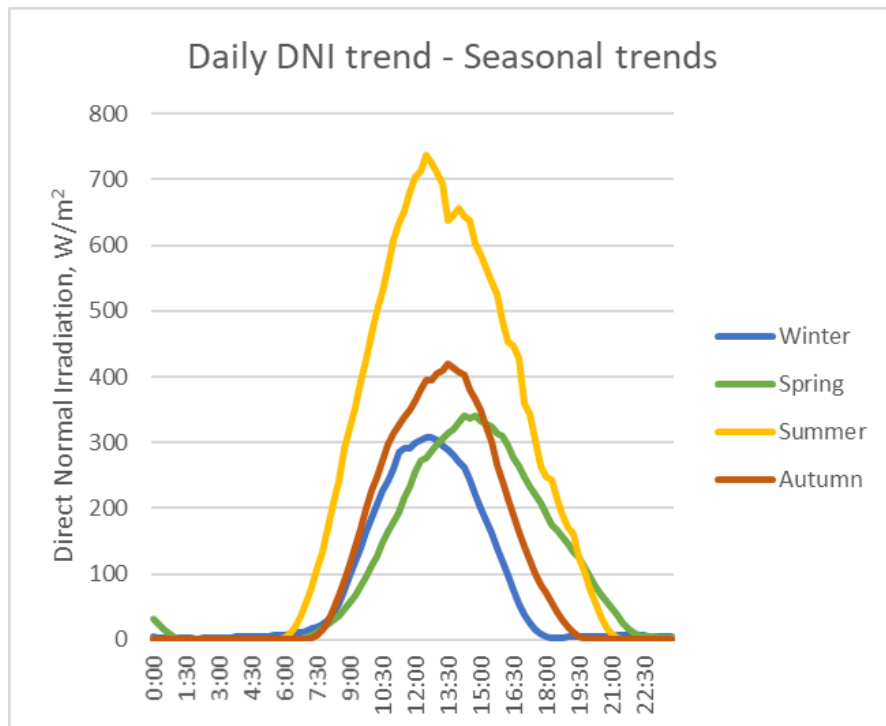


Figure 35 - Daily DNI trend recorded in Torino during 2020. Each season's curve stands for the average trend between its months. Each month's curve stands for its significant-day's curve

Productivity

When sizing the system, both the solar field and the thermal energy storage sections, it is important to keep in mind that the meteorological data of the location taken into consideration are not exactly the data of a typical location suitable for hosting a CSP system: the DNI design value which is usually referred to is equal to $800 \frac{W}{m^2}$, while observing the data about Turin it is clear that, in 2020, on average, the DNI never reaches that value, and only approaches it in July and August. In general, the plant can rely on a huge solar resource in Summer, on a moderate solar resource in Autumn and Spring but cannot rely on it in Winter, when the peak value is about $400 \frac{W}{m^2}$. It is therefore decided to assume $500 \frac{W}{m^2}$ as the Direct Normal Irradiation value at nominal conditions.

In this way, knowing that the capturing surface of the single solar collector is equal to $4,5 m^2$, and assuming that the optical efficiency of the collector declared by the supplier in project conditions remains constant as the DNI varies, that means it is still equal to 80%, then the rated power of the single collector becomes:

$$\dot{Q}_{solar\ dish} = DNI \cdot S \cdot \eta_{optical} = 500 \frac{W}{m^2} \cdot 4,5 m^2 \cdot 0,8 = 1800 W \quad [55]$$

The single solar dish collector located on the rooftop of Politecnico di Torino Energy Center is not sufficient to power a 10 kW ORC unit since its rated power is much lower. In this regard, since the rated power of the single solar dish is equal to 1,8 kW, by rounding to the nearest unit it is found that the number of solar collectors needed to satisfy the thermal requirement in rated conditions is 40. Unfortunately, being the Energy Center's solar system being used only for education, the solar field is severely undersized with respect to the organic Rankine cycle, and as a consequence, the system cannot operate as intended so it is assumed that the system is perfectly ideal – no hypotheses are made on the efficiencies of the individual subsystems because they would be completely far from reality, since the plant is not even assembled - and that there are no thermal losses towards the environment along the path of the fluid that goes from the solar field to the power block, passing through the thermocline. Since the heat output required from the evaporator is equal to 76,86 kW, the number of solar collectors required to satisfy the power needs is:

$$Number\ of\ solar\ collectors = \frac{\dot{Q}_{solar\ field}}{\dot{Q}_{solar\ dish}} = \frac{76,86}{1,80} = 42,7 \approx 43 \quad [56]$$

After having quantified the number of collectors, the productivity analysis of the solar field can be carried out. The following graph shows the daily trend of the thermal power made available by the solar field, assumed to be made of 43 collectors, month by month. The orange, thick line stands for the constant power requested by the evaporator in the base-case ORC setup.

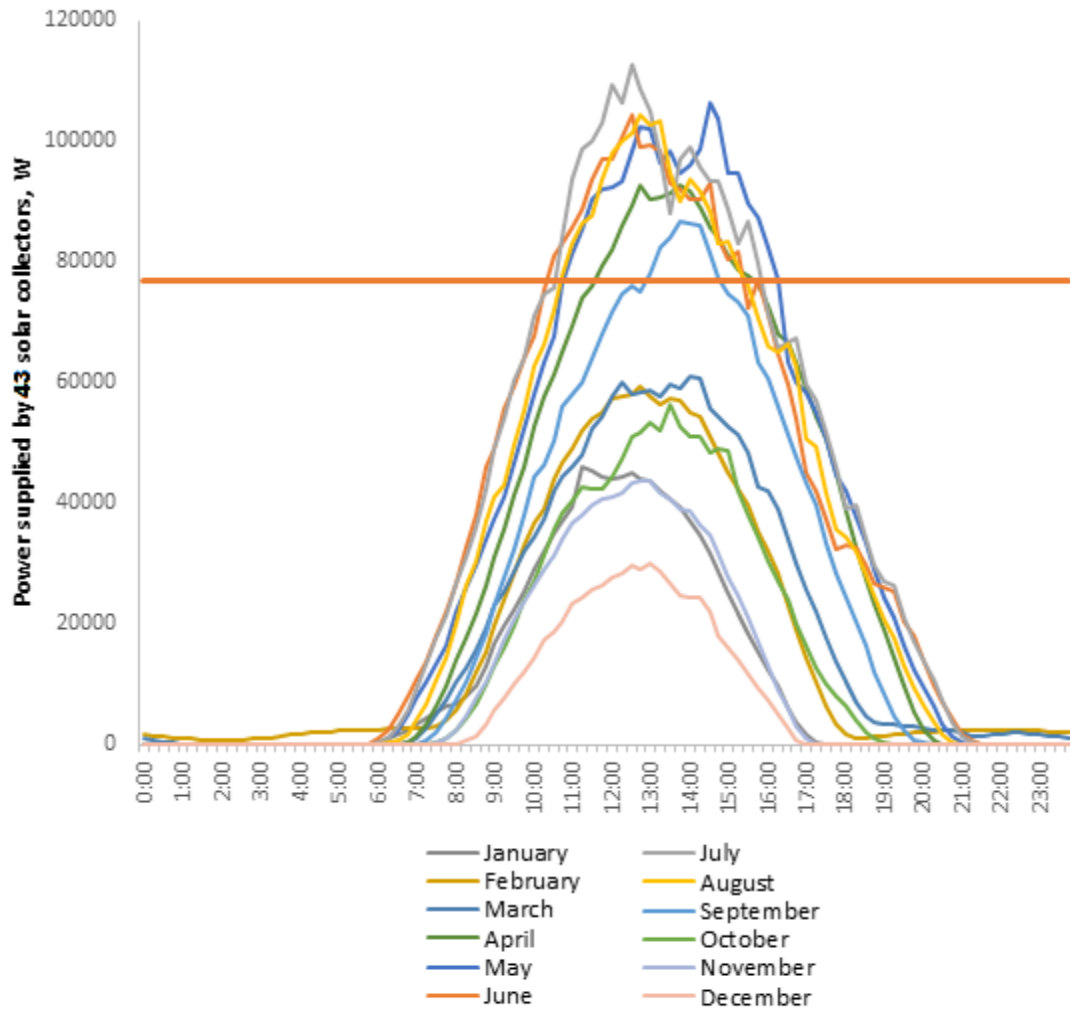


Figure 36 - Daily trend of the thermal power made available by the solar field with respect to the constant thermal power needs, month-by-month

In this way, that is, in the absence of any thermal energy storage, the system is able to work effectively for six months, that is, for half a year. In the months going from April to September, the power block would be active, running at full capacity, at the following daytime intervals:

| Month | Switch-on time | Switch-off time | Operating hours |
|-----------|----------------|-----------------|-----------------|
| April | 11:35 | 15:40 | 4 h 5 min |
| May | 10:45 | 16:15 | 5 h 30 min |
| June | 10:20 | 15:25 | 5 h 5 min |
| July | 10:30 | 15:50 | 5 h 20 min |
| August | 10:40 | 15:25 | 4 h 45 min |
| September | 12:55 | 14:50 | 1 h 55 min |

Table 5 - Power block operation times at working conditions

Thus, producing an amount of electrical energy equal to:

$$\text{Yearly energy} = \text{Rated power output} \cdot \text{Working hours at rated conditions} = 10 \text{ kW}_{el} \cdot 26,67 \text{ h} = 266,7 \text{ kWh}_{el} \text{ [57]}$$

It is noteworthy the large area of the solar field required to obtain a mild yearly energy production, also considering that the power unit is able to work for half a year only. The situation changes when the contribution of thermal energy storage is considered too. The system incorporates a TES to increase the stability of the solar field thermal production, as well as to allow for the production of electricity thanks to the solar resource until the end of the day. The TES system is designed as capable of storing the entire HTF volume required to match the TES energy content, and the volume is calculated considering average material property values for the tank design temperatures. The tank capacity is expressed in equivalent hours of the solar system operation at full load. The corresponding TES thermal capacity corresponds to the design-point thermal requirement that the solar system should provide, multiplied by the total number of desired storage hours, equal to 4. Thermal losses toward the environment, accounting for 2% of the power input, have to be considered too. Knowing that, at a temperature of 300 °C, Therminol® VP-1 has a density of $812 \frac{kg}{m^3}$ and a specific heat of $2319 \frac{J}{kg \cdot K}$ (Reddy, Jawahar, Sivakumar, & Mallick, 2017), and by using the following relation:

$$Q_{tank} = \dot{Q}_{evaporator} \cdot 1,02 \cdot h_{eq,tank} = m_{oil} \cdot c_{p,oil} \cdot (T_{inlet,tank} - T_{outlet,tank}) = V_{oil} \cdot \rho_{oil} \cdot c_{p,oil} \cdot (T_{inlet,tank} - T_{outlet,tank}) \quad [58]$$

It is found out that the tank has a theoretical capacity of about 314 kWh and a volume of $10,7 m^3$. Actually, when quantifying the practical storage capacity of a thermal storage system, it is advisable to compare it to the amount of energy the storage media could hold if the entire inventory were at its upper temperature and discharged completely to its lower temperature. This has been named the percent theoretical capacity. In a thermocline storage system, the percent theoretical capacity is a function of the tank height and is typically about 69% because of the space required by the thermal gradient (Pacheco, J.E., Showalter, & Kolb, 2001). For this reason, it is found out the actual volume of the thermocline to be $15,5 m^3$, in order to guarantee an actual storage having as top temperature 350 °C and as bottom temperature 293,95 °C. At the same time, the height and the radius of the cylindrical-shaped TES are fixed, respectively, at 3 m and 1,3 m.

At this point, it is possible to evaluate the yearly productivity of the plant by also taking into account the role of the thermal energy storage. In the following, it is possible to understand the weight that the storage assumes with respect to the solar contribution, month after month.

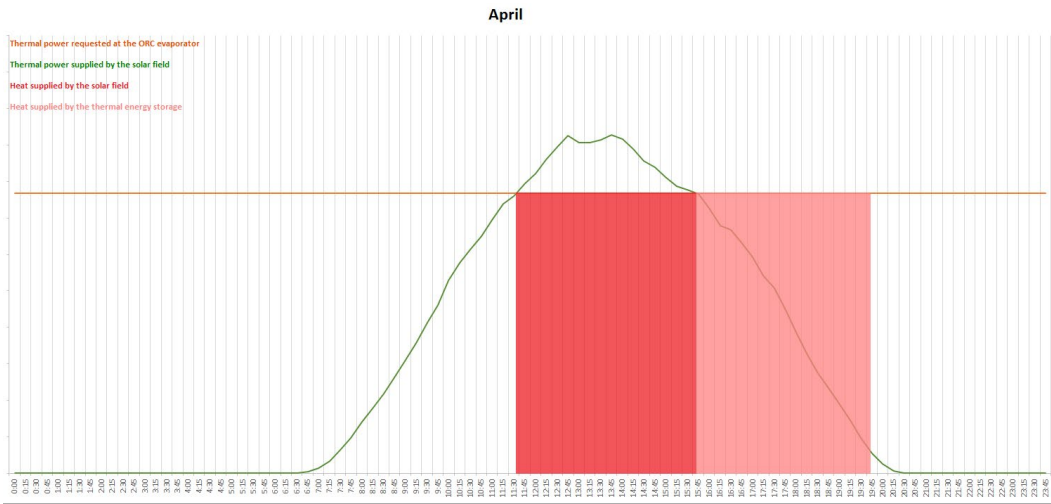


Figure 37 - Power profile during a typical April day

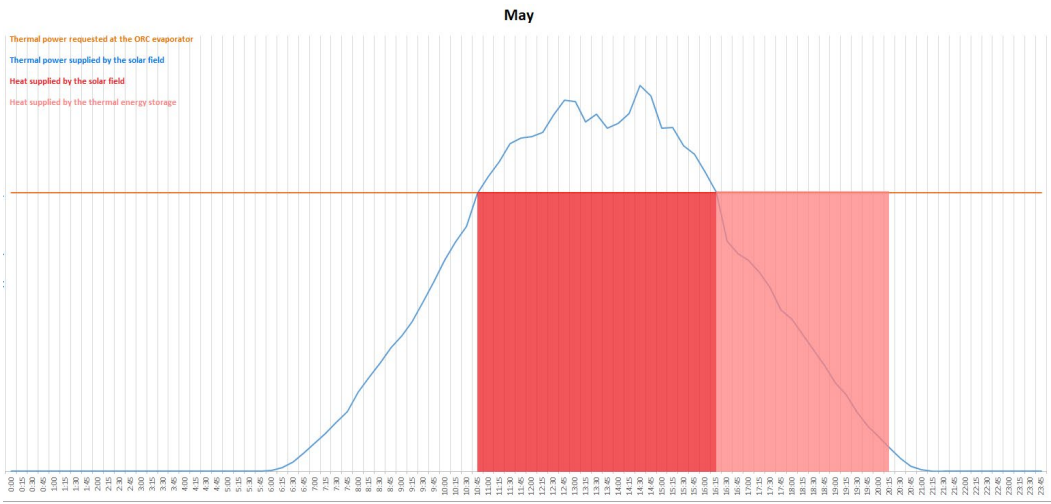


Figure 38 - Power profile during a typical May day



Figure 39 - Power profile during a typical June day

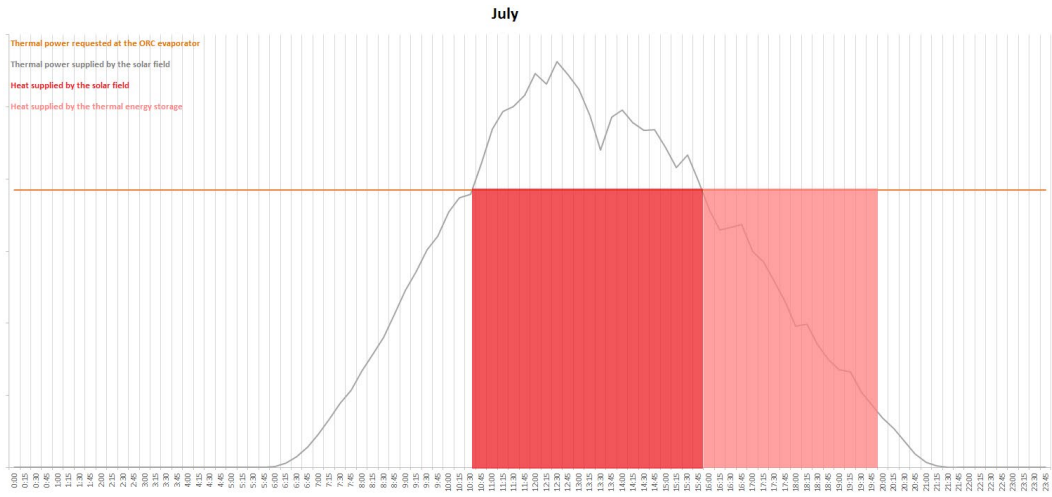


Figure 40 - Power profile during a typical July day

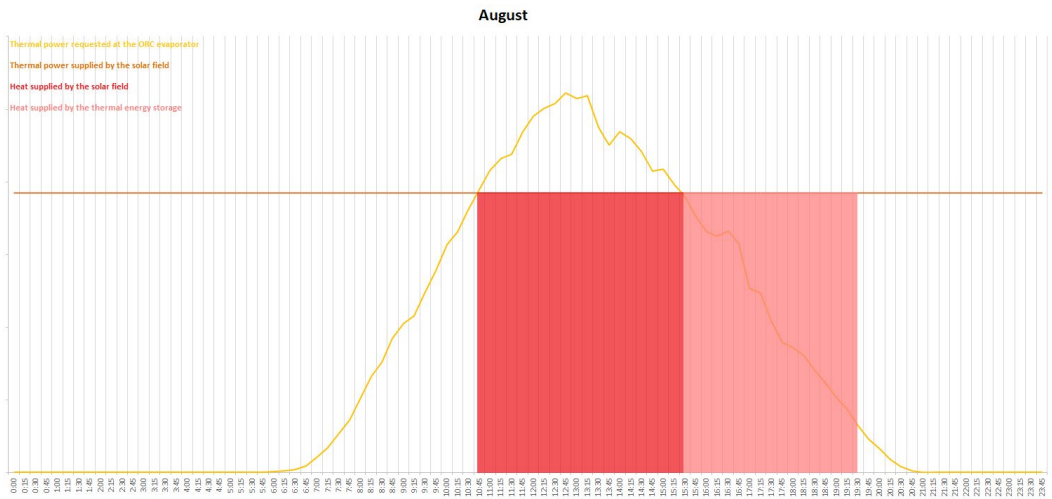


Figure 41 - Power profile during a typical August day

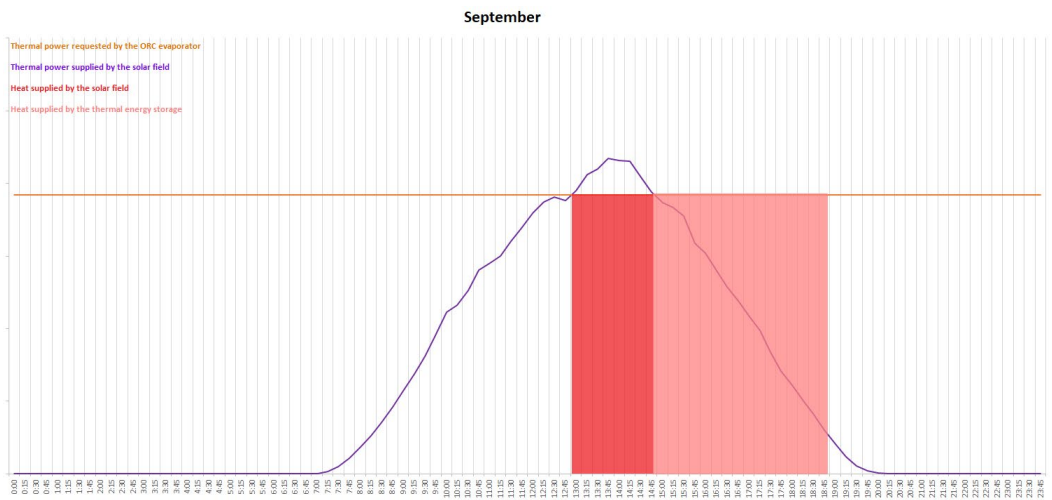


Figure 42 - Power profile during a typical September day

In this way, that is, in the absence of any thermal energy storage, the system is be able to work effectively for six months, that is, for half a year. In the months going from April to September, the power block would be active, running at full capacity, at the following daytime intervals:

| Month | Switch-on time | Switch-off time | Operating hours |
|-----------|----------------|-----------------|-----------------|
| April | 11:35 | 19:40 | 8 h 5 min |
| May | 10:45 | 20:15 | 9 h 30 min |
| June | 10:20 | 19:25 | 9 h 5 min |
| July | 10:30 | 19:50 | 9 h 20 min |
| August | 10:40 | 19:25 | 8 h 45 min |
| September | 12:55 | 18:50 | 5 h 55 min |

Table 6 - Power block operation times at new working conditions

And, applying again [57], the amount of yearly produced electrical energy equal to 506,7 kWh_{el}. Yearly energy production is about doubled thanks to the integration of the single-tank thermal energy storage: this reason justifies its presence within the system.

Exergy analysis

At this point, willing to consider the entire CSP – TES – ORC system, it is needed to analyze the other subsystems apart from the ORC unit from an exergy perspective.

In the following, a simplified model of the TES during its three operating stages - charging, storing, and discharging – is presented, following the discussion presented in (Borunda, Jaramillo, Dorantes, & Reyes, 2016).

In the charging stage, the extra energy collected by the solar field is transferred by the flow of the HTF to the TES. The HTF flow mass is then determined as follows by considering the following equation:

$$\dot{m}_{coll} = \frac{\dot{Q}_{solar}}{(h_{out}-h_{in})_{coll}} \quad [59]$$

where \dot{m}_{coll} is the mass of the HTF to the TES during charging.

An exergy balance for the TES system during the charging stage can be written as:

$$Ex_{solar} - Ex_{destr} - Ex_{loss} = Ex_{\Delta,Ch} \quad [60]$$

where Ex_{solar} is the exergy delivered by the parabolic arrangement, Ex_{destr} is the exergy destruction, Ex_{loss} is the exergy loss, and $Ex_{\Delta,Ch}$ is the exergy accumulation during the charging stage period.

The exergy loss Ex_{loss} is due to the energy flux to the surroundings Q_{loss} and it can be estimated considering:

$$Ex_{loss} = Q_{loss} \cdot \left(1 - \frac{T_a}{T_e}\right) \quad [61]$$

where T_e is the equivalent temperature of a mixed TES, and it can be expressed as:

$$T_e = \exp\left(\frac{T_t[\ln(T_t-1)]-T_b[\ln(T_b-1)]}{(T_t-T_b)}\right) \quad [62]$$

where T_t is the temperature at the top of the TES, and T_b is the temperature at the bottom.

The exergy accumulation $Ex_{\Delta,Ch}$ during the charging stage is described by:

$$Ex_{\Delta,Ch} = Ex_{out} - Ex_{in} = m_{coll} \cdot (u_{out} - u_{in} - T_a \cdot (s_{out} - s_{in})) \quad [63]$$

where u_{out} and u_{in} are the specific internal energy at the outlet and inlet states of the TES respectively, and s_{out} and s_{in} are the outlet and inlet specific entropy of the TES.

The exergy destruction Ex_{destr} is quantified by:

$$Ex_{destr} = N \cdot m_{coll} \cdot ((h_{out} - T_a s_{out}) - (h_{in} - T_a s_{in}))_{coll} - Q_{loss} \cdot \left(1 - \frac{T_a}{T_e}\right) - m_{coll} \cdot (u_{out} - u_{in} - T_a \cdot (s_{out} - s_{in})) \quad [64]$$

The exergy efficiency $\eta_{Ex,ch}$ of the TES during the charging stage is described by:

$$\eta_{Ex,ch} = \frac{Ex_{\Delta,ch}}{Ex_{solar}} \quad [65]$$

The storing stage is the interim stage for a TES to store energy without charging or discharging. An exergy balance for the storing stage can be expressed as:

$$-Ex_{loss} - Ex_{destr} = Ex_{\Delta,st} \quad [66]$$

where $Ex_{\Delta,st}$ is the exergy of the storage and the exergy efficiency of storing period $\eta_{Ex,st}$ is quantified by:

$$\eta_{Ex,st} = \frac{Ex_{\Delta,st}}{Ex_{\Delta,ch}} \quad [67]$$

Finally, during the discharge stage, the stored energy in the TES is recovered to use it in the power block. The outlet oil flow mass m_{ORC} can be evaluated as:

$$\dot{m}_{ORC} = \frac{\dot{Q}_{evap}}{(h_{out}-h_{in})_{evap}} \quad [68]$$

Where \dot{Q}_{evap} denotes the recovered energy from the TES and h_{in} and h_{out} are the specific enthalpies, at inlet and outlet, respectively.

An exergy balance for the TES can be expressed as follows:

$$-(Ex_{evap} + Ex_{loss}) - Ex_{destr} = Ex_{\Delta,Dis} \quad [69]$$

Where Ex_{destr} is the exergy destruction, Ex_{loss} is the exergy loss, $Ex_{\Delta,Dis}$ is the exergy accumulation during discharging stage period, and Ex_{evap} is quantified by:

$$Ex_{evap} = m_{evap} \cdot (h_{out} - h_{in} - T_a \cdot (s_{out} - s_{in})) \quad [70]$$

Here, Ex_{evap} denotes the recovered exergy, h_{out} and h_{in} are the specific enthalpy of the TES outlet and inlet oil respectively, and s_{out} and s_{in} represent the specific entropy of outlet and inlet oil from/to the TES respectively.

Also:

$$Ex_{\Delta,Dis} = Ex_{out} - Ex_{in} = m_{evap} \cdot (u_{out} - u_{in} - T_a \cdot (s_{out} - s_{in})) \quad [71]$$

and

$$Ex_{destr} = m_{evap} \cdot ((h_{out} - T_a s_{out}) - (h_{in} - T_a s_{in}))_{evap} - Q_{loss} \cdot \left(1 - \frac{T_a}{T_e}\right) - m_{evap} \cdot (u_{out} - u_{in} - T_a \cdot (s_{out} - s_{in})) \quad [72]$$

where u_{out} and u_{in} are the outlet and inlet states internal energy of the TES respectively.

The exergy efficiency of the TES during the discharging period, $\eta_{Ex,Dis}$, can be expressed as:

$$\eta_{Ex,Dis} = \frac{Ex_{evap}}{Ex_{\Delta,St}} \quad [73]$$

In this way, an overall exergy balance for the TES during a period of time is defined by:

$$Ex_{solar} - (Ex_{evap} - Ex_{loss}) - Ex_{destr} = Ex_{\Delta} \quad [74]$$

Where Ex_{Δ} is change in the exergy accumulation. Then, the overall Second Law efficiency of the TES can be written as:

$$\eta_{Ex,TES} = \eta_{Ex,Ch} \cdot \eta_{Ex,Dis} \cdot \eta_{Ex,Ch} = \frac{Ex_{evap}}{Ex_{solar}} \quad [75]$$

or in explicit form as:

$$\eta_{Ex,TES} = \frac{m_{ORC} \cdot ((h_{out} - h_{in}) - T_a \cdot (s_{out} - s_{in}))_{evap}}{N \cdot m_{coll} \cdot ((h_{out} - h_{in}) - T_a \cdot (s_{out} - s_{in}))_{coll}} = \frac{Q_{evap} \cdot \left(1 - \frac{T_a}{T_{rec}}\right)}{Q_{solar} \cdot \left(1 - \frac{T_a}{T_{out}}\right)} \quad [76]$$

It is important to point out that the overall efficiency established by the First Law η_{TES} is:

$$\eta_{TES} = \frac{Q_{evap}}{Q_{solar}} \quad [77]$$

Considering the available exergy by the solar field system $\eta_{Ex,solar\ coll}$, the instantaneous Second Law efficiency taking into account the TES, can be described by:

$$\eta_{Ex, TES-solar\ coll} = \eta_{Ex,solar\ coll} \cdot \eta_{Ex, TES} = \frac{\dot{Q}_{solar} \cdot \left(1 - \frac{T_a}{T_{evap}}\right)}{DNI \cdot A_c \cdot \left(1 - \frac{T_a}{T_{sol}}\right)} \quad [78]$$

When the whole system is taken into account, that is the control volume to which the exergy balance applies is extended to the whole system CSP – TES – ORC, then the exergy consumption of the solar dishes has to be taken into account too. For this purpose, it is possible to use the Petela model (Petela, 2003), and set the temperature of the Sun at 5770 K, being it a representative value for the outer layer of the Sun:

$$E_{solar} = Q_{solar} \cdot \left[1 - \frac{4}{3} \cdot \left(\frac{T_{env}}{T_{Sun}}\right) + \frac{1}{3} \cdot \left(\frac{T_{env}}{T_{Sun}}\right)^4\right] \quad [79]$$

By repeating the same procedure applied for the base case, thus applying FLT and SLT together, it is possible to write the exergy balance of each single component and then of the entire system. The application of [29] allows us to obtain the irreversibility generated in the entire CSP-TES-ORC:

| | Irreversibility, kW |
|---------------|---------------------|
| System | 110,347 |

Table 7 - Exergy consumption of the whole system

By applying again, the definition of energy [37] and exergy efficiency [38], the following results are obtained.

| | Power generation | Combined heat and power generation |
|-----------------------------|------------------|------------------------------------|
| Energy efficiency, % | 9,9% | 79,1% |

Table 8 - Obtained energy efficiency of the whole CSP-TES-ORC system

| | Power generation | Combined heat and power generation |
|-----------------------------|------------------|------------------------------------|
| Exergy efficiency, % | 10,6% | 20,8% |

Table 9 - Obtained exergy efficiency of the whole CSP-TES-ORC system

Again, we see that the system can exploit only a tenth of its potential exergy. Although the result is quite disappointing, it should be emphasized that the obtained value is absolutely in line with the typical range of exergetic efficiency of such a system, as already, and widely, discussed in the literature review. ORCs are characterized by rather low efficiencies, typically in the range of 8–12% (Schuster, Karellas, Kakaras, & Spliethoff, 2009), but they are viable for small-scale unsupervised power generation systems because they exhibit great flexibility, high safety, good reliability, and simplicity.

Again, these results are expressed by means of a pie chart showing the percentage weight of each component in exergy consumption:

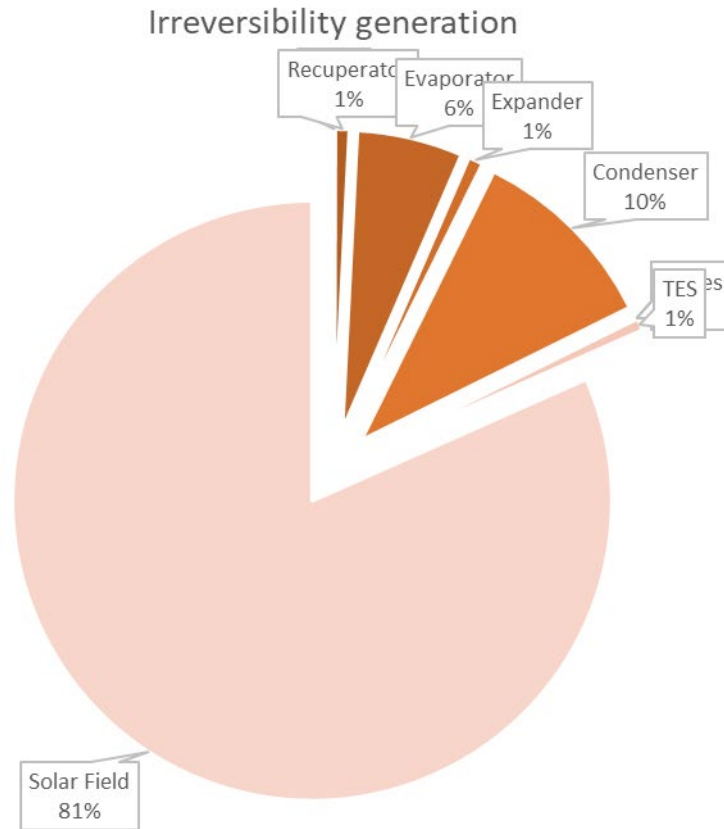


Figure 43 - Pie chart representing irreversibility generation

It is now appreciable the weight of the solar field in the exergy analysis: irreversibilities mostly come from the solar collectors. The thermal energy storage accounts for 1% of the total exergy destruction because of the thermal losses towards the environment, thus having the same contribution of a very efficient heat exchanger as the regenerator, having $\varepsilon \approx 80\%$. On the other hand, the contribution of the new components – the three valves and the sink – is absolutely negligible, accounting for less than 1%. It is difficult to establish whether this result is accurate or not, given the scarcity of scientific papers on the subject. The only scientific article that studies the exergetic behavior of valves that is known by the author, up to now, deals with a non-regenerative organic Rankine cycle – so a different setup with respect to the one considered in the thesis, and identifies the weight of the valves equal to 1% apart for one valve, placed downstream of the turbine, which appears to have a weight of 8%. That said, the graphs showing the general performance of the system are shown.

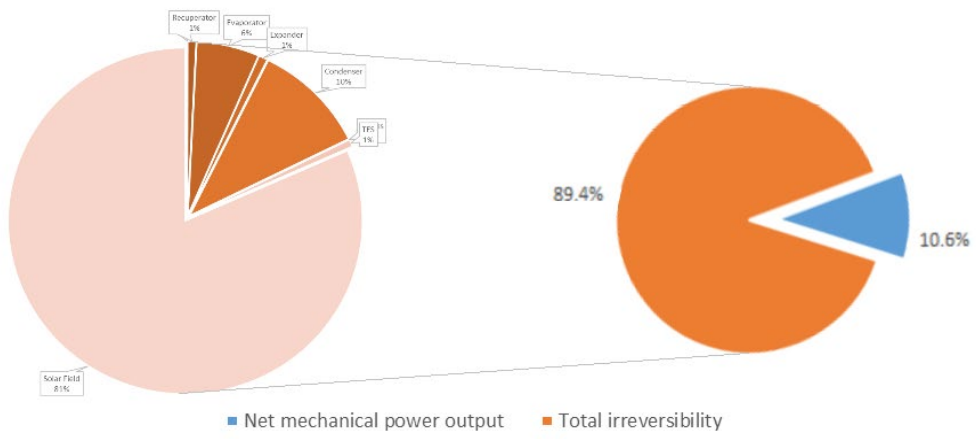


Figure 44 - Exergy output and destruction in the case of sole power generation

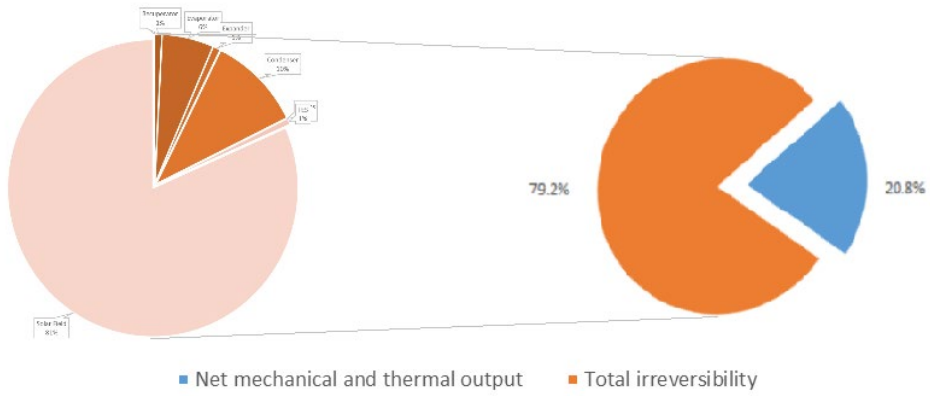


Figure 45 - Exergy output and destruction in the case of combined heat and power generation

Sensitivity analysis

As already extensively described in the previous sections, the analysis of the system in off-design conditions goes beyond the purpose of this thesis. To obtain reliable results, it would be necessary to know the characteristics of the individual components, their technical data sheets, the issues deriving from their assembly, and so on. On the other hand, the desire to study a system as close as possible to a real system is clear, and it is in part fulfilled in the introduction of the valves and of the thermal energy storage. In fact, the presence of the valves not only ensures that the pressure drops, distributed and concentrated, are taken into account in the exergetic analysis, but leads the way for a future, more detailed study on the regulation of this system, as also indicated in the conclusion of this thesis.

With regard to the regulation of the ORC unit, this type of power plant is usually regulated by means of a sliding pressure technique, easy to implement and leading to a reliable operation. Applying this regulation means that the turbine inlet pressure decreases proportionally to the reduction of turbine inlet mass flow, which is usually caused by a reduction of thermal input following the solar radiation variation (Casartelli, et al., 2015). In this case, a slight decrease of the isentropic efficiency of the expander also happens (Petrolese, Cau, & Cocco, 2020). In similar working conditions, a change in the power output depends on the modified evaporator outlet pressure. In addition, the temperature difference between the organic working fluid side and the cooling water side in the condenser is also required to be fixed at a constant value: this ensures that the turbine back pressure does not increase as it can affect the system performance. An adjustment in the mass flow rate of cooling water can maintain the temperature difference between the organic working fluid and the cooling water constant.

The working conditions of the condenser, evaporator and expander are interconnected and decisive for the operation of the plant. For this reason, this thesis is closed by a parametric study concerning the role of the temperature and the pressure at the expander inlet, the condensation temperature and the evaporation temperature. The starting data refer to the system in its full setup. For each of the design parameters, the sensitivity analysis is conducted on 5 different values falling within a reasonable range, which has to be considered within $\pm 20\%$ as suggested in the literature (Ozturk & Dincer, 2021). The five values include the design-condition parameter, the $\pm 10\%$ of its value and the $\pm 20\%$ of its value, to have a symmetric overview of the behaviour. Nevertheless, in a sensitivity analysis the considered values can also be extreme, anyway they are included as long as they are useful to study the behaviour of the system.

The graphical results of the parametric analysis are hereafter reported.

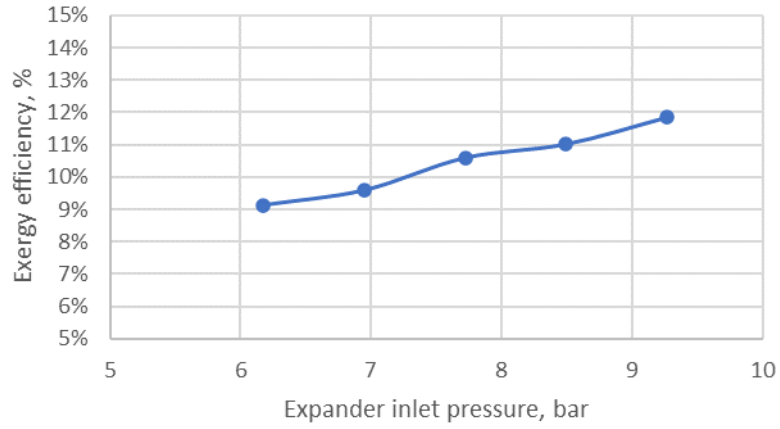


Figure 46 - Exergy efficiency as a function of the expander inlet pressure

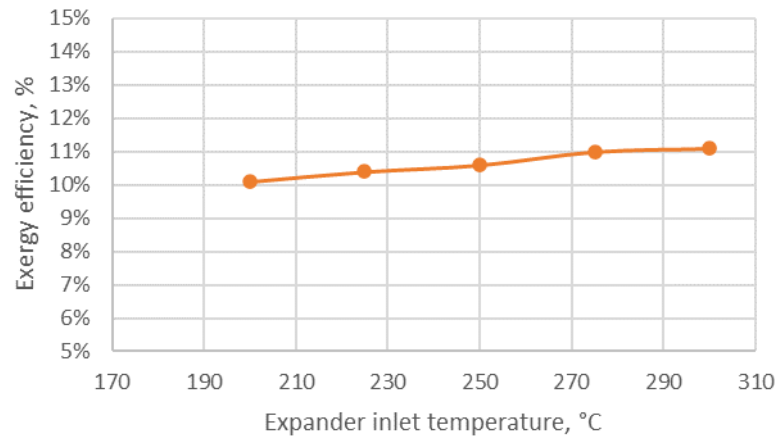


Figure 47 - Exergy efficiency as a function of the expander inlet temperature

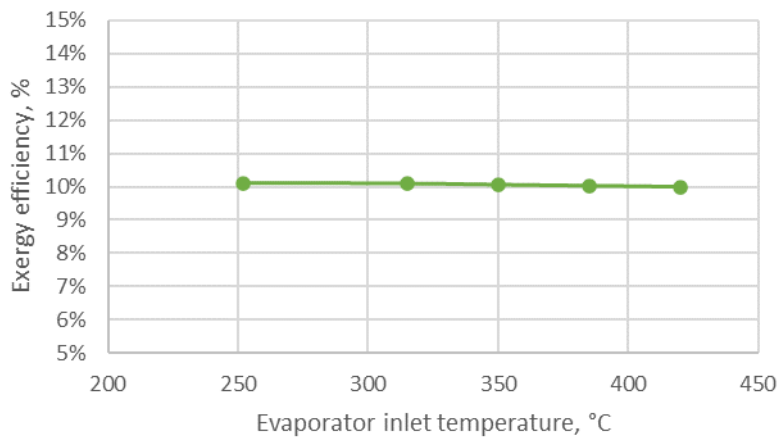


Figure 48 - Exergy efficiency as a function of the evaporator inlet temperature, from the TES side

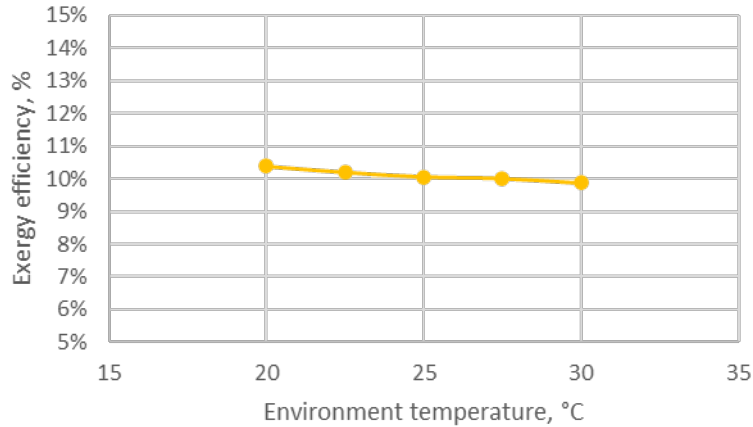


Figure 49 - Exergy efficiency as a function of the environment temperature and, subsequently, of the condensing conditions

First, it has to be pointed out that exergy destruction, in all the system components, is a function of the difference in entropy between inlet and outlet, and exergy efficiency increases with a reduction in exergy destruction. Therefore, as a general rule, as the entropy gradient becomes less significant at lower environment temperatures, the exergy efficiency increases.

The exergy efficiency reduces with the increasing condensation temperature. If the condensation temperature increases, then the specific enthalpy of the organic working fluid at the inlet of evaporator increases, and the heat absorbed by the working fluid from waste heat decreases, leading to a reduction of the net power output of the ORC system. Therefore, the ORC system is suggested to operate at a lower condensation temperature.

Note that the condensation temperature depends on the environment temperature, that is expected to vary significantly because of daily and seasonal temperature variation. When the environment temperature increases, for example in summer, the temperature of cooling water also rises, resulting in an increase in condensing temperature of the existing condenser with unchanged heat transfer surface. The increasing condensing temperature elevates the temperature of the organic working fluid entering the evaporator, where the same amount of transferred heat produces more organic vapor to elevate the evaporation pressure, resulting in an increase in turbine inlet pressure. The mass flow rate of the working fluid entering the turbine also increases. The variation of the turbine mass is consistent with the mass flow rate of working fluid yielded in the vapor generator. In this way, the increasing environment temperature increases the mass flow rate of the working fluid which is regulated by the control system.

The net power output and the average exergy efficiency both decreases when the environment temperature increases: this is because the increased environment temperature increases the condensing temperature, resulting in a rise in turbine back pressure. Thus, although the turbine inlet pressure increases with an increased environment temperature, the enthalpy drop across the turbine still decreases because the increased turbine back pressure has a significantly negative effect on the enthalpy drop across the turbine. Therefore, the reduced enthalpy drop across the turbine contributes to the decrease in turbine power output despite the increase in mass flow rate through the turbine due to higher environment temperature. Due to small power

consumption in the pump, the net power output decreases with the increased environment temperature, also contributing to a decrease in the average exergy efficiency of the system.

In addition, the increased environment temperature enables the heat loss in the thermal storage tank to decrease, while the exergy destruction in the solar field can be reduced by a reduction in reference state temperature, as a result of the fact that solar collectors operate more efficiently at lower temperatures since the lower environment temperature for the solar collectors improves their cooling (Sinasc & Jianu, 2021).

The ORC operating in cold areas generally has a higher exergy efficiency than that in warm areas under given conditions. Thus, the condensation temperature is recommended to be as low as possible under a given environment temperature (Sun, Yue, & Wang, 2017).

It can be also noted that the exergy efficiency of the system slightly increases with the increase of the expander inlet pressure and temperature: that is because the total exergy destruction rate decreases.

If, then, the oil inlet temperature in the evaporator is increased, the exergy efficiency decreases, whereas the system exergy loss increases with the increase in the hot gas temperature. With an increase of the evaporation temperature, the flow rate of the organic working fluid decreases, and the net power output per unit working fluid increases. Hence, the total net power output decreases. Basically, the difference between the evaporator temperature and the hot oil temperature entering the evaporator affects the system performance. The smaller this temperature difference is, the better the exergy efficiency, and less exergy loss are present in the system.

The importance of the operating temperatures of heat exchangers deserves to be investigated, apart from the exergetic considerations already discussed. According to the FLT, both the higher evaporation temperature and the lower condensation temperature lead to an increase of the system thermal efficiency. However, the evaporation temperature and condensation temperature are restricted by the critical temperature of the organic working fluid and the ambient temperature, respectively. The increasing evaporation temperature reduces the heat transfer flux in the evaporator, which may lead to a decrease of the net power output. At the same time, the pinch point temperature difference of the heat exchanger not only influences the evaporation temperature and condensation temperature but also plays an essential role in the well-known cost-efficiency trade-off. The heat exchangers' surface contributes largely to the total cost of an ORC unit, therefore it is necessary to discuss the effect of the PPTD on the heat transfer area.

When the total PPTD is given, with the variation of the PPTD of the evaporator, the heat transfer surface of evaporator and condenser changes simultaneously: it means that the variation of the PPTD of the evaporator affects the area of not only of the evaporator but also of the condenser. In general, the area of the heat exchanger decreases with the increase of the PPTD at the same heat transfer flux. The rational allocation of the PPTDs in evaporator and condenser to achieve more net power output with less heat transfer area by reducing the system irreversibility is the main task in a common optimization process.

The evaporator surface decreases and the condenser surface increases with the increase of the PPTD of the evaporator. Because the heat transfer coefficient of evaporator is generally larger than that of condenser, and the temperature variation of the cooling fluid between the inlet and outlet of the condenser is lower than the one of the thermal oil flowing in the evaporator, the condenser area has the biggest weight on the total heat transfer area (Li, Wang, & Du, 2012).

With the decrease of the pinch point temperature difference, higher evaporation temperature and lower condensation temperature can be achieved between the inlet temperature of waste heat and the heat sink temperature. Meanwhile, more heat transfer area is required with the decrease of the PPTD, which results in an increase of cost for the ORC system.

Part III – Final remarks

The aim of this thesis is to emphasise the significance of the results obtained from an exergy-analysis point of view, especially when applied to new, hybrid concepts of an energy system. From the first exergetic analysis, the one applied only to the organic Rankine cycle aimed at the production of electricity, an exergetic efficiency equal to 25,6% is obtained and the weight of the heat exchangers in the exergetic economy of the system is emphasized: the condenser is the most exergy-consuming component of the system, followed by the evaporator, the expander, the recuperator and finally the pump. The second exergetic analysis, on the other hand, underlines that the vast majority of exergy destruction occurs in the solar field, 81% to be exact; at the same time, the contribution of the new thermal energy storage is equal to 1%, while that of the valves and tank is negligible. The exergetic efficiency of the system composed of concentrated solar power-thermal energy storage-organic Rankine cycle is equal to 10,6% if the production of electricity alone is considered as the useful effect. Finally, the behaviour of exergetic efficiency is parametrically evaluated as the operating conditions of the plant vary. The results are in line with the scientific literature.

The developments presented in this work open a whole area of further research: the relevance of the addressed issue is crystal clear, as it is of the new hybrid-plant configurations that are rapidly providing themselves a space in the scientific literature. The models and methods could be adapted to alternative ORC configurations or advanced cycle designs – perhaps, in the future, included within energy systems having a high degree of flexibility - such as supercritical ORC units, ORCs using zeotropic substances, two-phase expansion cycles or multiple evaporation pressure cycles, just to name a few.

On the other hand, the strong limitations of this thesis work have to be taken into account too. The models themselves could be further validated, as in steady-state as in transient-state conditions. The control strategies developed for the particular case could be further improved, validated and proof-tested on other applications, such as a highly transient solar ORC, with or without any storage, by taking into account the switching-on and switching-off time requested by the plant too. Moreover, a more detailed analysis of the thermocline degradation during a yearly operation could be done, in order to understand the thermo-physical degradation of the materials under different operational cycles.

Nevertheless, the different results proposed in this work show that small-scale ORC systems are feasible from a technical point of view. The reached energy and exergy efficiencies are low, having magnitude of about 10%, but this is counterbalanced by the inexpensive nature of the heat source – solar energy - and by the low cost of the system, except for the solar field which usually has only a significant initial cost.

In addition to the realization of a working, small-sized system connected to the solar concentrator located on the rooftop of Energy Center, and beyond a subsequent experimental validation of the results obtained, more work will be needed to evaluate the economic profitability of such small-scale systems, as well as their potential contribution to the current general effort towards sustainable energy conversion, given that the economic aspect of a new energy system powered by renewable sources is fundamental and its profitability is as important as its efficiency.

In this context, two prospective studies are proposed to illustrate the utility of the developed results. The first one is a thermo-economic and exergo-economic analysis of the same small-scale solar-ORC system, to improve economic evaluations that, up to now, mainly deal with the evaluation of Levelized Cost of Electricity. The second prospective study, aimed at addressing specifically the environmental issue, is an exergo-environmental analysis. We know that exergy will become more integrated with environmental and ecological assessments, through tools like industrial ecology, life cycle assessment, and others, and applied more widely, so it would be interesting to apply these tools to the system already examined in the thesis.

In the spirit of developing such an evaluation, the emergy concept could also be used. The concept of emergy is an acceptable alternative for the word of conventional monetary index and the assessment of the environmental impact: the types of energy and resources needed can be considered as emergy or “energy memory” to create a specific product or service (Aghbashlo & Rosen, 2018); (Zhang, Guan, Ding, & Liu, 2018). The basic hypothesis of this concept is that life on Earth is created by sustainable solar energy, and any flow of energy, matter and even money can be expressed using the emergy concept, for example the solar equivalent joule (sej) of available energy. The monetary and environmental costs of a given energy flow can be combined using this concept (Chen, Liu, Brown, Gao, & Wu, 2017); (Wang, et al., 2017). Small-scale, RES-based power generation systems have significant impacts on the environment, so analysis of these systems is and will be environmentally necessary.

Bibliography

- Aghbashlo, M., & Rosen, M. (2018). Consolidating exergoeconomic and exergoenvironmental analyses using the emergy concept for better understanding energy conversion systems. *J. Clean. Prod.* 172, 696-708. doi:<https://doi.org/10.1016/j.jclepro.2017.10.205>
- Al-Ali, M., & Dincer, I. (2014). Energetic and Exergetic Studies of a Multigenerational Solar-Geothermal System. *Applied Thermal Engineering*. doi:<http://dx.doi.org/10.1016/j.applthermaleng.2014.06.033>
- Alibaba, M., Pourdarbani, R., Khoshgoftar Manesh, M., Valencia Ochoa, G., & Duarte Forero, J. (2020). Thermodynamic, exergo-economic and exergo-environmental analysis of hybrid geothermal-solar power plant based on ORC cycle using emergy concept. *Heliyon* 6. doi:<https://doi.org/10.1016/j.heliyon.2020.e03758>
- Al-Sulaiman, F. (2014). Exergy analysis of parabolic trough solar collectors integrated with combined steam and organic Rankine cycles. *Energy Conversion and Management* 77, 441-449. doi:<http://dx.doi.org/10.1016/j.enconman.2013.10.013>
- Al-Sulaiman, F., Dincer, F., & Hamdullahpur, F. (2011). Exergy modeling of a new solar driven trigeneration system. *Solar Energy* 85, 2228-2243. doi:<http://dx.doi.org/10.1016/j.solener.2011.06.009>
- Andersen, W., & T.J., B. (2005). Rapid screening of fluids for chemical stability in organic Rankine cycle applications. *Industrial and Engineering Chemistry Research* 44, 5560-5566.
- Bellos, E., & Tzivanidis, C. (2017). Parametric analysis and optimization of a solar driven trigeneration system based on ORC and absorption heat pump. *Journal of Cleaner Production* 161, 493-509. doi:<http://dx.doi.org/10.1016/j.jclepro.2017.05.159>
- Bellos, E., Tzivanidis, C., & Tsimpoukis, D. (2017). Thermal enhancement of parabolic trough collector with internally finned absorbers. *Solar Energy* 157, 514-531.
- Bellos, E., Vellios, L., Theodosiou, I., & Tzivanidis, C. (2018). Investigation of solar-biomass polygeneration system. *Energy Convers. Manag.* 173, 283-295. doi:<https://doi.org/10.1016/j.enconman.2018.07.093>
- Borghero, L. (2021). *Methane-assisted iron oxides chemical looping in a solar concentrator: tests in real conditions on the Energy Center rooftop*. Retrieved from Politecnico di Torino.
- Borunda, M., Jaramillo, O., Dorantes, R., & Reyes, A. (2016). Organic Rankine cycle coupling with a parabolic trough solar power plant for cogeneration and industrial process. *Renew. Energy* 86, 651-663. doi:<http://dx.doi.org/10.1016/j.renene.2015.08.041>
- Boyaghchi, F., & Heidarnejad, P. (2015). Thermo-economic assessment and multi objective optimization of a solar micro CCHP based on Organic Rankine Cycle for domestic application. *Energy Conversion and Management* 97, 224-234. doi:<http://dx.doi.org/10.1016/j.enconman.2015.03.036>
- Buonomano, A., Calise, F., Palombo, A., & Vicidomini, M. (2015). Energy and economic analysis of geothermal-solar trigeneration system: A case study for a hotel building in Ischia. *Appl. Energy* 138, 224-241. doi:<https://doi.org/10.1016/j.apenergy.2014.10.076>

- Calise, F., Dentice d'Accadia, M., Macaluso, A., Piacentino, A., & Vanoli, L. (2016). Exergetic and exergoeconomic analysis of a novel hybrid solar– geothermal polygeneration system producing energy and water. *Energy Conversion and Management* 115, 200-220. doi:http://dx.doi.org/10.1016/j.enconman.2016.02.029
- Casartelli, D., Binotti, M., Silva, P., Macchi, E., Roccaro, E., & Passera, T. (2015). Power block off-design control strategies for indirect solar ORC cycles. *International Conference on Concentrating Solar Power and Chemical Energy Systems, SolarPACES 2014*. doi:http://dx.doi.org/10.1016/j.egypro.2015.03.166
- Casati, E., Desideri, A., Casella, F., & Colonna, P. (2012). Preliminary Assessment of a Novel Small CSP Plant Based on Linear Collectors, ORC and Direct Thermal Storage. *Proceedings SolarPACES 2012*.
- Casati, E., Galli, A., & Colonna, P. (2013). Thermal energy storage for solar-powered organic Rankine cycles engines. *Sol. Energy* 96, 205-219.
- Cau, G., & Cocco, D. (2014). Comparison of Medium-size Concentrating Solar Power Plants based on Parabolic Trough and Linear Fresnel Collectors. *Energy Procedia* 45, 101-110.
- Chen, W., Liu, W. G., Brown, M., Gao, C., & Wu, R. (2017). Recent progress on emergy research: a bibliometric analysis. *Renew. Sustain. Energy Rev.* 73, 1051-1060.
- Cocco, D., & Serra, F. (2015). Performance comparison of two-tank direct and thermocline thermal energy storage system for 1 MWe class concentrating solar power plants. *Energy*, 1-11.
- Cocco, D., Petrollese, M., & Tola, V. (2017). Exergy analysis of concentrating solar systems for heat and power production. *Energy* 130, 192-203. doi:http://dx.doi.org/10.1016/j.energy.2017.04.112
- Cornelissen, R. (1997). Thermodynamics and Sustainable Development. *Ph.D. Thesis, University of Twente, The Netherlands*.
- Dincer, I., & Rosen, M. (2013). *Exergy Energy, Environment And Sustainable Development*. Elsevier.
- Dow. (n.d.). *DOWTHERM™ T Heat Transfer Fluid*. Retrieved from DOWTHERM™: <https://www.dow.com/en-us/pdp.dowtherm-t-heat-transfer-fluid.50720z.html>
- Eastman. (n.d.). *Therminol Heat transfer fluid by Eastman*. Retrieved from Eastman Chemical Company: <http://www.therminol.com/>
- F., K., Dincer, I., Rosen, & . (2015). Energy and exergy analyses of a solar-biomass integrated cycle. *Solar Energy* 112, 290-299. doi:http://dx.doi.org/10.1016/j.solener.2014.11.027
- Ferruzza, D. (2015). *Thermocline Storage for Concentrated Solar Power - Techno-economic performance evaluation of a multi-layered single tank storage for Solar Tower Power Plant*. Retrieved from KTH School of Industrial Engineering and Management.
- Fontalvo, A., Solano, J., Padraza, C., Bula, A., Gonzalez Quiroga, A., & Vasquez Padilla, R. (2017). Energy, Exergy and Economic Evaluation Comparison of Small-Scale Single and Dual Pressure Organic Rankine Cycles Integrated with Low-Grade Heat Sources. *Entropy* 19, 476.

- Gaggioli, R., & Petit, P. (1977). Use the second law first. *Chemtech* 7, 496-506.
- Google. (n.d.). *Maps*. Retrieved from <https://www.google.it/maps>
- Grosu, L., Marin, A., Dobrovicescu, A., & Queiros-Conde, D. (2015). Exergy analysis of a solar combiner cycle: organic Rankine cycle and absorption cooling system. *Int. J. Energy Environ. Eng.*
- Guerriero, E. (2021). *Modellazione di un Ciclo Rankine Organico su piccola scala alimentato da un Sistema a Concentrazione Solare*. Retrieved from Politecnico di Torino.
- Hafez, A., Soliman, A., El-Metwally, K., & Ismail, I. (2017). Design analysis factors and specifications of solar dish technologies for different systems and applications. *Renewable and Sustainable Energy Reviews* 67, 1019-1036. doi:<https://doi.org/10.1016/j.rser.2016.09.077>
- Haller, M., Yazdanshenas, E., Andersen, E., Bales, C., Streicher, W., & Furbo, S. (2010). A method to determine stratification efficiency of thermal energy storage processes independently from storage heat losses. *Solar Energy* 84, 997-1007. doi:<https://doi.org/10.1016/j.solener.2010.03.009>
- Hammond, G., & Stapleton, A. (2001). Exergy analysis of the United Kingdom energy system. *Proceedings of the Institution of Mechanical Engineers* 215 (2), (pp. 141-162). doi:<https://doi.org/10.1243/0957650011538424>
- Hassoun, A., & Dincer, I. (2015). Analysis and performance assessment of a multigenerational system powered by Organic Rankine Cycle for a net zero energy house. *Applied Thermal Engineering* 76, 25-36. doi:<http://dx.doi.org/10.1016/j.applthermaleng.2014.11.017>
- IRENA. (2020). *Global Renewables Outlook: Energy transformation 2050*. Retrieved from International Renewable Energy Agency.
- Javaherdeh, K., Amin Fard, M., & Zoghi, M. (2016). Thermo-economic analysis of organic Rankine cycle with cogeneration of heat and power operating with solar and geothermal energy in Ramsar. *Modares Mechanical Engineering, Proceedings of the Second International Conference on Air-Conditioning, Heating and Cooling Installations, Vol. 16, No. 13,* (pp. 56-63).
- Karellas, S., & Braimakis, K. (2015). Energy–exergy analysis and economic investigation of a cogeneration. *Energy Conversion and Management*. doi:<http://dx.doi.org/10.1016/j.enconman.2015.06.080>
- Kestin, J. (1980). Availability: the concept and associated terminology. *Energy* 5, 679-692. doi:[https://doi.org/10.1016/0360-5442\(80\)90088-2](https://doi.org/10.1016/0360-5442(80)90088-2)
- Khalid, F., Dincer, I., & Rosen, M. (2016). Techno-economic assessment of a renewable energy based integrated multigeneration system for green buildings. *Applied Thermal Engineering*, 1286-1294. doi:<http://dx.doi.org/10.1016/j.applthermaleng.2016.01.055>
- Khan, Y., & Mishra, R. (2020). Parametric (exergy-energy) analysis of parabolic trough solar collector-driven combined partial heating supercritical CO₂ cycle and organic Rankine cycle. *Energy Sources, Part A: Recovery, Utilization, and Environmental Effects*. doi:<https://doi.org/10.1080/15567036.2020.1788676>

- Kretzschmar, H. (2019). *Property Library for Octamethyltrisiloxane (MDM)*. Retrieved from KCE-ThermoFluidProperties.
- Lai, N., Wendland, M., & Fischer, J. (2011). Working fluids for high-temperature organic Rankine cycles. *Energy* 36, 199-211. doi:<https://doi.org/10.1016/j.energy.2010.10.051>
- Li, Y., Hung, T., Feng, Y., Xi, H., & Wang, C. (n.d.). Effect of valve on the performance of a 3-kW ORC system: a rationally based off-design modelling and exergy analysis. *Applied Energy*.
- Li, Y., Wang, J., & Du, M. (2012). Influence of coupled pinch point temperature difference and evaporation temperature on performance of organic Rankine cycle. *Energy* 42, 503-509. doi:<http://dx.doi.org/10.1016/j.energy.2012.03.018>
- Macchi, E., & Astolfi, M. (2016). *Organic Rankine Cycle (ORC) Power Systems*. Woodhead Publishing. doi:<https://doi.org/10.1016/C2014-0-04239-6>
- Maccioni, C. (n.d.). *Scelta dei componenti e progettazione di un impianto ORC di piccola taglia*. Retrieved from Università di Pisa - Dipartimento di Ingegneria dell'Energia, dei Sistemi, del Territorio e delle Costruzioni.
- Morosuk, T., Tsatsaronis, G., & Schult, M. (2013). Conventional and Advanced Exergetic Analyses: Theory and Application. *Arab. J. Sci. Eng.* 38, 395-404. doi:<https://doi.org/10.1007/s13369-012-0441-9>
- Nishith, B., & Bandyopadhyay, S. (2009). Process integration of organic Rankine cycle. *Energy* 34, 1674-1686. doi:<https://doi.org/10.1016/j.energy.2009.04.037>
- Oyekale, J., Heberle, F., Petrollese, M., Brüggemann, D., & Cau, G. (2019). Biomass retrofit for existing solar organic Rankine cycle power plants: Conceptual hybridization strategy and techno-economic assessment. *Energy Conversion and Management* 196, 831-845. doi:<https://doi.org/10.1016/j.enconman.2019.06.064>
- Ozturk, M., & Dincer, I. (2021). A new geothermally driven combined plant with energy storage option for six useful outputs in a sustainable community. *Sustainable Energy Technologies and Assessments* 45, 101-180. doi:<https://doi.org/10.1016/j.seta.2021.101180>
- Pacheco, J.E., Showalter, S., & Kolb, W. (2001). Development of a molten-salt thermocline thermal storage system for parabolic trough plants. *Proceedings of Solar Forum 2001 - Solar Energy: The Power to Choose*. doi:<https://doi.org/10.1115/1.1464123>
- Pantaleo, A., Camporeale, S., Sorrentino, A., Miliozzi, A., Shah, N., & Markides, C. (2020). Hybrid solar-biomass combined Brayton/organic Rankine-cycle plants integrated with thermal storage: Techno-economic feasibility in selected Mediterranean areas. *Renewable Energy* 147, 2913-2931. doi:<https://doi.org/10.1016/j.renene.2018.08.022>
- Patil, V., Biradar, V., Shreyas, R., Garg, P., Orosz, M., & Thirumalai, N. (2017). Technoeconomic comparison of solar organic Rankine cycle (ORC) and photovoltaic (PV) systems with energy storage. *Renew. Energy* 113, 1250-1260. doi:<https://doi.org/10.1016/j.renene.2017.06.107>
- Pavlovic, S., Daabo, A., Bellos, E., Stefanovic, V., Mahmoud, S., & Al-Dadah, R. (2017). Experimental and numerical investigation on the optical and thermal performance of

- solar parabolic dish and corrugated spiral cavity receiver. *J. Clean. Prod.* 150, 75-92. doi:<https://doi.org/10.1016/j.jclepro.2017.02.201>
- Petela, R. (2003). Exergy of undiluted thermal radiation. *Solar Energy* 74 (6), 469-488. doi:[https://doi.org/10.1016/S0038-092X\(03\)00226-3](https://doi.org/10.1016/S0038-092X(03)00226-3)
- Petrollese, M., Cau, G., & Cocco, D. (2020). The Ottana solar facility: dispatchable power from small-scale CSP plant based on ORC systems. *Renewable Energy* 147, 2932-2943. doi:<https://doi.org/10.1016/j.renene.2018.07.013>
- Pina, E., Lozano, M., Serra, L., Hernandez, A., & Lazaro, A. (2021). Design and thermoeconomic analysis of a solar parabolic trough – ORC – Biomass cooling plant for a commercial center. *Solar Energy* 125, 92-107. doi:<https://doi.org/10.1016/j.solener.2020.11.080>
- Prabhu, E. (2006). *Solar trough ORC. Subcontract report SR-550-39433*. NREL.
- Quoilin, S. (2011). *Sustainable energy conversion through the use of Organic Rankine Cycles for waste heat recovery and solar applications*. Retrieved from Energy Systems Research Unit - University of Liège.
- Quoilin, S., & Lemort, V. (2009). Technological and economical survey of Organic Rankine Cycle systems. *5th European Conference Economics and Management of Energy in Industry*, (pp. 14-17).
- Quoilin, S., Orosz, M., Hemond, H., & Lemort, V. (2011). Performance and design optimization of a low-cost solar organic Rankine cycle for remote power generation. *Solar Energy* 85, 955-966. doi:<http://dx.doi.org/10.1016/j.solener.2011.02.010>
- Rampello, G. (2018). *Simulazione in ambiente Aspen Plus Dynamics dei transitori di un ciclo ORC alimentato da calore di scarto a media temperatura*. Retrieved from Università degli Studi di Padova - Dipartimento di Ingegneria Industriale .
- Rank®. (2019). *ORC operating principle*. Retrieved from Rank® Technology: <https://www.rank-orc.com/2019/06/21/rank-technology-orc-operating-principle/>
- Reddy, K., Jawahar, V., Sivakumar, S., & Mallick, T. (2017). Performance investigation of single-tank thermocline storage systems for CSP plants. *Solar Energy* 144, 740-749. doi:<http://dx.doi.org/10.1016/j.solener.2017.02.012>
- Rodríguez, J., Sánchez, D., Martínez, G., Bennouna, E., & Ikken, B. (2016). Techno-economic assessment of thermal energy storage solutions for a 1 MWe CSP-ORC power plant. *Solar Energy* 140, 206-218. doi:<http://dx.doi.org/10.1016/j.solener.2016.11.007>
- Rosen, M., & Dincer, I. (1997). On exergy and environmental impact. *International Journal of Energy Research* 21, 643-654.
- Schuster, A., Karellas, S., Kakaras, E., & Spliethoff, H. (2009). Energetic and economic investigation of Organic Rankine Cycle application. *Appl. Therm. Eng.* 29, 1809-1817. doi:<http://dx.doi.org/10.1016/j.applthermaleng.2008.08.016>
- Sebelev, A., Saychenko, A., Zabelin, N., & Smirnov, M. (2016). Numerical analysis of the expansion process in a two-stage axial turbine operating with MDM siloxane. *St Petersburg State Polytechnical University Journal* 249 (3), 29-38. doi:<http://dx.doi.org/10.5862/JEST.249.4>

- Sinasac, Z., & Jianu, O. (2021). Parametric study on the exergetic and cyclic performance of a solar-powered organic Rankine cycle coupled with a thermal energy storage and complete flashing cycle. *Sustainable Energy Technologies and Assessments* 45. doi:<https://doi.org/10.1016/j.seta.2021.101172>
- Singh, H., & Mishra, R. (2018). Energy and exergy-based performance evaluation of solar powered combined cycle (recompression supercritical carbon dioxide cycle/organic Rankine cycle). *Clean Energy*, Vol. 2, Issue 2, 140-153. doi:<https://doi.org/10.1093/ce/zky011>
- Singh, H., & Mishra, R. (2018). Performance analysis of solar parabolic trough collectors driven combined supercritical CO₂ and organic Rankine cycle. *Engineering Science and Technology, an International Journal*. doi:<https://doi.org/10.1016/j.jestch.2018.03.015>
- Suleman, F., Dincer, I., & Agelin-Chaab, M. (2014). Development of an integrated renewable energy system for multigeneration. *Energy*, 1-9. doi:<http://dx.doi.org/10.1016/j.energy.2014.09.082>
- Sun, W., Yue, X., & Wang, Y. (2017). Exergy efficiency analysis of ORC (Organic Rankine Cycle) and ORC-based combined cycles driven by low-temperature waste heat. *Energy Conversion and Management* 135, 63-73. doi:<http://dx.doi.org/10.1016/j.enconman.2016.12.042>
- Tchanche, B., Petrisans, M., & Papadakis, G. (2014). Heat Resources and organic Rankine cycle machines. *Renew. Sustain. Energy Rev.* 39, 1185-1199. doi:<http://dx.doi.org/10.1016/j.rser.2014.07.139>
- Tribus, M., & McIrvine, E. (1971). Energy and Information. *Scientific American* 225 (3), 179-188. doi:<https://doi.org/10.1038/SCIENTIFICAMERICAN0971-179>
- Turboden. (n.d.). *ORC systems*. Retrieved from Turboden S.p.a. - Clean energy ahead: <https://www.turboden.com/products/2463/orc-system>
- Tzivanidis, C., Bellos, E., & Antonopoulos, K. (2016). Energetic and financial investigation of a stand-alone solar-thermal Organic Rankine Cycle power plant. *Energy Conver. Manag.* 126, 421-433. doi:<http://dx.doi.org/10.1016/j.enconman.2016.08.033>
- UN. (2021). *Goal 7 - Ensure access to affordable, reliable, sustainable and modern energy for all*. Retrieved from United Nations - Department of Economic and Social Affairs - Sustainable Development: <https://sdgs.un.org/goals>
- Van Gool, W. (1997). Energy policy: Fairy Tales and Factualities. *Innovation and Technology - Strategies and Policies*, 93-105. doi:https://doi.org/10.1007/978-0-585-29606-7_6
- Van Lew, J., Li, P., Chan, C., Karaki, W., & Stephens, J. (2011). Analysis of heat storage and delivery of a thermocline tank having solid filler material. *J. Sol. Energy Eng.* 133. doi:<http://dx.doi.org/10.1115/1.4003685>
- Wang, J., Yan, Z., Zhao, P., & Dai, Y. (2014). Off-design performance analysis of a solar-powered organic Rankine cycle. *Energy Conversion and Management* 80, 150-157. doi:<http://dx.doi.org/10.1016/j.enconman.2014.01.032>

- Wang, X., Li, Z., Long, P., Yan, L., Gao, W., Chen, Y., & Sui, P. (2017). Sustainability evaluation of recycling in agricultural systems by energy accounting. *Resour. Conserv. Recycl.* 117, 114-124. doi:<https://doi.org/10.1016/j.resconrec.2016.11.009>
- Xiang, J., Cali, M., & Santarelli, M. (2004). Calculation for physical and chemical exergy of flows in systems elaborating mixed-phase flows and a case study in an IRSOFC plant. *International Journal of Energy Research* 28, 101-115. doi:<https://doi.org/10.1002/er.953>
- Zarei, A., Akhavan, S., Babaie Rabiee, M., & Elahi, S. (2021). Energy, exergy and economic analysis of a novel solar driven CCHP system powered by organic Rankine cycle and photovoltaic thermal collector. *Applied Thermal Engineering* 194. doi:<https://doi.org/10.1016/j.applthermaleng.2021.117091>
- Zhang, H., Baeyens, J., Cáceres, G., Degrève, J., & Lv, Y. (2016). Thermal energy storage: Recent developments and practical aspects. *Progress in Energy and Combustion Science* 53, 1-40. doi:<https://doi.org/10.1016/j.pecs.2015.10.003>
- Zhang, H., Guan, X., Ding, Y., & Liu, C. (2018). Exergy analysis of Organic Rankine Cycle (ORC) for waste heat power generation. *J. Clean. Prod.* 183, 1207-1215. doi:<http://dx.doi.org/10.1016/j.jclepro.2018.02.170>